



UNIVERSITAT POLITÈCNICA DE CATALUNYA  
BARCELONATECH

Escola Superior d'Enginyeries Industrial,  
Aeroespacial i Audiovisual de Terrassa

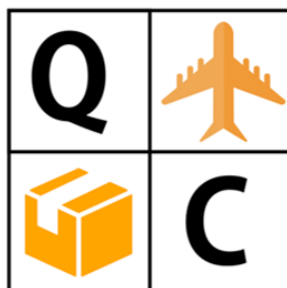
**Degree:** AEROSPACE ENGINEERING

**Course:** Engineering Projects

---

# Quick-change regional aircraft

QCRA



**QC AIRCRAFT**

---

**Contents:** REPORT

**Group:** G04-AE-2020/21-Q1

**Delivery date:** 17/12/2020

**Students:**

Asensio Garcia, Cristian

León Delgado, Alexis

Navarro Gorgojo, Pablo

Busquets i Soler, Lluc

López Flores, Arnau

Pérez Gil, Hugo

Chaler Tost, Clàudia

Martí Arasa, Marc

Roig Cererols, Marta

Ferrer Brao, Jordi

Molina Cuadrado, Alba

Ruiz Álvarez, Óscar

González Chirivella, Víctor

Montilla Garcia, Carles

Villalonga Domínguez, Pablo

**Supervisor:** Nualart Nieto, Pau

# Contents

<b>1 Aim</b>	<b>1</b>
<b>2 Scope</b>	<b>2</b>
<b>3 Requirements</b>	<b>3</b>
<b>4 Background</b>	<b>4</b>
<b>5 State of the art</b>	<b>5</b>
<b>6 Main alternatives considered and selection of the best one</b>	<b>8</b>
6.1 Wing system decisions . . . . .	8
6.1.1 Vertical configuration . . . . .	8
6.1.2 Wing's subsystems decisions . . . . .	9
6.2 Tail system decisions . . . . .	11
6.2.1 Configuration . . . . .	11
6.2.2 Materials choice . . . . .	12
6.3 Fuselage system decisions . . . . .	12
6.3.1 Fuselage shape . . . . .	12
6.3.2 Section shape . . . . .	13
6.3.3 Materials choice . . . . .	13
6.3.4 Fuselage's subsystems decisions . . . . .	13
6.4 Landing gear system decisions . . . . .	14
6.4.1 Geometry configuration . . . . .	14
6.4.2 Landing gear's subsystems decisions . . . . .	14
6.5 Power plant system decisions . . . . .	15
6.5.1 Type of engine . . . . .	15
6.5.2 Number of engines . . . . .	15
6.5.3 Positioning of the engines . . . . .	15
6.5.4 Engine selection . . . . .	15
<b>7 Development and design of the chosen solution</b>	<b>17</b>
7.1 Aerodynamics . . . . .	17
7.1.1 Weights estimation for design point selection . . . . .	17
7.1.2 Weight-range diagram . . . . .	19
7.1.3 Design point selection . . . . .	19
7.1.4 Airfoil selection . . . . .	20

7.1.5	Wing planform . . . . .	21
7.1.6	Wing parameters . . . . .	21
7.1.7	High-lift devices . . . . .	27
7.1.8	Tail and rear fuselage sizing . . . . .	29
7.1.9	Longitudinal and lateral-directional control surfaces . . . . .	33
7.1.10	Fuselage . . . . .	38
7.2	Structures . . . . .	41
7.2.1	Wing . . . . .	41
7.2.2	Fuselage . . . . .	45
7.2.3	Tail . . . . .	56
7.2.4	Landing gear . . . . .	63
7.2.5	Stability . . . . .	67
7.2.6	Cabin floor rail system . . . . .	69
7.2.7	Final QCRA aircraft CAD model . . . . .	75
7.3	Propulsion . . . . .	77
7.3.1	Type, positioning and number of engines . . . . .	77
7.3.2	Maximum power required . . . . .	77
7.3.3	Selection of the engine . . . . .	77
7.3.4	Propeller . . . . .	77
7.3.5	Positioning of the engine . . . . .	77
7.3.6	Performance . . . . .	78
7.4	Systems . . . . .	79
7.4.1	Avionics . . . . .	79
7.4.2	Electrical system . . . . .	80
7.4.3	Control system . . . . .	86
7.4.4	Fuel system . . . . .	93
<b>8</b>	<b>Economic feasibility analysis</b>	<b>96</b>
8.1	Cumulative Cash flow . . . . .	96
8.2	Net present value at the end of the Project . . . . .	98
8.3	Payback time and Break-even point . . . . .	98
8.4	Return on Investment . . . . .	99
8.5	Internal rate of return . . . . .	100
8.6	Final conclusions . . . . .	100
<b>9</b>	<b>Environmental impact analysis</b>	<b>102</b>
9.1	General considerations . . . . .	102
9.2	Structure materials . . . . .	102

9.3 <i>CO<sub>2</sub></i> emissions . . . . .	104
9.3.1 <i>CO<sub>2</sub></i> emissions in the aviation industry . . . . .	104
9.3.2 <i>CO<sub>2</sub></i> emissions reduction plan . . . . .	105
<b>10 Safety considerations</b>	<b>107</b>
<b>11 Planning and scheduling for the follow-up of the project</b>	<b>108</b>
11.1 Preliminary Design . . . . .	108
11.2 Design Phase . . . . .	109
11.3 Prototyping Phase . . . . .	109
11.4 Certification Phase . . . . .	110
11.5 Manufacturing Phase . . . . .	110
<b>12 Conclusions and recommendations</b>	<b>111</b>
<b>13 Bibliography and regulations</b>	<b>113</b>

## List of Figures

1	Comparison of major operating cost fractions with time. Source: [4]. . . . .	5
2	Wing vertical positioning configuration alternatives (low, high and mid wing). Source: [16]. . .	8
3	Box beam type structure. Source: [16]. . . . .	10
4	Different spar sections used depending on the aircraft. Source: [17]. . . . .	11
5	Tail configuration alternatives (T-tail, conventional and cruciform). Source: [16]. . . . .	11
6	T-Tail configuration scheme. Source: [18]. . . . .	12
7	Weight-range diagram for Quick-Change Regional Aircraft (QCRA). . . . .	19
8	Matching plot, acceptable region and design point. . . . .	20
9	Douglas LA203A airfoil section. Source: [25]. . . . .	20
10	3D modelling of wing planform obtained from XFLR5. . . . .	21
11	3D modelling of wing winglets from XFLR5. . . . .	22
12	Winglets addition XFLR5 results. . . . .	23
13	Wing incidence values for reference turboprop regional aircraft. Source: [22]. . . . .	24
14	$c_l$ distribution along the span. . . . .	25
15	% decrease in bending moment. . . . .	25
16	Sweep angle for three types of wings: rectangular, swept wing and tapered wing. Source: [22].	26
17	Final wing polars. . . . .	27
18	Flaps deflected 20 degrees in XFLR5. . . . .	28
19	$\delta C_L$ vs. Flap Deflection Degree. . . . .	29
20	Top view of aft position of the aircraft and $l_t$ characterization. Source [22] . . . . .	29
21	Variation of wetted area with respect to tail arm. Source: [22]. . . . .	30
22	Horizontal tail configurations studied. . . . .	31
23	Conventional aircraft in longitudinal trim. Source: [22]. . . . .	31
24	Polar graphs with main wing and horizontal stabilizer in XFLR5. . . . .	32
25	Horizontal stabilizer design in XFLR5 . . . . .	32
26	Vertical stabilizer design in XFLR5. . . . .	33
27	Design possibilities for the longitudinal control system. Source: [22]. . . . .	33
28	+20° degree deflection in the elevator. . . . .	34
29	+20° degree deflection in the elevator and +20° rudder . . . . .	35
30	Physics of a right turn for an aircraft and its adverse yaw. . . . .	36
31	Diagram of lengths. . . . .	37
32	The frontal tip (or nose) of the fuselage and the root leading edge of the wing are separated 10.51 m from each other. This is because the fuselage's nose is located at -9.51m from the global reference system and the leading edge of the wing is positioned at 1m from the same coordinate system. . . . .	38

33	Assisted Body Generator of XFLR5. According to the Structures Department, the fuselage's cross-section is not fully round shaped, but rather an oval shape. . . . .	39
34	Perspective view of the aircraft. . . . .	39
35	Pressure coefficient distribution on surfaces (note the limitations due to the homogeneous distribution of the pressure coefficient). . . . .	40
36	Polars of the VLM1 analysis (Vortex Line Method). . . . .	40
37	Top view of the final wing model. . . . .	41
38	Ribs and spar sections on three different cuts of the wingspan (at 0.90 m, 5.16 m and 10.84 m from the center). . . . .	42
39	Top view of the internal wing configuration. Note the three different rib spacings. . . . .	42
40	View of the internal wing configuration. . . . .	43
41	Most demanding lift distribution over the semiwing. . . . .	44
42	Predicted deflection from one-dimensional analysis. . . . .	44
43	Deflection with combined Titanium-Aluminum configuration. . . . .	45
44	Factor of safety with combined Titanium-Aluminum configuration. . . . .	45
45	Seat dimensions. . . . .	46
46	Dimensions for every row. . . . .	46
47	Internal dimensions of the fuselage. . . . .	47
48	General seating arrangement in passenger operation mode. . . . .	47
49	Space claims of a typical aircraft lavatory. . . . .	48
50	General seating arrangement and lavatory installation. . . . .	48
51	Type I and Type IV doors dimensions. . . . .	49
52	Aircraft's interior layout. . . . .	50
53	Cockpit design and layout. . . . .	50
54	Frame disposition for the cabin. . . . .	51
55	Longeron disposition for the cabin. . . . .	52
56	Longeron and frame disposition for the cabin. . . . .	52
57	Longeron and frame disposition for the cabin (3D model). . . . .	52
58	Window sizing and structure. . . . .	53
59	Final window placement. . . . .	53
60	An approximation of a tubular fuselage using elementary solids. . . . .	54
61	Cargo door dimensions. . . . .	55
62	Dismounted cargo door. . . . .	55
63	Mounted cargo door. . . . .	56
64	Spars and ribs distribution of the HS. . . . .	57
65	Horizontal stabiliser's airframe configuration. . . . .	58
66	Spars and ribs distribution of the HS. . . . .	59

67	Spars and ribs distribution of the HS. . . . .	60
68	Spars and ribs distribution of the HS. . . . .	60
69	Rear fuselage-tail joint scheme. . . . .	61
70	Rear fuselage (elliptical section) to tail (lower rectangular and upper elliptical section) transition. . . . .	62
71	Rear fuselage - tail joint and VS 3D model (cargo door not implemented). . . . .	62
72	Final empennage 3D model. . . . .	63
73	Landing gear disposition scheme according to stability criteria (units in mm). . . . .	65
74	3D model of the landing gear and the corresponding nacelle . . . . .	66
75	Weight breakdown of the airplane, with the corresponding centers of mass located in the sideview. . . . .	67
76	Excursion diagram of the longitudinal position of the estimated center of gravity of the airplane. . . . .	68
77	Excursion diagram of the vertical position of the estimated center of gravity of the airplane. . . . .	68
78	Fuselage rail system. . . . .	69
79	Pallet design. . . . .	70
80	Pallet rail system. . . . .	70
81	Rail system. . . . .	70
82	Rail system. Source: [30]. . . . .	71
83	Assembly of the palletized seats in the fuselage structure. . . . .	71
84	Pallets distribution along the cabin. . . . .	72
85	Pallets distribution along the cabin (3D model). . . . .	72
86	Roller conveyor strips mounted on the fuselage floor. Source: [32]. . . . .	73
87	Usable area of the cabin. . . . .	73
88	Quick-change system render . . . . .	74
89	Cabin configuration modes. . . . .	75
90	QCRA aircraft CAD models. . . . .	76
91	Cockpit of the <i>Avions de Transport Régional</i> (ATR)42-600. Source: [34]. . . . .	80
92	Power Requirements of an ATR 42. Source: [35]. . . . .	81
93	DC powered emergency supplies. . . . .	82
94	Alternate Current (AC) circuit scheme with normal supply in flight and both AC generators online. Source: [35]. . . . .	83
95	Exterior lightning of the aircraft. Source: [36]. . . . .	83
97	Spot lights of the ATR flight compartment. Source: [36]. . . . .	84
98	Interior lightning. Source: [36]. . . . .	85
100	Emergency lighting system of the ATR-42. Source: [36]. . . . .	86
101	Primary flight controls. Source: [45]. . . . .	88
102	Electro-Mechanical Actuator. Source: [46]. . . . .	88
103	Roll control through the joystick. Source: [47] (modified). . . . .	89
104	Rudder system layout of the ATR42-300. Source: [48]. . . . .	90

105	Flap control lever (white) in the ATR42-600s and its allowable deflections. Source: [34]. . . . .	91
106	Boeing 717 approach phase: cruise flight (left), descending flight (center) and landing (right). Source: [49]. . . . .	91
107	Electric brake. Source: [50]. . . . .	92
108	Cockpit controls layout in an Airbus A320. Source: [51]. . . . .	92
109	Scheme of the four tanks situated in the wings (the front of the wing corresponds to the top of the image). . . . .	94
110	Estimation of the amount of airplanes sold per year. . . . .	96
111	Cumulative cash flow in the three scenarios. . . . .	97
112	Cumulative Net Cash Flow. . . . .	97
113	Total units sold per year. . . . .	99
114	Top aluminum exporters in 2019 by dollar value and % share of global sales. . . . .	103
115	<i>CO<sub>2</sub></i> emissions from commercial aviation, 2004 to 2009. Source: [56]. . . . .	104
116	Average fuel burn of new commercial jet aircraft, 1960 to 2019. Source: [56]. . . . .	105
117	Planning and scheduling for the follow up of the project. . . . .	108
118	Internal organization structure. . . . .	109

## List of Tables

1	Display of the basic specifications of eleven regional Quick-Change aircraft. . . . .	6
2	Engine candidates. Sources: [20] and [21]. . . . .	16
3	Ordered Weighted Average (OWA) to select the engine. . . . .	16
4	Reference methodologies for OEW estimation. . . . .	18
5	Obtained fuel-fraction values for all mission flight profile stages. . . . .	18
6	Geometric characteristics of the wing. . . . .	21
7	Typical dihedral angles. . . . .	26
8	Parameters of QCRA flap design. . . . .	28
9	Table comparing flaps parameters of turboprop aircraft. Source: [22]. . . . .	28
10	Horizontal stabilizer planform dimensions. . . . .	32
11	Vertical stabilizer planform dimensions . . . . .	33
12	Ailerons chord and span ratios, and maximum deflection values. . . . .	36
13	Longitudinal position values for our model aircraft. . . . .	37
14	Wing spar properties along the span (provided by Solidworks). . . . .	41
15	Definition of seat dimensions for economy class passengers. . . . .	46
16	Number of required exits on each side of the fuselage for 40 - 50 passengers. . . . .	49
17	Internal cabin dimensions (see Figure 47). . . . .	51
18	Typical tail spar positioning in transport aircraft, where $x_{\text{spar}}$ refers to the chord direction relative to the root's TE. Source: [24] . . . . .	56
19	HS spar positioning in QCRA aircraft. . . . .	57
20	HS's spar properties along the span (provided by Solidworks). . . . .	58
21	Conditions of the study. . . . .	59
22	Estimated most fore-and-aft CG limits for QCRA aircraft, where $x$ refers to the aircraft's longitudinal axis, being its nose the origin. . . . .	64
23	Landing gear's stability design variables. . . . .	64
24	QCRA's nose and main landing gear distances, being $l_{\text{nose}}$ the distance between the mean CG and the nose, and $l_{\text{main}}$ the one between the main gear and the mean CG. Refer to Figure 73a for a visual representation. . . . .	64
25	Landing gear loads and wheel sizing. . . . .	66
26	Types of pallets. . . . .	72
27	Take-off Field Length (TOFL) and Landing Field Length (LFL) for different altitudes. . . . .	78
28	Compulsory instrumentation. . . . .	79
29	Commercially available electrical components. . . . .	86
30	Control systems. . . . .	87
31	Fuel mass calculations. . . . .	93

## Acronyms list

<b>4G LTE</b>	Fourth Generation Long Term Evolution
<b>AC</b>	Alternate Current
<b>ACARS</b>	Aircraft Communications Addressing and Reporting System
<b>ACW</b>	Alternate Current Wild frequency
<b>ADF</b>	Automatic Direction Finding
<b>ADS-B</b>	Automatic Dependent Surveillance-Broadcast
<b>AHRS PB</b>	Attitude and Heading Reference System Push Button
<b>AoA</b>	Angle of Attack
<b>APU</b>	Auxiliar Power Unit
<b>AR</b>	Aspect Ratio
<b>ARALL</b>	Aramid aluminum laminate
<b>ATR</b>	<i>Avions de Transport Régional</i>
<b>BTC</b>	Bus Tie Contactor
<b>BEP</b>	Break-Even Point
<b>CFR</b>	Code of Federal Regulations
<b>CG</b>	Center of Gravity
<b>CMU</b>	Communications Management Unit
<b>CS</b>	Certification Specifications
<b>CSD</b>	Constant Speed Driver
<b>CVR</b>	Cockpit Voice Recorder
<b>DC</b>	Direct Current
<b>DFDR</b>	Digital Flight Data Recorder
<b>EADI</b>	Electronic Aircraft Direction Indicator
<b>EASA</b>	European Union Aviation Safety Agency
<b>EBHA</b>	Electric Backup Hydraulic Actuator

<b>EBITDA</b>	Earnings Before Interest, Taxes, Depreciation & Amortization
<b>EBT</b>	Earnings Before Taxes
<b>EFIS</b>	Electronic Flight Instrument System
<b>EHSI</b>	Evolved Horizontal Situation Indicator
<b>ELA</b>	Electrical Load Analysis
<b>EMA</b>	Electro-Mechanical Actuator
<b>EW</b>	Empty Weight
<b>FAA</b>	Federal Aviation Agency
<b>FAR</b>	Federal Aviation Regulations
<b>FBW</b>	Fly-By-Wire
<b>FFAP</b>	Forward Flight Attendant Panel
<b>GCU</b>	Ground Control Unit
<b>GPS</b>	Global Positioning System
<b>GPU</b>	Ground Power Unit
<b>HLD</b>	High-lift device
<b>HLPDU</b>	High-Lift Power Drive Unit
<b>HS</b>	Horizontal Stabilizer
<b>IAS</b>	Indicated Air-Speed
<b>ICAO</b>	International Civil Aviation Organization
<b>IRR</b>	Internal Rate of Return
<b>ILS</b>	Instrument Landing System
<b>JAR</b>	Joint Aviation Requirements
<b>LE</b>	Leading Edge
<b>LEHLDs</b>	Leading Edge High-Lift Devices
<b>LFL</b>	Landing Field Length
<b>LLT</b>	Lifting Line Theory
<b>MAC</b>	Mean Aerodynamic Chord

<b>MCDU</b>	Multi-function Display Control Unit
<b>MCP</b>	Multi-function Control Panel
<b>MFW</b>	Maximum Fuel Weight
<b>MGC</b>	Mean Geometric Chord
<b>MPL</b>	Maximum PayLoad
<b>MRO</b>	Maintenance, Repair & Operations
<b>MTOW</b>	Maximum Take-Off Weight
<b>MU</b>	Management Unit
<b>MZFW</b>	Maximum Zero Fuel Weight
<b>NACA</b>	National Advisory Committee for Aeronautics
<b>ND</b>	Navigation Display
<b>NPV</b>	Net Present Value
<b>OEW</b>	Operational Empty Weight
<b>OWA</b>	Ordered Weighted Average
<b>PBT</b>	Pay-Back Time
<b>PF</b>	Primary Flight Display
<b>PL</b>	Payload
<b>PNT</b>	Position, Navigation and Timing
<b>PSU</b>	Passenger Service Unit
<b>QC</b>	Quick-Change
<b>QCRA</b>	Quick-Change Regional Aircraft
<b>RAT</b>	Ram Air Turbine
<b>RCDR</b>	ReCorDeR
<b>RFM</b>	Reserve Fuel Mass
<b>ROC</b>	Rate Of Climb
<b>ROI</b>	Return On Investment
<b>RPM</b>	Revolutions per minute

**SATCOM** SATellite COMmunications

**SESAR** Single European Sky ATM Research

**SFC** Specific Fuel Consumption

**STOL** Short Take-Off and Landing

**TE** Trailing Edge

**TO** Take-off

**TOFL** Take-off Field Length

**TOW** Take-off weight

**THSA** Trimmable Horizontal Stabilizer Actuator

**TRU** Transformer-Rectifier Unit

**VHF** Very High Frequency

**VLM** Vortex Line Method

**VOR** VHF Omni-directional Range

**VS** Vertical speed

**VS** Vertical Stabilizer

**WAAS** Wide Area Augmentation System

**WBS** Work Breakdown Structure

**ZFW** Zero Fuel Weight

## **1 Aim**

The aim of the project is to design a quick-convertible aircraft between passengers and cargo operational modes specifically conceived to operate in short regional range flights and following both EASA and FAA regulations.

## 2 Scope

In order to carry out the design of the aircraft, the following processes and analysis will be included:

- A justification on the general configuration selection aiming on being optimal in both possible aircraft's operational modes (passenger and cargo), while studying different seating arrangements and cargo configurations.
- The study and design of the "quick change" system, including the decisions taken to select the best configuration.
- The study and design of the propulsion, aerodynamics and payload capabilities of the plane, as well as decisions and considerations taken to justify the selected design options.
- A brief study on the systems that compose the aircraft, such as avionics, controls and illumination.
- Definition and justification of materials to be used in the aircraft to satisfy requirements, as well as structural concept definition.
- An extensive study and preliminary design of the doors that will allow an easy access to the cabin.
- The three views of the aircraft's drawing including its dimensions.
- A feasibility study that justifies the existence of an aircraft of this characteristics at a competitive price.
- A research and study on maintaining competitive jet sales price with special focus on fuel consumption with a component-by-component contribution and saving analysis.
- A brief study of the FAA and EASA regulations in order to broaden the market possibilities of this new concept of aircraft.
- An environmental study that ensures that the standards imposed by the government are met.

Take into account that the following aspects will not be included in the preliminary design:

- Detailed structural simulations including the final load distribution on all the aircraft elements.
- In-depth aerodynamic simulations (CFD) beyond the basic parametric wing configuration calculations.
- Detailed fuselage's aerodynamics study and free bending moment generated determination.

### **3 Requirements**

When it comes to designing a quick-change regional aircraft, there are some specifications that must be taken into account to fulfil the requirements of the customer. The main requirements of the project are the following:

- The aircraft must have a certified seating capacity of 50 passengers, and be able to carry 2 pilots and 2 flight attendants
- All aircraft parts and subsystems, as well as its general layout, must follow both EASA and FAA regulations.
- The aircraft must be able to operate in both passenger and cargo modes.
- Maximum range greater than 1500 km in the design conditions.
- Maximum take-off field length of 1100 meters with MTOW.
- Fuel consumption should be at least 10% lower than similar aircraft.

## 4 Background

Given the current situation of the Covid-19 pandemic and the resulting decrease in the number of passengers, companies are interested in being able to adapt quickly to satisfy new market demands. A versatile aircraft capable of frequently switching from passenger to cargo transportation provides them the possibility of embracing a wider market, due to the fact that it can take advantage of both cargo and commercial businesses.

Although there are precedents of aircraft designed to be adaptable to both passenger and cargo such as the ATR42-600, there is not any option capable of doing so in a quick turnaround.

On the one hand, this configuration of the aircraft can help companies make the otherwise under demanded short range passenger flights worthwhile, since a single aircraft could be used in the same route and adapted to the marked necessities on the go. Possible niche markets could be islands, where this convertibility feature is commonly needed.

On the other hand, one possible drawback of this project is that, as a consequence of the double configuration, the design of the aircraft could not result as efficient as a conventional plane for a particular single market. However, being a regional aircraft makes it less critical to fly fast when carrying passengers, making the classical cargo aircraft configuration more optimal for both situations.

## 5 State of the art

Convertible aircraft in commercial aviation are aircraft that can be used to carry either passengers, as an airliner, or cargo as a freighter, and may have a partition in the aircraft cabin to allow both uses at the same time in a mixed passenger/freight combination.

This system dates back to the 1960s, when some jet transports were introduced to the cargo service because of the increase in air freight. Since 1962, total free world air cargo increased by over 70%, reaching an air freight increase of over 25% in 1965 alone. A year later, in April 1966, Northwest Airlines purchased the first Quick Change jet aircraft, the Boeing 727QC [1].

Nowadays, the cargo service is still increasing. In 2014, more than 51 million tonnes of cargo was flown around the world, of which 56% of this total was flown on dedicated freighter aircraft, that is, aircraft whose only function is to transport cargo. The other 44% travelled as belly-freight in the holds of passenger flights, on combi-aircraft or QC-aircraft. In 2015, the 9% of total airline revenues was generated by freight, which represents more than twice the derived from first class products [2].

With these great changes on the aviation industry, the idea of the Quick-Change aircraft arose so as to take profit of the non-operative time for conventional passenger transporters. Thanks to this system, airlines are able to alternate between passengers and cargo layouts on a daily, weekly or seasonal basis depending on market demands, which results in much more profitable aircraft. However, due to the conditions in which this type of aircraft operate, this operation is practical only with small narrow-body aircraft, where the conversion time between both configurations is considerably reduced [3].

According to a study of the economic benefit potential of these aircraft [4], it is claimed that, nowadays, the largest cost that airlines must face is the ownership costs, such as depreciation, interest, insurance, etc., as it is shown below in Figure 1.

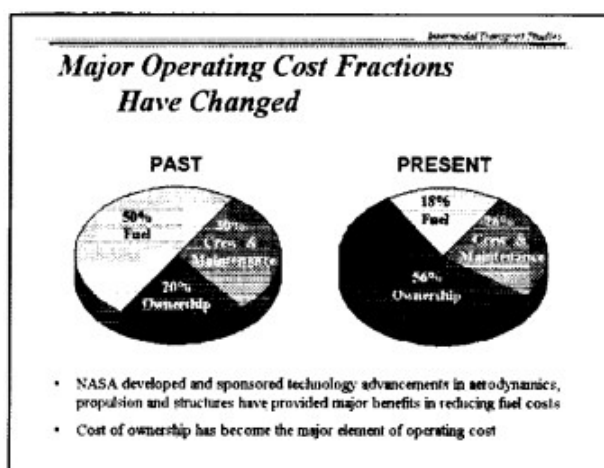


Figure 1: Comparison of major operating cost fractions with time. Source: [4].

For that reason, reducing the cost of air transportation requires to improve the aircraft utilization. By increasing daily utilization it can be reduced the share of ownership cost charged to each trip. One of the most useful solution to this issue is to change operating modes from passenger during the day to cargo at night, which provides the usage of the aircraft throughout the day. An example of utilization would be one explained in [1]: *"A daytime passenger flight from New York to Miami and back might be followed by a cargo flight from New York to Atlanta and back within the 24-hr period, still leaving sufficient time for conversion and maintenance."*. But this system can also travel at day time according to market demand changes. A profit improvement by a factor of two or more can be obtained with this system, resulting in an operating cost reduction of up to 20%.

Second hand freighter market has become another of the uses for the Quick-Change aircraft. The global recession of 2008 or the current living situation of the Covid-19 pandemic lead to an increased number of passenger to freight aircraft conversions. This is the case, for example, of Dubai-based airline with 85 of Emirates' Boeing 777-300ERs operating as stand-in freighters. Virgin Atlantic and Finnair are two more examples of other carriers that have also taken advantage of the airfreight market so as to minimize losses [5].

Airbus A330, A340, A350, A380 and Boeing 737NGs, 767-300, 777-200, 777-300 are some examples of large capacity aircraft that have been converted from passenger to cargo during this situation. In fact, the huge demand on these conversions had been noticed for the German MRO, who claimed that more than 40 airlines had interest in its technical and engineering services for these operational changes from passenger to cargo aircraft [5].

Table 1: Display of the basic specifications of eleven regional Quick-Change aircraft.

	<b>Length [m]</b>	<b>Wingspan [m]</b>	<b>Height [m]</b>	<b>MTOW [kg]</b>	<b>Cruise Speed [km/h]</b>	<b>Range [km]</b>	<b>Crew</b>	<b>Passengers</b>
<b>Boeing 737-300 [6]</b>	33.4	28.88	11.13	62,820	920	4,204	5	149
<b>ATR 42-500 [7]</b>	22.67	24.57	7.59	18,200	484	1,470	2	48
<b>ATR 72-500 [8]</b>	27.16	27.05	7.65	22,800	511	1,650	2	78
<b>British Aerospace ATP [9]</b>	26.00	30.63	7.14	22,930	496	1,825	2	66
<b>Fokker 50 [10]</b>	25.25	29	8.32	20,820	500	1,700	2	56
<b>Saab 340 [11]</b>	19.7	21.4	7.0	13,150	460	1,500	2	37
<b>BOMBARDIER DASH 8-Q400F [12]</b>	32.81	28.4	8.3	29,260	667	2,522	2	148
<b>Airbus A320/A321 [13]</b>	44.51	35.80	11.76	93,500	833	5,930	4	220
<b>Antonov An-140 [14]</b>	22.6	24.5	8.2	21,500	460	1,380	4	52
<b>British Aerospace 146-300 [15]</b>	31	26.34	8.61	44,225	789	3,340	2	112

In the matter of common Quick-Change aircraft, some models must be highlighted. With up to 149 passengers or 41,420 lb of cargo on 8 pallets, the American company Boeing produces the B737-700 in a Quick-Change configuration. And for military purposes, the US Navy adopted the C40, the army's evolution of the 737-700. As regards Quick-Change regional aircraft, the project's specific field of study, the Franco-Italian company

Avions de Transport Régional, or more commonly known as ATR, produces the ATR72 and ATR42, being the latter the most similar aircraft in terms of performance in comparison with the project's requirements. A part from these models, the turbofan aircraft CASA/IPTN CN-235 is co-produced by Construcciones Aeronáuticas (Spain) and IPTN (Industri Pesawat Terbang Nusantara, Indonesia), whereas the DASH 8 aircraft is produced by De Havilland Canada. Additionally, a newcomer to this niche is the Ukraine's Antonov An-140.

Finally, after analyzing the specifications of the prior variety of regional quick-change aircraft and some more examples, a comparative Table 1 can be assembled as follows.

## 6 Main alternatives considered and selection of the best one

The aircraft to be developed is named QCRA, a clear identifier of the project's aim. In this matter, the QCRA project requirements fulfilment have implied the consideration of different design alternatives. In terms of decision making, various methodologies have been applied depending on the aspect to assess. In some cases in which the decision was logical, a pros and cons comparison has been performed, whereas when a more technical and precise decision was needed, the OWA method has been used.

### 6.1 Wing system decisions

#### 6.1.1 Vertical configuration

The wing vertical location, inside the wing-fuselage configuration, depends on the operational and technical requirements that the aircraft would be designed for. It must be said that, although the aerodynamic and structural differences are not without importance, they cannot be deciding factors when choosing between the following three main conventional vertical positioning configurations that are considered:



Figure 2: Wing vertical positioning configuration alternatives (low, high and mid wing). Source: [16].

The selection of the best configuration has been performed taking into account both the project and the operational requirements of the aircraft. Thus, a high wing configuration has been selected as it presents the best advantages in relation to what just stated (please see Aerodynamic Attachment section 1.13 for a further detail containing all configurations' advantages and disadvantages):

- Provides a clear, unobstructed view of the ground as well as more ground clearance for avoiding low obstacles. Then, it also provides a better operational organization in platform around the aircraft, thus reducing time and costs for airlines, being more competitive.
- Ability to both takeoff and land within shorter distances due to lessened impact of ground effect, as there is no close proximity of the wing to the ground that may cause mentioned pronounced and generally undesirable ground effects (thus aircraft won't only takeoff because of the effect).
- Provides enough vertical distance to fit a turboprop engine that will also have less blades-runway aerodynamic interference and, as it will be further commented, is the one offering the least fuel consumption.
- Presents an inherent stable configuration since the center of mass is situated below the center of lift.

- It is easier to chock and unchock the main wheels, and allows landing gear to be attached to the fuselage instead of the wing, thus reducing structural fatigue and both manufacturing and maintenance costs.
- Gravity helps fuel flow from the tank to engine without the need for a very highly sophisticated fuel pumping system.
- Provides some aerodynamic advantages in wing's extrados.

### 6.1.2 Wing's subsystems decisions

#### 6.1.2.1 Airfoil type selection

The airfoil selection is a crucial step in the design of an airplane. Its effect goes beyond the pure aerodynamic behavior, and structural constraints must be considered. Since designing a specific airfoil was beyond the scope of this project, several already existing ones were considered. The major specifications looked for were thickness, stall behavior, and overall lift coefficient. The theoretical information on which this decision is based is presented in section 1.5.1 of the Aerodynamics Attachment.

The most weighting factors when deciding the type of airfoil selected, from the aerodynamic point of view, were the cruise speed and the TO capabilities. Since the aircraft is turboprop driven, the speeds where the supercritical airfoil performs best will never be reached, so the option was discarded. Moreover, for achieving a shorter takeoff distance, high lift coefficient values will be required, without the need for excessive Angle of Attack (AoA). For these reasons, the type of airfoil selected was a high-lift one.

#### 6.1.2.2 Airfoil model selection

To decide which airfoil model best suits the aircraft, existing airfoils have been analyzed extracting the usable data from the polar plots obtained with the XFLR5. The final candidates were the DEFIANT CANARD BL110, the DOUGLAS LA203A, the NACA 7315, the NACA 2315 and the NACA 4216.

From the **OWA** done in the Aerodynamics Attachment in section 1.5.6, it is known that the best airfoil for our aircraft is the LA203A.

What makes this airfoil better than the others is specially its great efficiency at cruise stage and also that it has the best  $C_{L,max}$  between all studied airfoils. These two characteristics are of great importance for our plane, since two of the main design requirements are a STOL configuration where high-lift is necessary and low fuel consumption where good efficiency is needed.

#### 6.1.2.3 High-lift devices

With regards to high-lift devices, two types of devices are used in commercial aviation: trailing edge devices and leading edge devices. Trailing edge devices are used in all types of aircraft, due to their simplicity and that they are the most wide-spread practice. On the other hand, Leading Edge High-Lift Devices (LEHLDs) are not

used as commonly as the previous ones. Therefore, the decision of implementing LEHLDs should be taken (for further pros and cons comparison, please refer to the Aerodynamics Attachment, section 1.7).

Thereby, no Leading Edge High-Lift Devices will be implemented since the airfoil can generate enough extra lift with only the trailing edge flaps. Regarding the type of Trailing edge high lift device, it will be a plain flap due to its simplicity.

#### 6.1.2.4 Wing internal structure

Refer to Structures Attachment, section 2.3.2 to see the detailed analysis of the most suitable type of wing structure. In short, the best option has been found to be a box beam internal structure, which means that the main elements that resist the loads are the spars but the combination of ribs and skin takes a significant part in the overall structural behavior. This means that, unlike in mass boom structures, a failure in the spars is not catastrophic for the whole wing. Figure 3 shows a schematic of such structure, in this case formed by three spars (the thicker vertical lines), the ribs (with their observable section, consisting of the other vertical lines and the airfoil contour) and the skin.

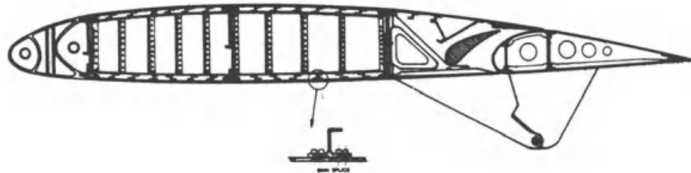


Figure 3: Box beam type structure. Source: [16].

#### Spars section

The box beam structure is commonly formed by two longitudinal spars (main and rear) in the wingspan direction to which the ribs are subjected. The section of these spars can take several forms depending on the material used and type of aircraft, as seen in Figure 4.

As it can be seen, the nature of metallic materials allows the central webs to be thinner, which allows the material to be concentrated near the extremes and thus increase the inertia of the section. Bearing in mind that the developed aircraft is far from light and the materials study (see Structures Attachment section 2.2) has yield to aluminium as a great candidate, the chosen section for the wing spars has been D from Figure 4.

#### Materials choice

After having studied the main materials used in aircraft industry and analyzing their properties (see Structures Attachment, section 2.2.2), the materials chosen for the wing structure are the following. The spars are made out of Aluminium alloy (7075 - T651) and Titanium alloy (Ti - 6Al - 4V), being the latter used only in the initial section of the spars (from 0 to 4.33 m); the ribs are made from Aluminium alloy (7075 - T651) and

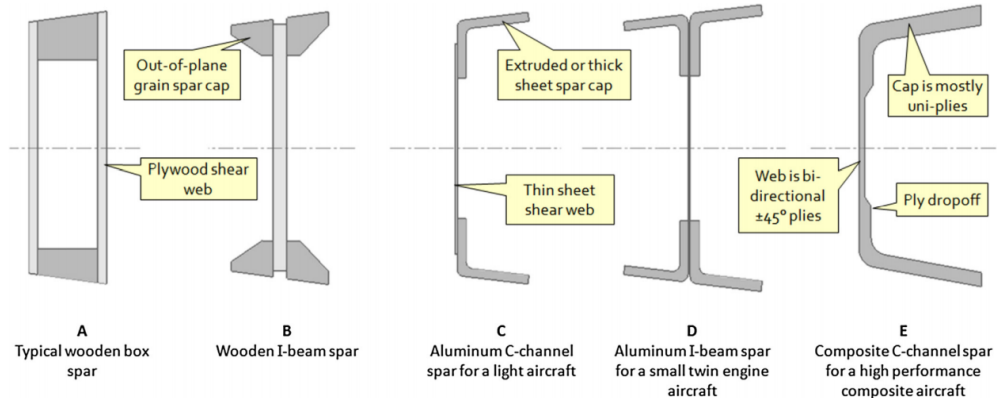


Figure 4: Different spar sections used depending on the aircraft. Source: [17].

Aramid aluminum laminate (ARALL) composite is used for the skin. The material selection is based on the study in Structures Attachment section 2.3.3. It is observed that they show a proper performance regarding the deflection and safety factor.

## 6.2 Tail system decisions

### 6.2.1 Configuration

Aerodynamics and structural standpoints and factors have been taken into account for selecting an appropriate configuration for the empennage. Some of the commonly used tails are considered, which are those mentioned in Figure 5. Both structural and aerodynamic features of each tail configuration are explained in detail in Structures Attachment, section 2.5.2.



Figure 5: Tail configuration alternatives (T-tail, conventional and cruciform). Source: [16].

It is evident that the conventional tail is the most structurally suitable due to its high stiffness and low weight. However, a general aircraft context has to be considered.

Because of the high wing configuration and after looking at some examples of existing planes (mainly cargo ones, that are the ones that commonly use the high-wing configuration), it has been decided that a T-tail disposition (Figure 6) is the most reasonable one for the following main factors:

- Less interference with machinery and cargo when loading the plane from the rear door.

- Avoiding the interference and turbulence of the trail and downwash generated by the high-wing on the horizontal stabilizer.
- Accounts for a smaller horizontal stabilizer that reduces skin drag and produces less vibration or buffet, thus providing a greater efficiency.

It is true that this configuration is considerably demanding in terms of structural loads, but a proper aerodynamic performance and efficient cargo loading must be assured.

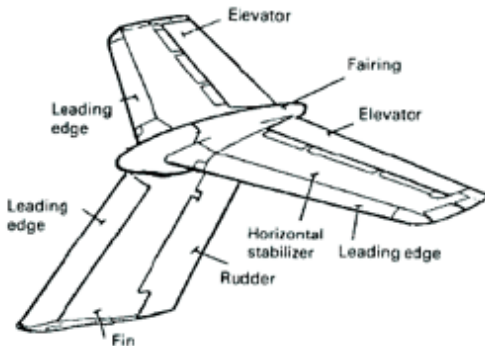


Figure 6: T-Tail configuration scheme. Source: [18].

### 6.2.2 Materials choice

After having studied the main materials used in aircraft industry and analyzing their properties (see Structures Attachment, section 2.2.2), the materials chosen for the tail structure are the following. The spars and ribs made out of Aluminium alloy and ARALL composite is used for the skin. The material selection is based on their properties, they show a proper performance regarding the deflection and safety factor.

## 6.3 Fuselage system decisions

To start with, there are some general requirements that need to be fulfilled as part of the aim of the project. Those consist in the aircraft being able to transport 50 or more passengers and its evacuation taking less than 90 seconds, making sure emergency doors are placed in order to make it possible.

### 6.3.1 Fuselage shape

In the first instance, the fuselage overall shape needs to be determined. Hence, the different options regarding this aspect are the following ones: frustum-shaped fuselage, pressure tube fuselage and tadpole fuselage. If desired, see Structures Attachment, section 2.4.2 for a detailed pros/cons comparison.

Finally, after analysing and studying current models and balancing the cons and pros, a tube fuselage is chosen due to its higher passenger and cargo capacity and its versatility.

### 6.3.2 Section shape

Secondly, the shape of its section is chosen. There are three main section configurations: rectangular shaped, elliptical shaped and circular shaped. Once again, a detailed pros/cons comparison is proposed in Structures Attachment, section 2.4.4.

An elliptical-shaped fuselage is chosen due to its equilibrium between pressurization support, which is a need for passenger transport, and internal volume, which is required for optimal cargo transport.

### 6.3.3 Materials choice

After having studied the main materials used in aircraft industry and analyzing their properties (see Structures Attachment, section 2.2.2), the materials chosen for the fuselage structure are the following. Frames and longerons are made out of Aluminium alloy (7075 - T651) and ARALL composite is used for the skin. They show proper performance regarding factor of safety and deformation.

### 6.3.4 Fuselage's subsystems decisions

#### 6.3.4.1 Cargo door position

On a Quick-Change aircraft the position of the cargo door will not only affect on the velocity of the cargo loading operations, but also on the switching process between both configurations. The two main placements of cargo doors are on a side of the fuselage and on its rear part, although there is a third possibility which consists on placing the cargo door on the nose of the aircraft. The placement will also be affected and will affect on the tail and wing configuration. In other words, a lateral cargo door usually implies a mid-wing and a conventional tail configurations while rear cargo doors normally use high-wing and T-tail configurations. For a further development of the different options, see Structures Attachment, section 2.4.7.

Finally, a rear cargo door would be implemented as a consequence of its agile and non-difficult loading process. Moreover, taking into account that the aim of the project is to design an aircraft from scratch, the difficulties involved when implementing a rear cargo door in already existent airplanes is no longer a problem.

Furthermore, as explained in following sections, this design is harmonious with the implementation of the selected Quick-Change system.

#### 6.3.4.2 Quick-change system

The design of the Quick-Change passenger/cargo system must take certain aspects into consideration, as minimum conversion times, simplicity, ruggedness, versatility of passenger and cargo loading, and compatibility with present cargo-handling systems. See Structures Attachment, section 2.8.1 for a more accurate explanation of the different possibilities (palletized interior system and folding seats).

Since one of the objectives of this design is to build an aircraft able to be competitive in both cargo and passengers markets, the idea is to guarantee that both operations can be developed reaching optimal values.

Therefore, the freight operation mode just offers conditions of this nature in the case of a palletized interior system, since it takes advantage of the hole cabin space.

Moreover, the compatibility between the cargo and the passengers interior is only guaranteed by the palletized seats system.

So, taking into account all the points mentioned above, the ideal option for this project regarding the Quick-Change nature is to implement a palletized interior system.

## 6.4 Landing gear system decisions

### 6.4.1 Geometry configuration

Some of the common configurations of landing gear must be discussed in order to choose the most suitable one. In this case, the possible layouts [16] are: classic, tricycle and tandem (for a detailed pros/cons comparison, see Structures Attachment, section 2.6.1.1).

Taking into account the aspects of each alternative, the tricycle landing gear is the most suitable layout in terms of stability, beating both classic and tandem options. Obviously, the stability aspect is a critical feature in every aircraft, but specially when using the Quick-Change airplane in cargo mode since its payload can be greater and more demanding. In addition, the tricycle offers a proper performance from a visibility and comfort standpoint, which cannot be achieved with a classic landing gear.

It is worth mentioning that even though the tricycle configuration implies a higher weight and nose structural modifications, it is definitely the best option to be adopted by the QCRA aircraft. In fact, almost all current passenger-cargo airplanes use this landing gear layout.

### 6.4.2 Landing gear's subsystems decisions

#### 6.4.2.1 Mounting

Two different options are available when deciding the landing gear's type of mounting [19]: wing/nacelle-mounted and fuselage-mounted (refer to section 2.6.1.2 of Structures Attachment for a detailed comparison).

On the one hand, the wing/nacelle-mounted landing gear provides high lateral stability, but a complex and heavy retraction system under the wing is required. Besides, the wing is further structurally demanded by the addition of ground loads. This configuration is commonly used among regional turboprop aircraft, such as De Havilland Canada Dash 7 and 8, Fokker 50/60 and Saab 2000.

On the other hand, a fuselage-mounted gear is still stable and does not interfere with the wing structure, thus needing a simpler and lighter retraction system. Both Antonov An-140 and the project's reference, ATR-42, feature this type of mounting.

Due to the advantages presented, the QCRA aircraft will feature a landing gear mounted under the fuselage.

## 6.5 Power plant system decisions

### 6.5.1 Type of engine

Regarding the power plant of regional aircraft the most wide-spread practice is to use turboprop engines rather than turbofan engines. As a consequence, the decision to be taken by the propulsion department is whether or not to implement a turboprop engine. In order to simplify the decision, a comparative study between the two types has been made (see Propulsion Attachment, section 3.1.1).

The final decision has been to use turboprop engines due to the fact that this type of engine has higher efficiency when flying at the speed of regional flights, enhances the initial climb and takeoff performance quite remarkably and is lightweight, so it can provide a better performance during takeoff while maintaining fuel efficiency. Although having slower cruising speed and shorter range than turbofan engines, it is enough to reach the requirements of the plane.

### 6.5.2 Number of engines

With the purpose of selecting the optimum number of engines, it has been displayed some of the advantages and disadvantages of the two types of configurations studied: single-engine and twin-engine (see section 3.1.1 of the Propulsion Attachment).

Finally, the twin-engine configuration was the chosen one. The main reason for the selection is the fact that safety is a major requirement, and with two engines the aircraft can still flight in case of engine failure. Another reason that justifies the selection of two engines is that they provide more power to the aircraft and they allow faster speeds and faster pickup.

### 6.5.3 Positioning of the engines

Commercial aircraft present two types of engine positioning, tail-mounted engines and wing-mounted engines. In order to decide which configuration is the optimal one, it has been studied their pros and cons (see Propulsion Attachment, section 3.1.1).

The final decision has been to select a wing-mounted engines configuration due to the fact that with this configuration it is possible to alter the position of the center of gravity by changing the positions of the engines in the spanwise direction. Another reason for this decision is its simplicity of construction and calculation of forces, and the reduction of the bending moment at the wing root produced due to the lift.

### 6.5.4 Engine selection

To decide which engine best suits the aircraft, a market study has been conducted. The Pratt & Whitney PW100 series all meet the requirements of being turboprop engines and being fuel compatible. They also provide enough power for the aircraft and are used in aircraft of similar characteristics. Three engines of this

series that meet the minimum requirements have been selected and an OWA study will be conducted in order to determine which one will be used in the aircraft. The criteria used to compare each engine is: the maximum continuous power (the highest weight will be for those closest to 1864kW, which was the maximum take-off power calculated), the maximum take-off power (same weight criteria used previously), the dry weight (higher mark for the lowest weight) and antiquity (this will be used as a measure of engine efficiency, the highest mark will be for the most recent engine). A higher weight has been given to the power related criteria, followed by the antiquity (a measure of efficiency) and, lastly, by the dry weight. These parameters can be seen in Table 2 and the OWA is shown in Table 3.

Table 2: Engine candidates. Sources: [20] and [21].

	<b>PW127F</b>	<b>PW127G</b>	<b>PW127N</b>
<b>Turboprop</b>	✓	✓	✓
<b>Biofuel compatible</b>	✓	✓	✓
<b>Maximum continuous power (kW)</b>	1864	2178	1864
<b>Maximum take-off power (kW)</b>	2051	2178	2051
<b>Dry weight (kg)</b>	480.8	484.4	481.7
<b>Antiquity (in years) [year of certification]</b>	23 [1997]	21 [1999]	6 [2014]

Table 3: OWA to select the engine.

<b>Criteria</b>	<b>Weight</b>	<b>PW127F</b>		<b>PW127G</b>		<b>PW127N</b>	
		g	p	gxp	p	gxp	p
<b>Maximum continuous power</b>	7	5	35	1	7	5	35
<b>Maximum take-off power</b>	8	5	40	1	8	5	40
<b>Dry weight</b>	4	5	20	1	4	4	16
<b>Antiquity</b>	6	1	6	1.5	9	5	30
<b>SUM (gxp)</b>	25		101		28		121
<b>OWA</b>			<b>0.81</b>		<b>0.75</b>		<b>0.97</b>

Finally, the engine selected is the PW127N, which obtained the highest mark, followed by the PW127F. The PW127N is one of latest models of this series and is currently used in the ATR-42 aircraft.

## 7 Development and design of the chosen solution

### 7.1 Aerodynamics

#### 7.1.1 Weights estimation for design point selection

In order to select design point in matching plot that will determinate aircraft reference wing surface (and required aircraft's engine power), an estimation on aircraft's MTOW need to be performed. Furthermore, for the performance estimation and certification purposes, rest of aircraft's main weights need to be estimated. Thus, in the present section certification weights that need to be approved in both EASA and FAA Type Certificate are presented. Please refer to Aerodynamic Attachment, section 1.1 for extended weights estimation procedure. Notice that the obtained results have been obtained by a trade-off study so that aircraft's weight configuration can satisfy project's requirements (maximum range longer than 1500 km in the design conditions and maximum take-off weight field length of 1100 meters with MTOW).

##### Maximum Takeoff Weight (MTOW):

By a general build-up technique purposed in [22], and taking into account weight-range conceptual configuration with reference aircraft values, the following MTOW for the aircraft has been obtained. Take into account that, as said before, this value must be suitable so that the requirements are met, but also allowing the weight configuration to be competitive in the market.

The following Maximum Takeoff Weight (MTOW) for our QCRA has been obtained, which is similar to reference aircraft values presented in Aerodynamics Attachment section 1.1.1:

$$MTOW_{QCRA} = 18800 \text{ kg}$$

##### Maximum Payload Weight (MPL):

When range allows to do so, commercial airlines will always try to fly as close to the MPL configuration as possible, as it will allow them to obtain the highest operational revenues. Thus, it is crucial that this value is obtained correctly and according to reference aircraft values so that our project is competitive. By means of methodology purposed in [16], estimate average weight values for passengers and baggage extracted from EASA's survey [23], both reference cargo goods and baggage densities purposed in [22], and available cargo volume when flying in passengers configuration that is obtained from reference aircraft and structures department general arrangement, the following MPL values has been obtained:

$$MPL_{QCRA} = 4956 \text{ kg}$$

### Operational Empty Weight (OEW):

Regarding the OEW, references and authors purpose different methodologies to asses an estimate value for the configuration. As seen in the Aerodynamic Attachment, section 1.1.5, a full comparison between all expressions has been performed with reference aircraft values, in order to determinate which presents the least error and will allow us to obtain a more accurate and representative estimation. Following table sums up the results, and it is possible to see why expression in [22] has been used:

Table 4: Reference methodologies for OEW estimation.

OEW	Methodology expression	Error
Torenbeek [16]	$OEW = 0.2 \cdot MTOW + W_{eng} + 500 + 130 \cdot l_f \cdot \frac{a_f + h_f}{2} - 1100$	• Average error of 5.85%
Roskam [24]	$\log(OEW) = 1.0366 \cdot (\log(OEW) - 0.3774)$	• Average error of 7.03%
Reference	$OEW = \alpha_{referenceaircraft} \cdot MTOW$	• Average error of 4.86%
Sadraey [22]	$OEW [lb] = 0.9675 \cdot (-8.2 \cdot 10^{-7} MTOW + 0.65) \cdot MTOW$	• Average error of 4.03%

Thus, the following OEW value has been obtained from MTOW mentioned above in this section, and as seen in Aerodynamics attachments section 1.1.5, it ranges between values for purposed reference aircraft:

$$OEW_{QCRA} = 11200 \text{ kg}$$

### Maximum Fuel Weight (MFW):

As purposed by many references, such [22] and [16], Maximum Fuel Weight is determined by selecting a typical mission flight profile according to the flight type (in our case, commercial configuration will be the most restrictive in terms of fuel weight) and to both EASA and FAA regulations for minimum required reserve and contingency fuel, and by dividing it into its different flight stages to find an specific weight ratio for each one (ratio between initial and final weight for each stage). The following results have been obtained for stages defined in the Aerodynamic Attachment, section 1.1.6:

Table 5: Obtained fuel-fraction values for all mission flight profile stages.

$\frac{W_9}{W_8}$	$\frac{W_8}{W_7}$	$\frac{W_7}{W_6}$	$\frac{W_6}{W_5}$	$\frac{W_5}{W_4}$	$\frac{W_4}{W_3}$	$\frac{W_3}{W_2}$	$\frac{W_2}{W_1}$	$\frac{W_1}{MTOW}$
0.995	0.9646	0.985	0.9715	0.8849	0.989	0.995	0.995	0.99

Then, by determining overall fuel weight ratio as the multiplication of all factors in Table 5, and applying a 5% contingency fuel, the following MFW has been determined:

$$MFW_{QCRA} = 4189 \text{ kg}$$

### 7.1.2 Weight-range diagram

The weight-range diagram illustrates the trade-off relationship between aircraft's weight and its range. It is a graphical way to determine the range under payload, fuel and takeoff weight restrictions. Furthermore, as a main project requirement, it is necessary that from weights configuration determined in the section before a maximum range longer than 1500 km in the design conditions is achieved, which will allow as to be competitive in the market.

The obtained weight-range diagram for our aircraft is presented below, and has been obtained from code that is found in the Aerodynamics Attachment, section 1.1.7, by numerically solving Breguet's equation for range performance:

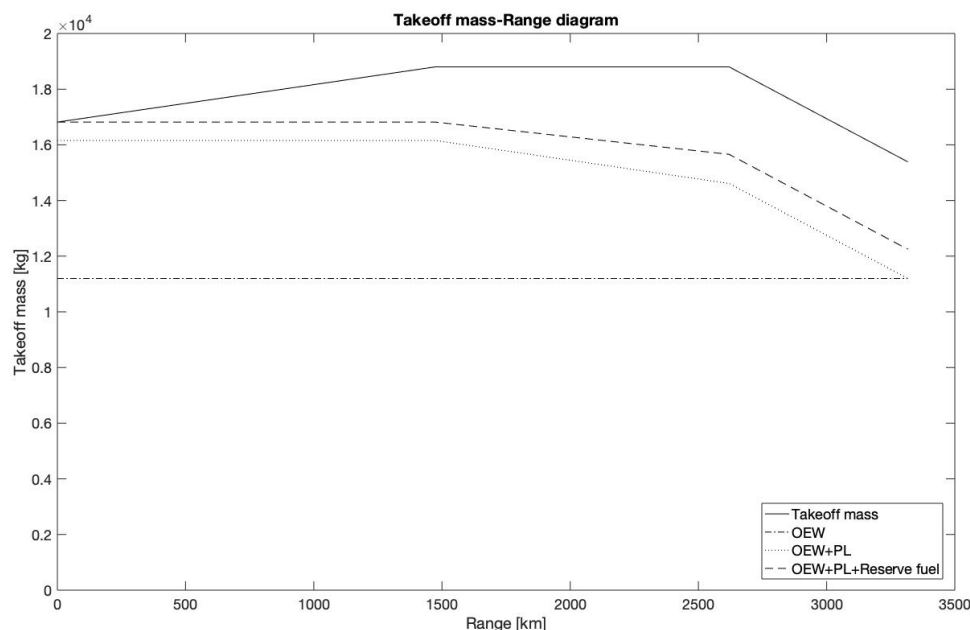


Figure 7: Weight-range diagram for QCRA.

### 7.1.3 Design point selection

Once determined an estimate value for aircraft's Maximum Take-Off Weight (MTOW), performance equations for stall speed, maximum speed, takeoff run, rate of climb and absolute ceiling are treated and solved for our design, in order to obtain the aircraft's matching plot that will allow us to obtain select design point for proceeding with preliminary design.

First, all equations for each performance requirement are derived in form of  $W/P$  as function of  $W/S$  (see Aerodynamics Attachment section 1.2 for the explanation of the equations and the code that derive and treat them). Then, all equations are sketched in one plot, so acceptable design regions can be identified inside

all equations permissible limits. Finally, design point is selected, and its  $W/S$  and  $W/P$  will allow to obtain reference wing surface and required engine power.

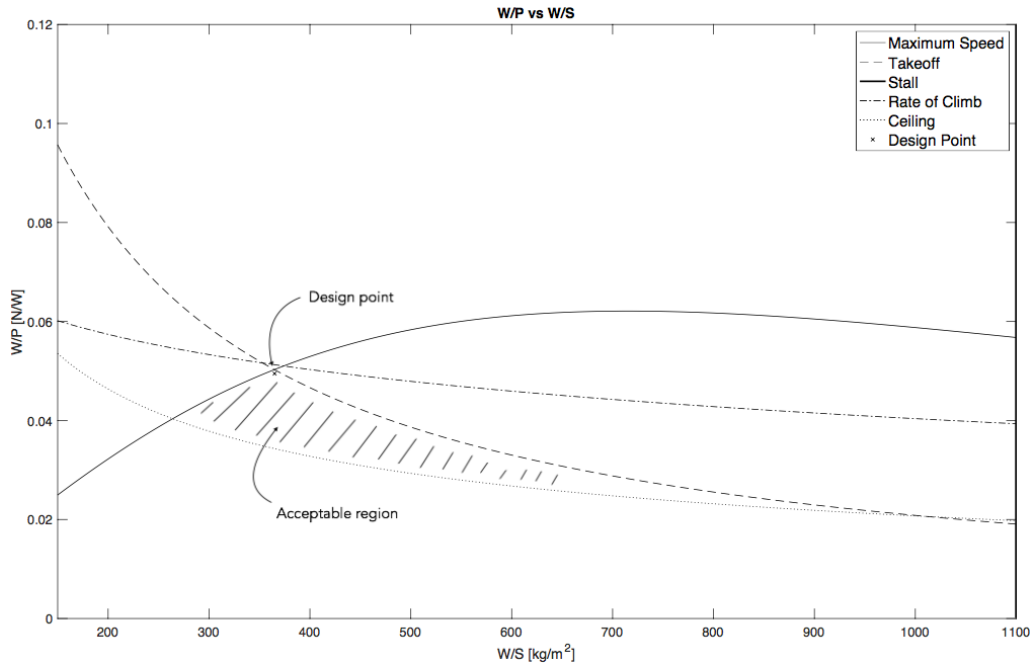


Figure 8: Matching plot, acceptable region and design point.

It is finally obtained that wing reference surface and engine power are to be, for our design:

$$\frac{W}{S} = 365.05 \text{ kg/m}^2 \rightarrow S = MTOW / 365.05 = 51.5 \text{ m}^2$$

$$\frac{W}{P} = 0.0495 \text{ N/W} \rightarrow P = MTOW \cdot g / 0.0495 = 1863 \text{ kW}$$

#### 7.1.4 Airfoil selection

Following the OWA selection method showed in Aerodynamics Attachment section 1.5.6, it has been stated that the best airfoil for the QCRA is the DOUGLAS LA203A. The airfoil parameters are a maximum thickness of 15.7% at 34.3% chord and maximum camber of 5.5% at 46% chord.

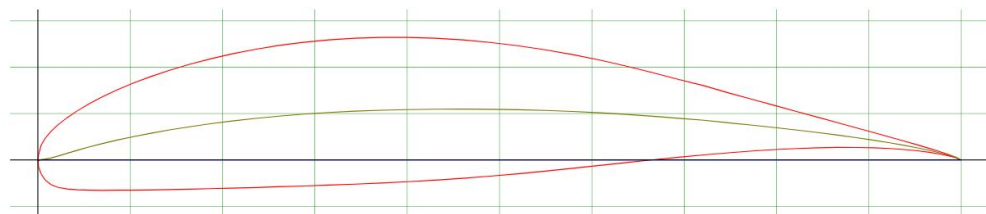


Figure 9: Douglas LA203A airfoil section. Source: [25].

### 7.1.5 Wing planform

Once defined aircraft's wing reference surface and airfoil, planform design process is performed. Based in reference aircraft, a first iteration proposal is studied and analyzed. From there, a refinement procedure by trial and error method from results directly presented by XFLR5 is performed in order to obtain the most adequate performance regarding project's requirements, that are a Short Take-Off and Landing (STOL) configuration and high aerodynamic efficiency for reducing fuel consumption. Up to ten trial and error iterations were made, and only final results are presented, which are to be taken for following design stages. Geometric characteristics are now presented, and a 3D model obtained from XFLR5 and values from Table 6 is shown. Notice that mean geometric chord stands for Mean Geometric Chord (MGC) and mean aerodynamic chord as Mean Aerodynamic Chord (MAC):

Table 6: Geometric characteristics of the wing.

Surface [m <sup>2</sup> ]	Span [m]	AR	MGC [m]	MAC [m]	$\lambda$	Sweep [°]
51.5	23.5	10.72	2.19	2.22	0.677	-0.47

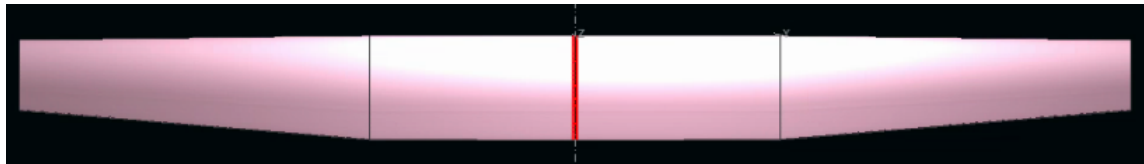


Figure 10: 3D modelling of wing planform obtained from XFLR5.

### 7.1.6 Wing parameters

When already an optimal and desirable wing planform has been selected for our aircraft, it is important to define and study the implementation of different typical wing parameters that will further increase the aerodynamic and structural behaviour of the wing. Take into account that a more detailed study is presented in the Aerodynamic Attachment, section 1.6, and that the scope of the present section is only to present the decisions and results that arose from it.

#### 7.1.6.1 Winglets

Winglets are mainly implemented in the aircraft in order to obtain a partial recover of tip vortex energy that will allow to improve overall efficiency. Nevertheless, while its implementation will allow to reduce aircraft's drag by reducing the so-called *lift due to drag* (or induced drag) because of an span extension, both increase on *skin drag* and strength and weight of the wing are major constraints for their implementation, that needs to be traded-off. The following chapter will try to design an implement winglets devices to the above presented 3D wing in Figure 10 and study its effectiveness, competitiveness and possible implementation to our design.

## Regulations

Before beginning with the dimensioning and design, a brief regulations study has been carried out, and few requirements or specifications were found in CS-25 regulations. Just, and when significant, CS-25.445 exposes that the aerodynamic influence between auxiliary surfaces (such winglets) and their supporting aerodynamic surfaces must be taken into account for all loading conditions including pitch, roll and yaw maneuvers. Furthermore, as the aircraft is assumed to be subjected to symmetrical vertical and lateral gusts in level flight, gust loads also need to be considered to be limited (they are determined by dynamic analysis on winglets in this case).

## General arrangement validation

[“Conceptual Design and Performance Optimization of a Tip Device for a Regional Turboprop Aircraft”](#) exposes that effects of its implementation to low cruise altitude and short range operating flights are low, and the penalization of weight is higher than drag reduction (reference presents an average of 3.25% vs 1.19% values respectively). Furthermore, and since the decision for its implementation into the design must not only be studied from aerodynamic and structural benefits and constraints, cost per flying hour also needs to be assessed (the longer time to earn back the return of investment or additional expenses such extra weight or maintenance, thus short regional flights are not this case).

Thus, from what has been extracted from specific research paper for turboprop regional aircraft, it is not worthy to retrofit winglets to our design, as it will mainly increase operating and design costs.

## XFLR5 design and validation

Although a first conception is obtained from above mentioned and analyzed research paper, an XFLR5 design is developed by means of reference aircraft data. It has to be said that benchmark has shown that, as mentioned before, none of them use this devices, so values for design have been chosen from bigger aircraft and dimensioned according to the proportional sizing difference. The final 3D result is presented below:

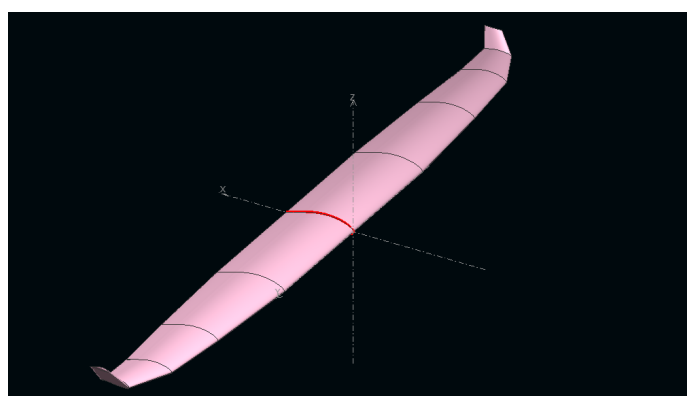


Figure 11: 3D modelling of wing winglets from XFLR5.

By means of this model, an XFLR5 analysis has shown a reduction in  $C_D$  of just 4% (see Figure 12). Thus, according to above mentioned research paper for winglets optimization in regional aircraft, the effect that this device will produce at the wing and its general performance is not worthy to compensate all constraints that have been mentioned, and will not be implemented in the design.

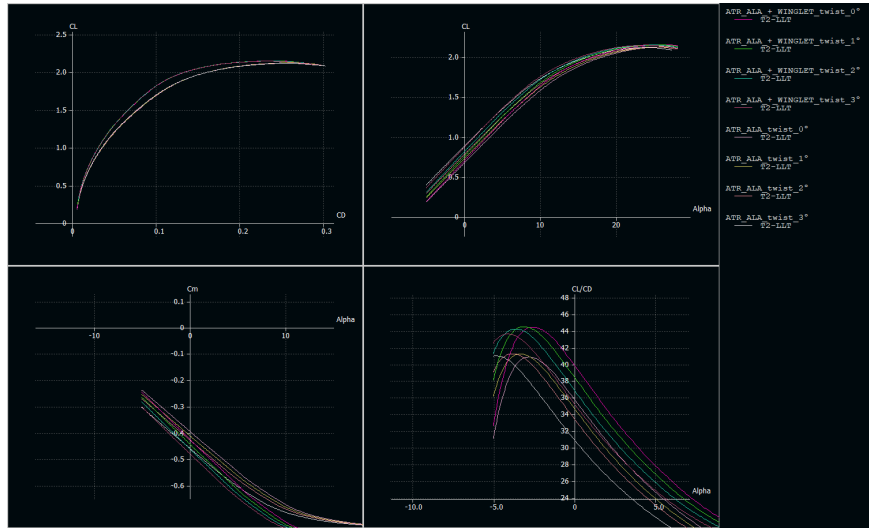


Figure 12: Winglets addition XFLR5 results.

### 7.1.6.2 Wing incidence

The wing incidence  $i_w$  is the angle between the fuselage center line and the wing chord line at its root. In order to determine the angle at which the wing is attached to the fuselage, the wing incidence must satisfy the following design requirements:

- The wing must be able to generate the desired lift coefficient during cruising flight.
- The wing must produce minimum drag during cruising flight.
- The wing incidence angle must be such that the fuselage generates minimum drag during cruising flight (i.e., the fuselage angle of attack must be zero in cruise).

These design requirements naturally match with the wing airfoil angle of attack corresponding to the airfoil ideal lift coefficient. Therefore, as soon as the wing ideal lift coefficient is determined, wing incidence can be easily obtained from the  $C_L = C_L(\alpha)$  graph. This angle is specially important in commercial aviation since it ensures that the fuselage is horizontal with respect to the ground, a factor that greatly affects the comfortableness of the passengers.

Procedure for selecting the appropriate wing incidence for our aircraft is presented in the Aerodynamic Attachment, section 1.6.1, and takes into account the lift coefficient for cruise level, the lift slope  $C_{L\alpha}$  extracted from 3D wing analysis, and the wing twist (which is extracted from following section).

It has been obtained for our design an incidence of  $i_w = 2^\circ$ , that is appropriate according to reference aircraft values presented in Figure 13 from reference turboprop regional aircraft. An additional confirmation of this value will be made after the following parameters are presented.

Aircraft	Type	Wing incidence	Cruising speed (knot)
Fokker 50	Prop-driven transport	$3^\circ 30'$	282
Kawasaki	Prop-driven transport	$0^\circ$	560
ATR 42	Prop-driven transport	$2^\circ$	265
Lockheed P-3C Orion	Prop-driven transport	$3^\circ$	328
Embraer FMB-120 Brasilia	Prop-driven transport	$2^\circ$	272

Figure 13: Wing incidence values for reference turboprop regional aircraft. Source: [22].

### 7.1.6.3 Twist

The benefits of adding twist to a wing are:

1. Avoiding tip stall before root stall.
2. Modification of the lift distribution to get closer to an elliptical one.
3. Reducing the bending moment at the wing root.

Its main disadvantage, however, is the reduction in the total lift for the same AoA of the wing.

After thorough consideration and balance of pros and cons, it has been decided to apply a geometrical twist to the wing design, although it complicates slightly its manufacturing process. By looking into similar types of aircraft, we have seen that the common values for geometrical twist lie between  $-2$  and  $-3^\circ$ . The values are negative because the tip has a lower incidence angle than the root.

Using the program XFLR5, we have applied values of sweep from  $0$  to  $-4^\circ$ , with intervals of  $-1^\circ$ , to study how it affects the wing performance. Figure 14 compare the lift distribution span-wise for the same value of  $C_L$  (the same area below the  $C_L$  curve,  $C_L = 0.767$ ). For this reason, the curves are for different AoA.

Moreover, as stated before, another benefit of adding twist is reducing the bending moment at the tip. Figure 15 shows how this moment decreases as we increase twist.

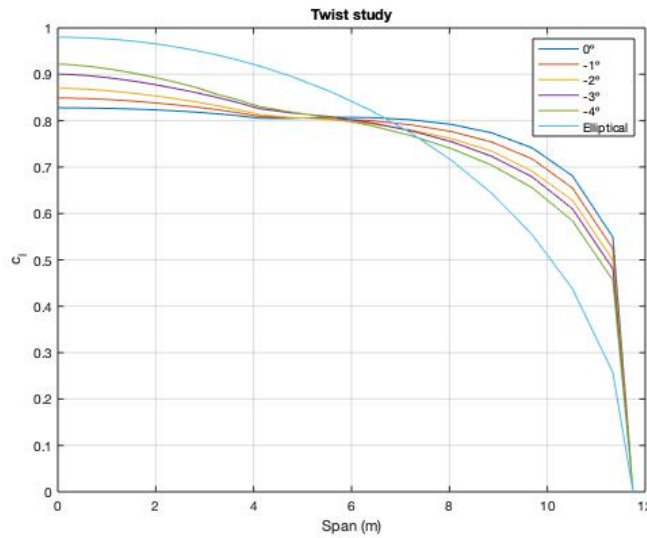
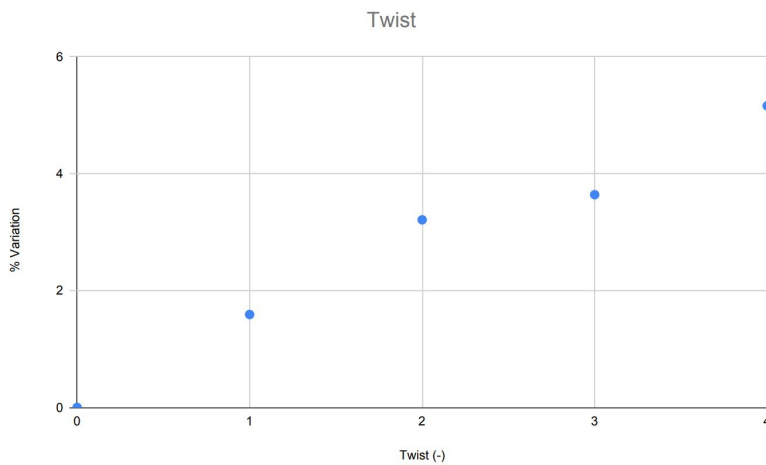
Figure 14:  $c_l$  distribution along the span.

Figure 15: % decrease in bending moment.

The best equilibrium for loss of efficiency (not shown in the graph) and reduction bending moment is found for  $\varepsilon_t = -3^\circ$ . It also resembles more an elliptical distribution than the untwisted wing, fits with the references we have looked into and doesn't complicate excessively the beam design of the wing. For all this reasons, we have settled for it.

#### 7.1.6.4 Dihedral

The dihedral angle of a wing is the angle formed by the chord line plane and the horizontal plane of the aircraft. By convention, when the wing tip is lower than the root, this angle is considered to be negative.

The primary reason for applying a wing dihedral is to improve the lateral stability of the aircraft, which it's

mainly the tendency of an aircraft to return to the original trim level-wing flight condition if disturbed by a gust and rolls around the longitudinal axis.

High mounted wings, which is our case, use to have negative dihedral in order to increase the aircraft's manoeuvrability.

Reference [22] gives an interval of typical values for dihedral angles, depending on the position of the wing relative to the fuselage, the sweep and the cruise speed.

Table 7: Typical dihedral angles.

Wing	Low wing	Mid-wing	High wing	Parasol wing
Unswept	5 to 10	3 to 6	-4 to -10	-5 to -12
Low-subsonic swept	2 to 5	-3 to 3	-3 to -6	-4 to -8
High-subsonic swept	3 to 8	-4 to 2	-5 to -10	-6 to -12

According to this, and with a deeper stability analysis in mind for the future, we have initially settled for a value of  $-4^\circ$ .

#### 7.1.6.5 Leading Edge Sweep Angle

The Leading Edge (LE) sweep angle  $\Lambda_{LE}$  on the leading edge is the angle between a constant percentage chord line along the semi-span of the wing and the lateral axis perpendicular to the aircraft center line (y-axis). In other words, it is the angle between the line of the leading edge and the y-axis of the aircraft. If the angle is grater than zero, with the wing inclined towards the tail, it is called aft sweep otherwise it is called forward sweep.

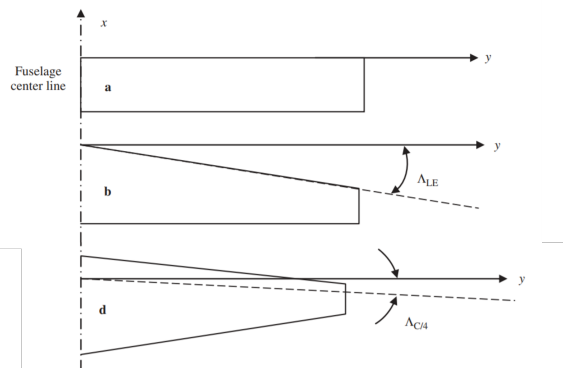


Figure 16: Sweep angle for three types of wings: rectangular, swept wing and tapered wing. Source: [22].

The main goal of a swept wing is to improve the wing aerodynamic features (lift, drag, and pitching moment) at transonic, supersonic, and hypersonic speeds by delaying the compressible effects. Plus it allows the designers to adjust the aircraft center of gravity.

However, since the cruise speed will not be such that compressible effects affect the aerodynamic features of the aircraft, **it is not structurally worthy to introduce a sweep angle to our design** to correct such effects that are unlikely to happen. Moreover, it has to be said that since a tapered wing has been designed, the wing will account with an intrinsic angle of sweep that can aid to the overall efficiency of the wing (see last configuration from Figure 16).

#### 7.1.6.6 Final results

Once the changes mentioned above (Twist =  $-3^\circ$  and Dihedral =  $-4^\circ$ ) have been applied, the final results of the wing are represented in Figure 17.

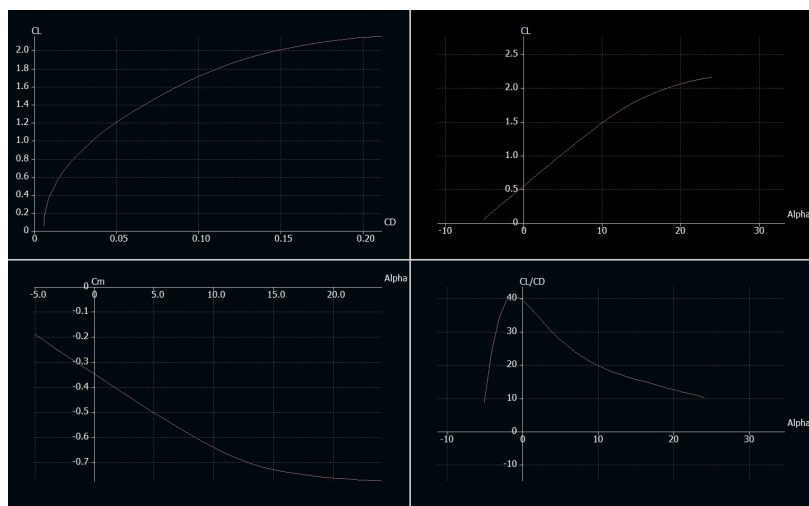


Figure 17: Final wing polars.

In the  $C_L - \alpha$  graph it can be seen that the  $C_{L_{cruise}}$  of 0.7 is achieved with a wing incidence of  $2^\circ$  so the result obtained in section 7.1.6.3 is now additionally confirmed.

#### 7.1.7 High-lift devices

Regarding the high-lift devices implemented in the aircraft, no Leading edge high lift devices will be implemented, as seen in section 6.1.2.3, therefore this section will cover the design of the Trailing edge high lift devices, specifically plain flaps due to their simplicity. It is important to note that the design must take into account the regulations affecting high lift devices, which are explained in section 1.7.1 Regulations, from the Aerodynamics Attachment.

As seen in the Aerodynamics Attachment, section 1.7.2 Trailing-edge devices, the procedure followed to design the trailing-edge devices high lift devices will be analytical, which in this case will be the implementation of the equations (1) for plain flaps extracted from [16].

$$\begin{aligned}\Delta C_{l0} &= C_{l\alpha} \cdot \tau \cdot \eta \cdot \delta_f = C_{l\alpha} \cdot \Delta \alpha_{eq} \\ \Delta C_{L,max} &= 0.92 \cdot \Delta C_{l,max} \cdot \frac{S_{fw}}{S_w} \cdot \cos \Lambda_{1/4}\end{aligned}\quad (1)$$

The chosen geometry of the flaps can be seen in section 1.7.2 Trailing-edge devices from the Aerodynamics Attachment, where the design of the flaps are based on the parameters of the Table 8, this configuration results in the design of the following picture:

Table 8: Parameters of QCRA flap design.

	$C_f/C (\%)$	$b_0$ (m)	$b_f$ (m)	$\delta_{max,TO}$ ( $^{\circ}$ )	$\delta_{max,L}$ ( $^{\circ}$ )
Flap	30	1.50	6.03	20	35

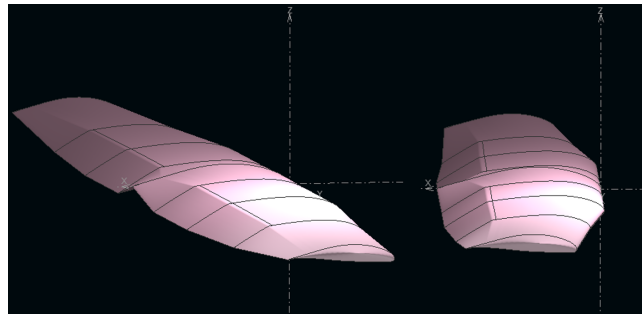


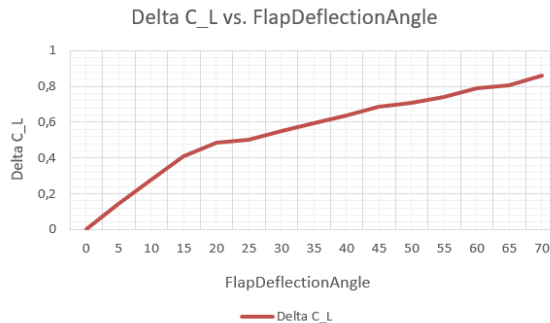
Figure 18: Flaps deflected 20 degrees in XFLR5.

Those parameters can be compared with similar turboprop aircraft, as can be seen in the table below: the chord ratio  $c_f/c$  and flap deflections  $\delta_{max}$  have similar values, and the selected type of HLD device is to be plain for construction process simplification purposes.

Table 9: Table comparing flaps parameters of turboprop aircraft. Source: [22].

Aircraft	Engine	HLD	$c_f/c$	$b_f/b$	$\delta_{max}$ ( $^{\circ}$ )	
Short Skyvan 3	Turboprop	Double slotted	0.3	0.69	TO	Landing
Fokker 27	Turboprop	Single slotted	0.313	0.69	18	45
Lockheed L-100	Turboprop	Fowler	0.3	0.7	16	40
Jetstream 41	Turboprop	Double slotted	0.35	0.55	18	36
QCRA	Turboprop	Plain	0.3	0.39	20	35

The result of equations (1) is a graph depicting the variation of the global lift coefficient  $\delta C_L$  versus the angle deflected of the flap, as can be seen in Figure 19:

Figure 19:  $\delta C_L$  vs. Flap Deflection Degree.

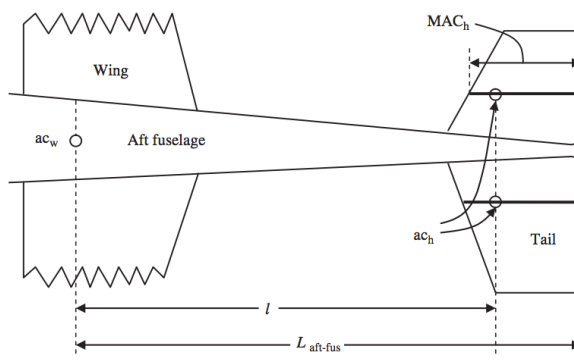
### 7.1.8 Tail and rear fuselage sizing

The aim of this section is to highlight the main decisions taken in the design of the tail and the rear fuselage. In the first place, the type of tail design is selected. Then, the distance between the tail's aerodynamic chord and the aircraft center of gravity, commonly referred as tail arm  $l_t$ , is optimised. With this result, the geometrical aspects of the stabilisers are designed and tested, through an iterative process.

As the design of the tail is a major point in this project, it has been studied in detail in section 6.2. The final result is a T tail design, with the horizontal stabiliser mounted in the top of the vertical one.

#### 7.1.8.1 Optimum tail arm

The optimum tail arm is determined as the tail arm that minimises the aircraft drag yet maximises the effectiveness of the control surfaces. The aircraft drag is assumed to be a function of the aircraft wetted area, so it will be the key parameter to minimise.

Figure 20: Top view of aft position of the aircraft and  $l_t$  characterization. Source [22]

In order to do so, certain approximations on the aircraft's surfaces will have to be made. This includes simplifying the aft portion of the fuselage as simply conical, and describing the stabilisers' wetted area as a function of the tail volume coefficient ( $\bar{V}_H = \frac{l}{C} \frac{S_h}{S}$ ), which is yet to be defined.

$$S_{wet,aft} = S_{wet,aft,f} + S_{wet,aft,h} = \frac{1}{2}\pi \cdot D_f L_{f,aft} + 2 \frac{\bar{C}SV_H}{l} \quad (2)$$

Another assumption to be made is that  $L_{f,aft} \approx l$ , which is commonly used according to [22]. After this changes, the optimum tail arm will be obtained as the value of  $l$  that minimises equation (2).

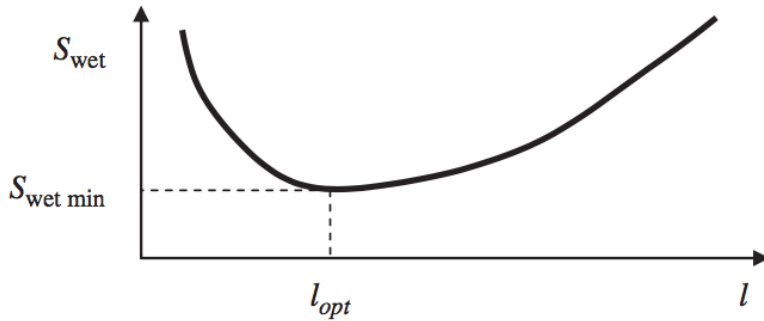


Figure 21: Variation of wetted area with respect to tail arm. Source: [22].

$$\frac{\partial S_{wet,aft}}{\partial l} = \frac{1}{2}\pi \cdot D_f - 2 \cdot \frac{\bar{C}SV_H}{l^2} = 0 \longrightarrow l = \sqrt{\frac{4\bar{C}SV_H}{\pi D_f}} \quad (3)$$

With the parameters presented in the Aerodynamics Attachment, section 1.8.2, the final result is:

$$l = 14.43 \text{ m}$$

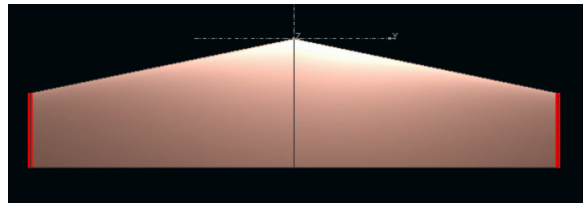
This value is slightly larger than those from similar aircraft, just as the overall length is (that, as will be seen further on, is mainly to the rear cargo compartment door). This increased overall length is the reason behind this larger value.

### 7.1.8.2 Tail sizing

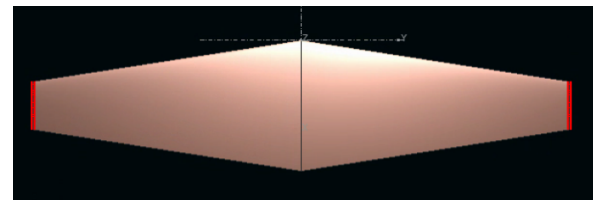
For the design of the horizontal stabilizer, different planforms were considered. They were studied in the XFLR5 program, and the final decision was made based on the aerodynamic and structural performance of each configuration.

For the same span, the reduced tip chord of Figure 22b reduced the bending moment at the root, yet its smaller surface made it lose efficiency. Increasing it in order to match the other options' aerodynamic performance would eliminate its structural advantage. As for the other options, wing sweep would slightly increase the tail arm but also would increase the torsional moment at the root. Also, the spar placement would be more complicated. For this reasons, the option selected was Figure 22c.

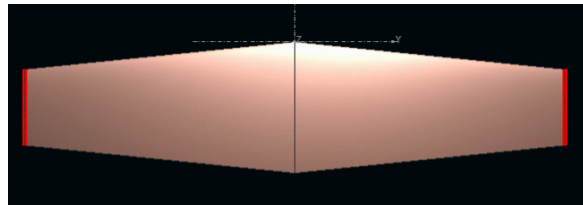
With the planform designed, a longitudinal stability analysis was made. Its objective is to determine the incidence angle of the horizontal stabilizers that guarantees a zero pitch moment coefficient at the cruise angle of attack.



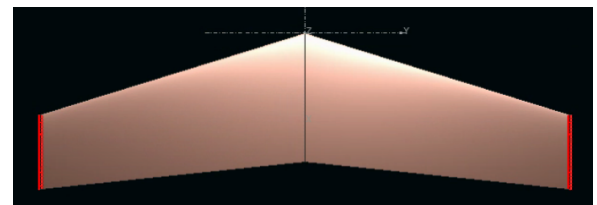
(a) Straight end tail



(b) Low aspect ratio, symmetric



(c) High aspect ratio, symmetric



(d) Swept back

Figure 22: Horizontal tail configurations studied.

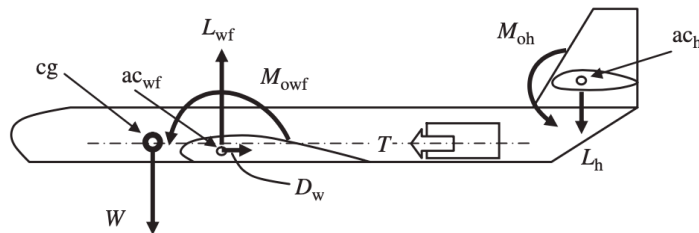


Figure 23: Conventional aircraft in longitudinal trim. Source: [22].

After an iterative process, this result was determined to be:

$$i_h = -2.9^\circ$$

Its associated polar curves are shown in Figure 24 in green. The final design is detailed in Figure 24 and Table 10.

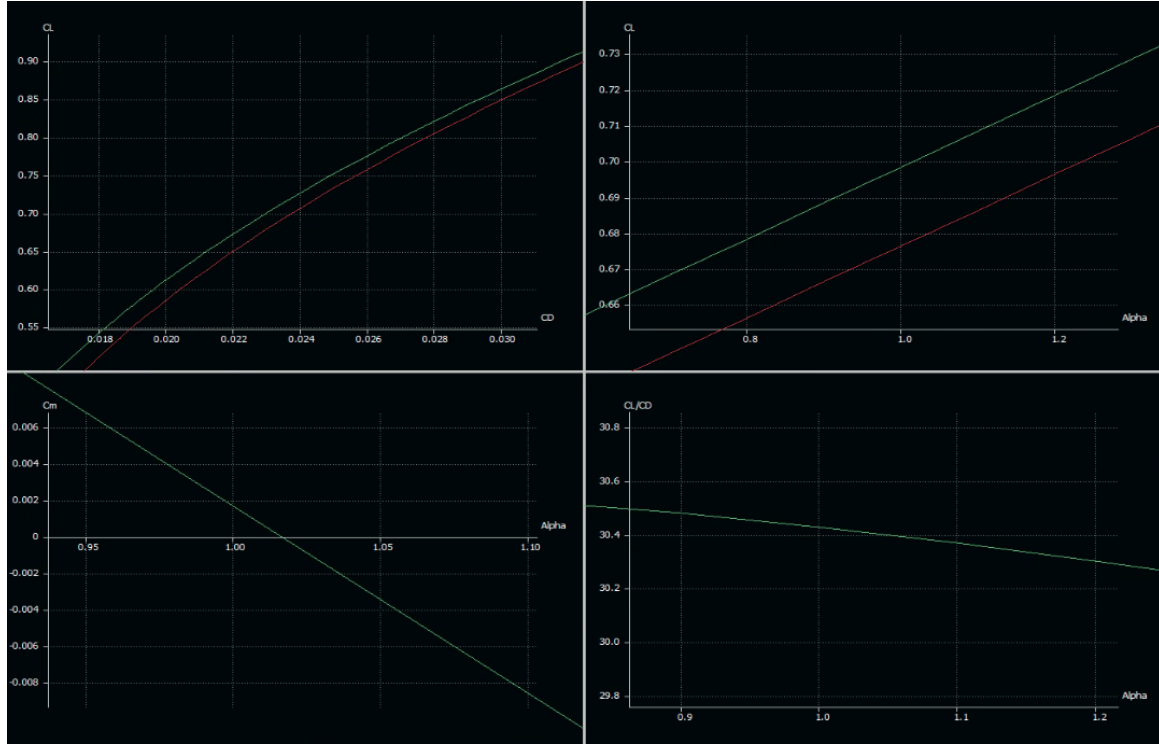


Figure 24: Polar graphs with main wing and horizontal stabilizer in XFLR5.

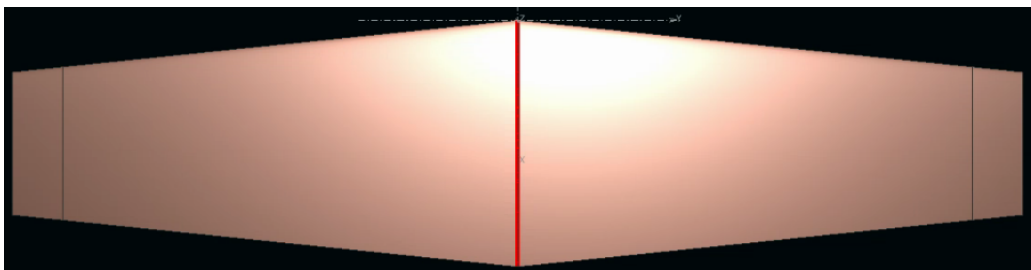


Figure 25: Horizontal stabilizer design in XFLR5

Table 10: Horizontal stabilizer planform dimensions.

Section	y [m]	Chord [m]	Offset [m]	Dihedral [°]	Twist [°]	Airfoil
1	0.00	1.9	0.00	0.0	-2.9	NACA 0009
2	3.5	1.1	0.4			

The vertical tail or fin design was made by looking into similar aircraft. The planform was set and the chords and spans were modified so as to have a surface ratio  $S_v/S = 0.2$  (appropriate value according to [22]) and to be able to fit the horizontal stabiliser. The final result is detailed in Figure 26 and Table 11

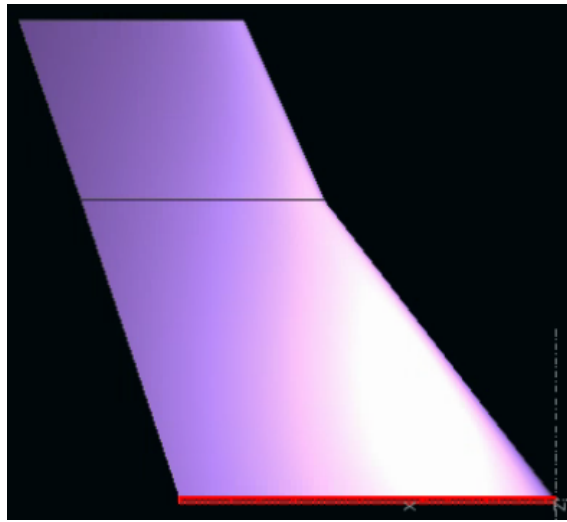


Figure 26: Vertical stabilizer design in XFLR5.

Table 11: Vertical stabilizer planform dimensions

Section	y [m]	Chord [m]	Offset [m]	Dihedral [°]	Twist [°]	Airfoil
1	0.00	3.50	0.00	0,0	0,0	NACA 0012
2	2.50	2.27	2.15			
3	4.00	2.10	290			

### 7.1.9 Longitudinal and lateral-directional control surfaces

#### 7.1.9.1 Elevator

Due to the placement of the horizontal tail, an all-movable approach (c) from Figure 27) was discarded for structural simplicity. A flap-like approach (a)) was taken for the elevator. From typical values from [22], and to offer enough space for the vertical stabiliser and the mechanisms required for the elevator movement, the values of  $C_E/C_h = 0.3$  and  $b_E/b_h = 0.9$  were selected. An arbitrary  $20^\circ$  deflection can be appreciated in Figure 28.

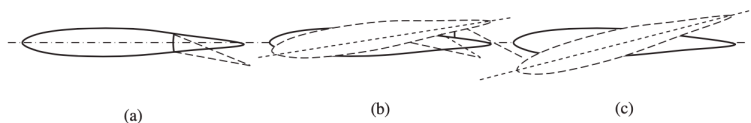


Figure 27: Design possibilities for the longitudinal control system. Source: [22].

#### 7.1.9.2 Rudder

The rudder possibilities were limited to the same configuration taken in the elevator, due to the characteristics

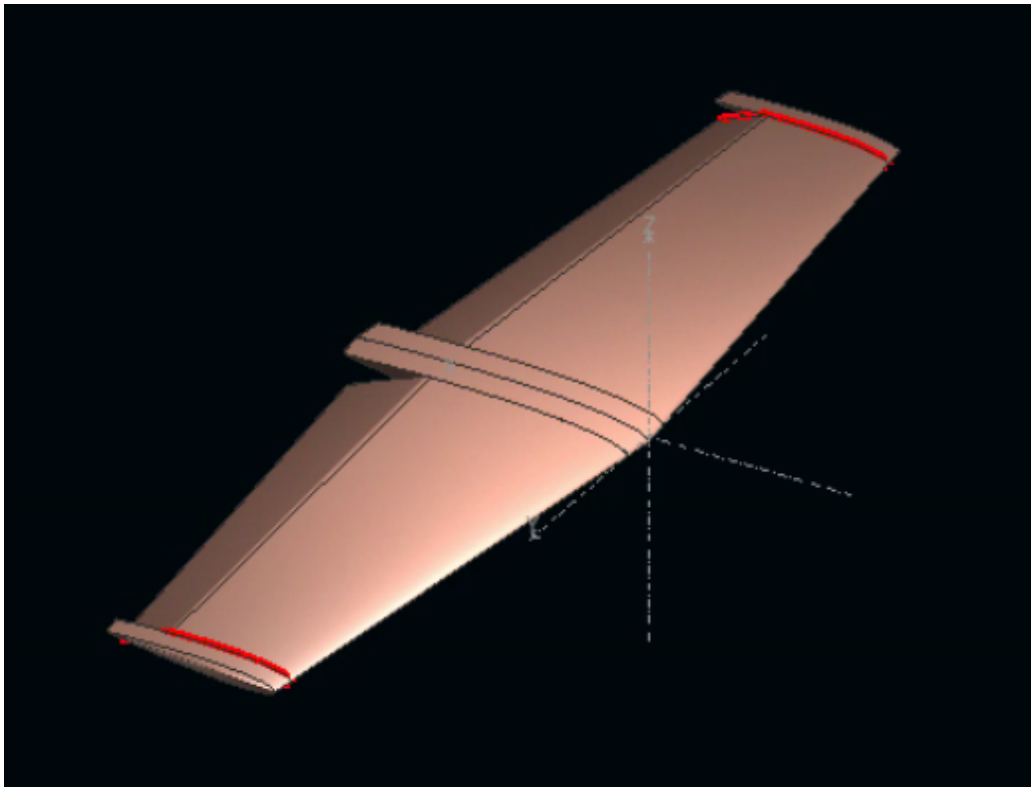


Figure 28:  $+20^\circ$  degree deflection in the elevator.

of our aircraft. Once again, values from [22] were followed for setting  $C_R/C_h = 0.3$ , and the  $b_E/b_h = 0.8125$  was limited by the T tail configuration. Figure 29 shows the configuration of wing and tail, with a certain deflection in the control surfaces to appreciate them.

#### 7.1.9.3 Ailerons

In order to control and maneuver to tilt the entire  $xz$  plane of the aircraft, thus to control its roll, ailerons are incorporated as a control surface. Ailerons are very similar to a trailing edge plain type flap, with the difference that it can be deflected both up and down. Nevertheless, unlike flaps, ailerons are deflected deferentially, meaning that when left wing aileron is in upward position, right must be downward. Furthermore, although some exceptions are accounted, both ailerons are typically used symmetrically, hence their geometries are identical.

The dimensioning of the ailerons has been performed by taking into account that four main parameters need to be found (planform area  $S_a$ , chord/span ratio  $C_a/b_a$ , maximum up and down deflection, and location of inner edge of the aileron along the wingspan  $b_{ai}$ ), and under the consideration for typical maneuverability requirements for regional turboprop aircraft and the following critical design constraints (which are further detailed in the Aerodynamics Attachment, section 1.9.3):

- **Ailerons reversal:** all aircraft, when flying near and at their maximum speed, are subject to important

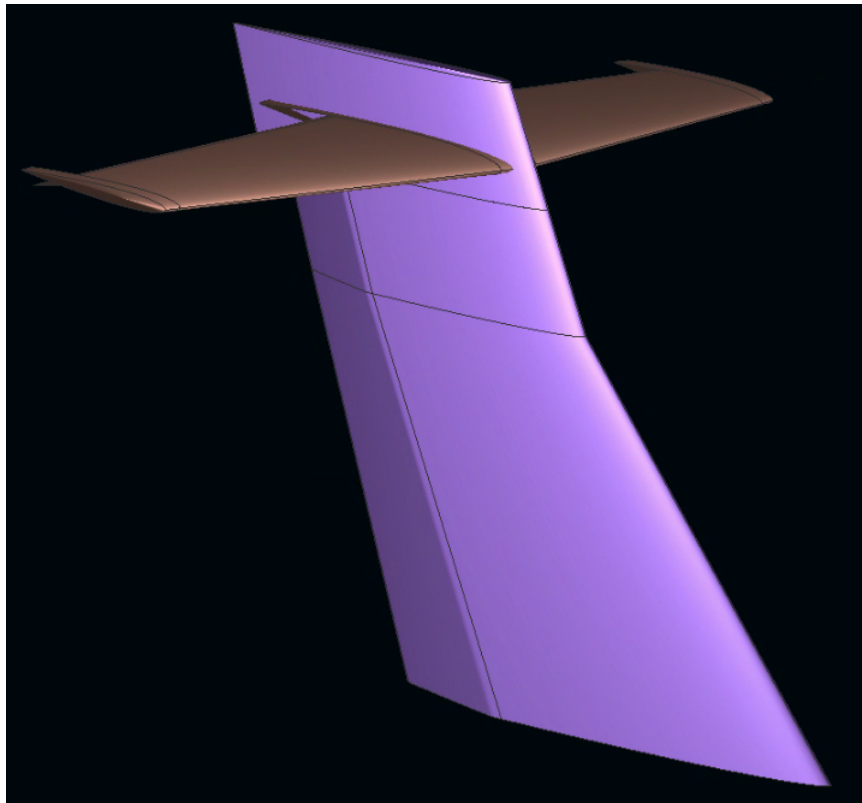


Figure 29:  $+20^\circ$  degree deflection in the elevator and  $+20^\circ$  rudder

aeroelastic phenomena (static and dynamic flexibility) as no real structure is ideally rigid, and light and flexible materials used for wings causes the wing to be unable to maintain its geometry (especially in high-speed cruise flights, which is not our case). Known as ailerons reversal, this effect implies that ailerons lose their effectiveness due to a change in the roll control derivative sign  $C_{l\delta A}$  since a change in the lift direction consequently generates a positive rolling moment.

- **Adverse yaw:** Figure 30 describes the physics of a right turn for an aircraft, with a corresponding appliance of positive aileron deflection (right up, left down), in order to modify the lift distribution such that the one in the left wing is higher, thus generating a positive rolling moment that will roll the aircraft clockwise. Nevertheless, such aileron deflection simultaneously alters differently the induced drag in each wing (as it depends on  $C_L$  as  $C_{D_i} = K \cdot C_L^2$ ). Thus, as left wing lift higher, so will be the induced drag, generating a yawing tendency towards the outside of the turn (adverse yaw).

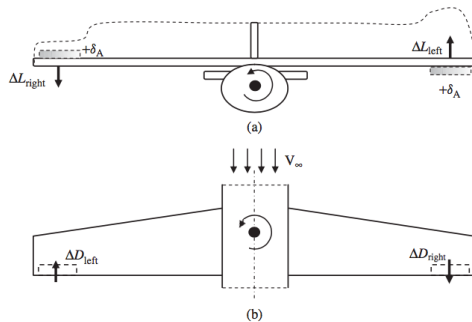


Figure 30: Physics of a right turn for an aircraft and its adverse yaw.

- **Flap:** as wing's trailing edge is home for both two control surfaces ailerons (primary) and high-lift devices such as flaps (secondary), and since they are next to each other, they impose a span limit on one other and a balance between aileron's span  $b_a$  and flap's span  $b_f$  must be found taking into account aircraft's priorities and roll performance requirements. A typical low-speed aircraft uses around 60% of the span for flaps, in order to increase take-off and landing performances and obtaining a lower stall speed for greater safety, thus leaving a free trailing edge span of around 35 to 40%.
- **Wing rear spar:** when designing wing's rear spar, and since the aileron needs a hinge line to rotate about with sufficient freedom to operate, a simplified configuration will advise to consider this rear spar to be the most forward limit for the aileron. Nevertheless, this will mean limiting the aileron chord (but improving wing's structural integrity).
- **Aileron stall:** it is seen by empirical approximations, simulations, and test, that deflection of around 20-25° in ailerons tends to generate flow separation. Thus, a design maximum deflection of 25° is recommended to never be exceed, both in upward and downward configurations.
- **Wing tip:** since a trailing vortex is created at each wing tip because of the spanwise component of airflow along the wing span that creates a tendency for the flow to leak around the wing tips.

The following dimensions are established for our design, according to references [16] and [22] proposed values for regional turboprop aircraft, that have been adapted to our structural constraints, maneuverability requirements and flaps dimensioning.

Chord ratio*	Span Ratio		$\delta_{a_{max}}$ (deg)	
$C_a/C$	$b_i/b/2$	$b_o/b/2$	Up	Down
0.23	0.67	0.94	25	20

Table 12: Ailerons chord and span ratios, and maximum deflection values.

\* Notice that the chord ratio is not fixed, and will vary with the tapered ratio of the wing. The value presented

in Table 12 is the proportion that needs to be satisfied at every span position according to the taper ratio  $\lambda$ . For further detail see the corresponding section in the Technical Sheets.

#### 7.1.9.4 Wing longitudinal position

In order to design an aircraft in such a way that good stability is obtained, it is necessary to arrange the design layout and specially the lifting surfaces so that acceptable forwards and backwards limits of center of gravity are established. With respect to the design of the wing, this should be taken into account when calculating the longitudinal position of the wing relative to the fuselage. Another important fact is that the main landing gear and the wing are approximately located at the center of gravity of the aircraft. In the QCRA the mean aerodynamic chord is approximately at the center of gravity.

As it can be seen in the Aerodynamics Attachment, section 1.9.4 Wing longitudinal position, the first calculations can be based on an average values of the percentage  $\%l_t/l_f$  and  $\%l_{nose-LE}/l_f$  of similar aircraft. Where the tail lever arm is  $l_t$ , the length of the fuselage is  $l_f$  and the distance between the nose of the fuselage and the leading edge of the wing  $l_{nose-LE}$ , as seen in the following figure:

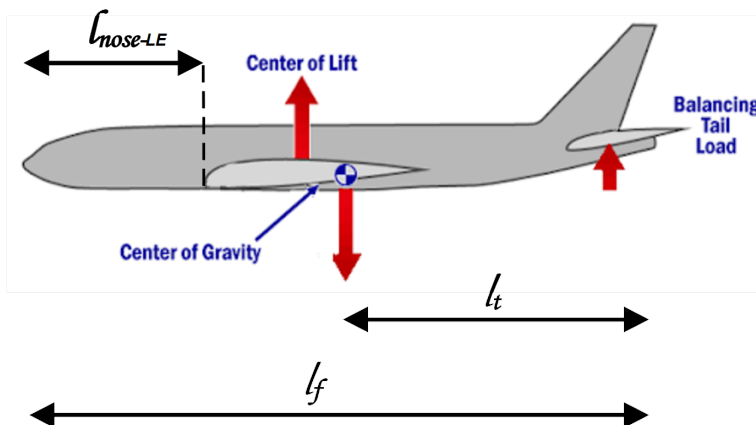


Figure 31: Diagram of lengths.

Then, since the tail arm has already been calculated in section 7.1.8.2a first approximation of the fuselage length and of the wing longitudinal position can be obtained, that will be later modified by the structural department in order to incorporate the rear cargo door. The values are shown in the following table:

Table 13: Longitudinal position values for our model aircraft.

Airplane	Fuselage length $l_f$ (m)	Tail arm $l_t$ (m)	$\% l_t/l_f$	$l_{nose-LE}$ (m)	$\% l_{nose-LE}/l_f$
Model	26.27	14.43	54	10.25	39

### 7.1.10 Fuselage

From the aerodynamic point of view, the fuselage is difficult to theoretically analyse. If it is done by an inviscid model, its resultant lift is equal to zero. However, flow separation near its rear end generates a certain negative resultant lift, located at around 60% to 80% of its length.

Inviscid models are useful to determine the unstable free pitching moment generated by the asymmetric pressure distribution along the fuselage. These results are usually over-predicted and have to be corrected.

Overall, the fuselage interaction with viscous flows is complicated and simulations are often used in order to obtain its aerodynamic characteristics. Further details on the results obtained with these analyses are found in the Aerodynamics Attachments, section 1.10.

In order to properly analyze the fuselage, simulations just like those mentioned before were used. The fuselage has been designed approximately according to the directions of the Structures Department. More precisely, it has been created with the Assisted Body Generator via XFLR5. Then, it has been attached to the aerodynamic surfaces, i.e. wing, horizontal and vertical stabilizers (using the same software program).

The fuselage has been positioned relatively to the wing and the distribution of the body as shown in Figure 32:

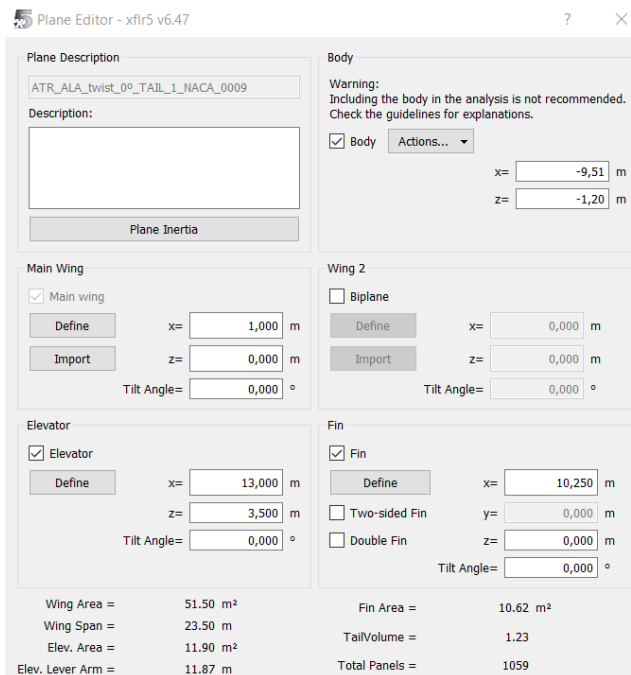


Figure 32: The frontal tip (or nose) of the fuselage and the root leading edge of the wing are separated 10.51 m from each other. This is because the fuselage's nose is located at -9.51m from the global reference system and the leading edge of the wing is positioned at 1m from the same coordinate system.

The XFLR5's Assisted Body-Generator consists of sizing every cross-section profile all along the longitudinal

axis. In this way, the width and height of the fuselage is defined with simple parameters at each position of its axis creating thus the desired shape of the aircraft's body.

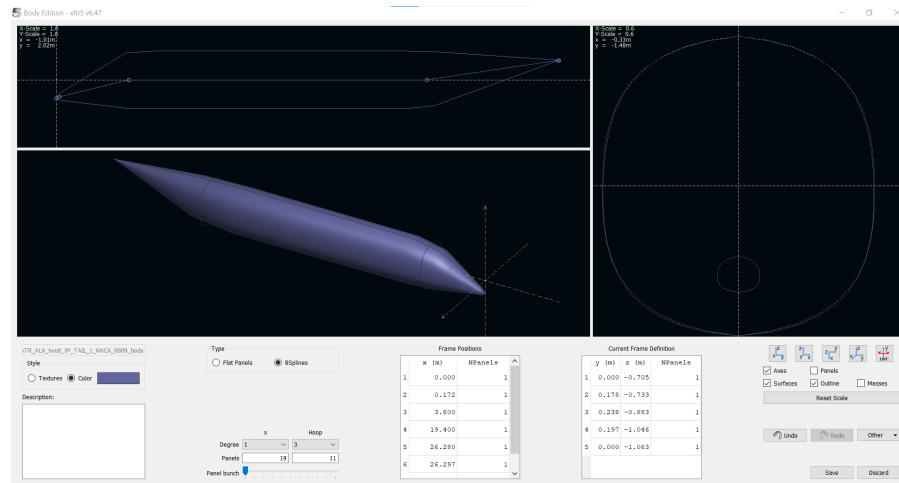


Figure 33: Assisted Body Generator of XFLR5. According to the Structures Department, the fuselage's cross-section is not fully round shaped, but rather an oval shape.

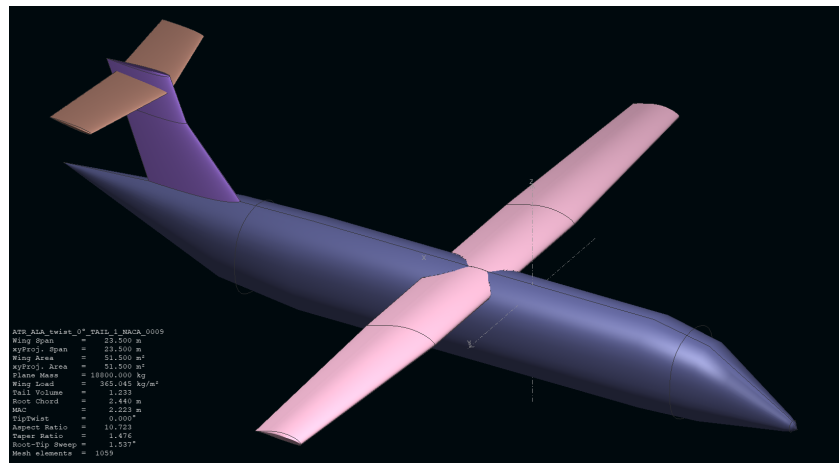


Figure 34: Perspective view of the aircraft.

Once defined the final arrangement of the aircraft, presented in Figure 34, the aerodynamic 3D analysis is done to determine the final CL, CD and polars of the aircraft. Results are presented in both Figures 35 and 36. In the first of them it can be appreciated the distribution of the pressure over the aerodynamic surfaces. Notice that the obtained result by the simulation present a slightly higher pressure coefficient on the upper wing, specially at the root, which shows the limitations of the software that was used, which is also warned by the XFLR5 itself when introducing the fuselage to the analysis, as it can bee seen in top right of Figure 32 (*Warning: including the body in the analysis is not recommended*, as it doesn't take into account the body panels nor the true viscous effects for it proceeds according to a simple aerodynamic theory, the Vortex Line Theory).

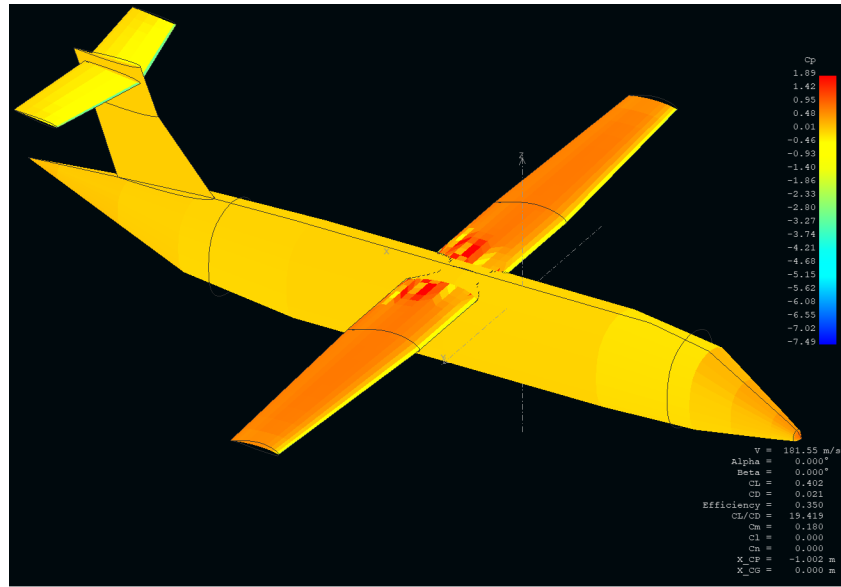


Figure 35: Pressure coefficient distribution on surfaces (note the limitations due to the homogeneous distribution of the pressure coefficient).

Due to the simplicity of the program, it has only been able to analyse an angle-of-attack range of 5 degrees, which is represented in the following polar charts:

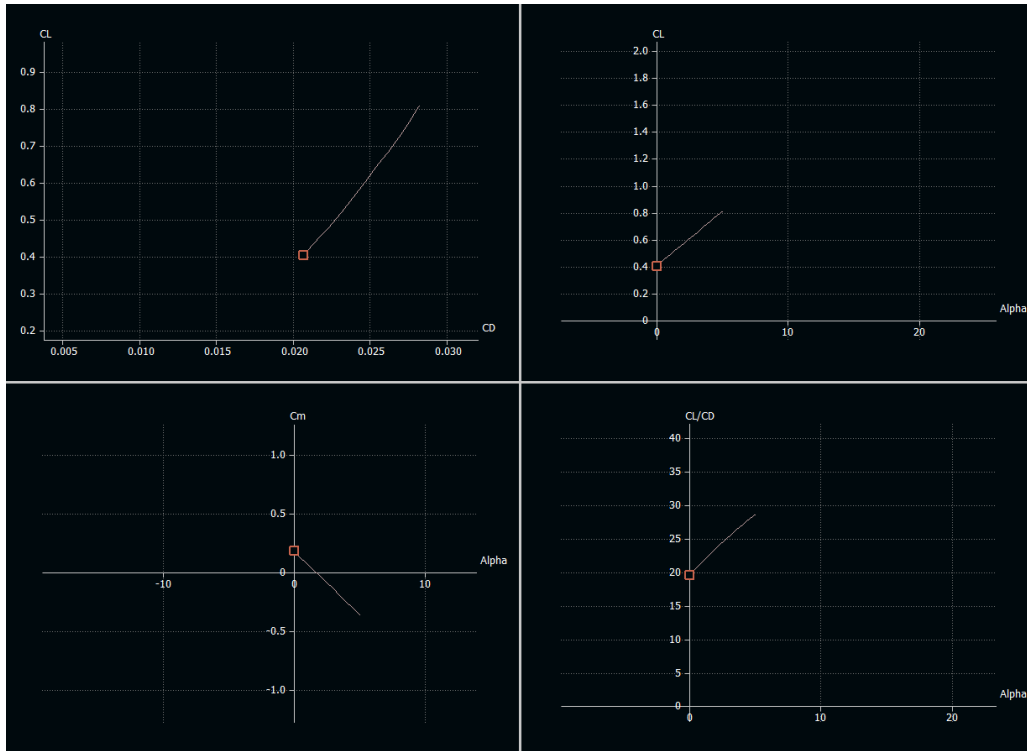


Figure 36: Polars of the VLM1 analysis (Vortex Line Method).

## 7.2 Structures

### 7.2.1 Wing

#### 7.2.1.1 Spar distribution

The aerodynamic wing planform design has determined the need of the Douglas LA203A airfoil, a tip twist of -3 degrees, a flap spanning from 0.87 m to 7.00 m and an aileron from 7.26 to 10.43 m. The external structure of the wing can be seen in Figure 37.



Figure 37: Top view of the final wing model.

In order to fulfill the structural requirements in the most constraining aerodynamic scenario, the wing spars have been divided in three longitudinal sections. This has allowed to fully take advantage of the room inside the wing as the chord decreases. Figure 38 and Table 14 show their different sections and properties. Refer to Drawings Section 4 to see a full detailed sketch of the wing structure.

Table 14: Wing spar properties along the span (provided by Solidworks).

Distance from root (m)	Area ( $m^2$ )	Inertia $I_y (m^4)$
<b>0 - 4,33</b>	$1,5638 \cdot 10^{-2}$	$2,4339 \cdot 10^{-4}$
<b>4,33 - 6,53</b>	$1,3926 \cdot 10^{-2}$	$1,7558 \cdot 10^{-4}$
<b>6,53 - 11,75</b>	$9,5120 \cdot 10^{-3}$	$5,5072 \cdot 10^{-5}$

Regarding the longitudinal positioning inside the wing, it must be taken into account that flaps usually take 25% to 40% chord (the former for simple plain and split flaps and the latter for slotted and Fowler flaps), and 5% to 10% chord should be available between the rear spar and the flap in order to fit the control system elements [16]. Thus, the main spar has been located at 15% of the root chord, whilst the rear spar has been located at 55%.

#### 7.2.1.2 Rib distribution

As explained in Structures Attachment section 2.3.2., the rib spacing has been adapted to the wing section divisions in order to enforce that there is a rib in the location of a section change, which makes these points less critical. The start value has been 61cm, as suggested by [24] for transport aircraft. The final rib thickness has been established at 0.5 cm for all ribs, based on similar models [26]. Regarding the ribs orientation, all of

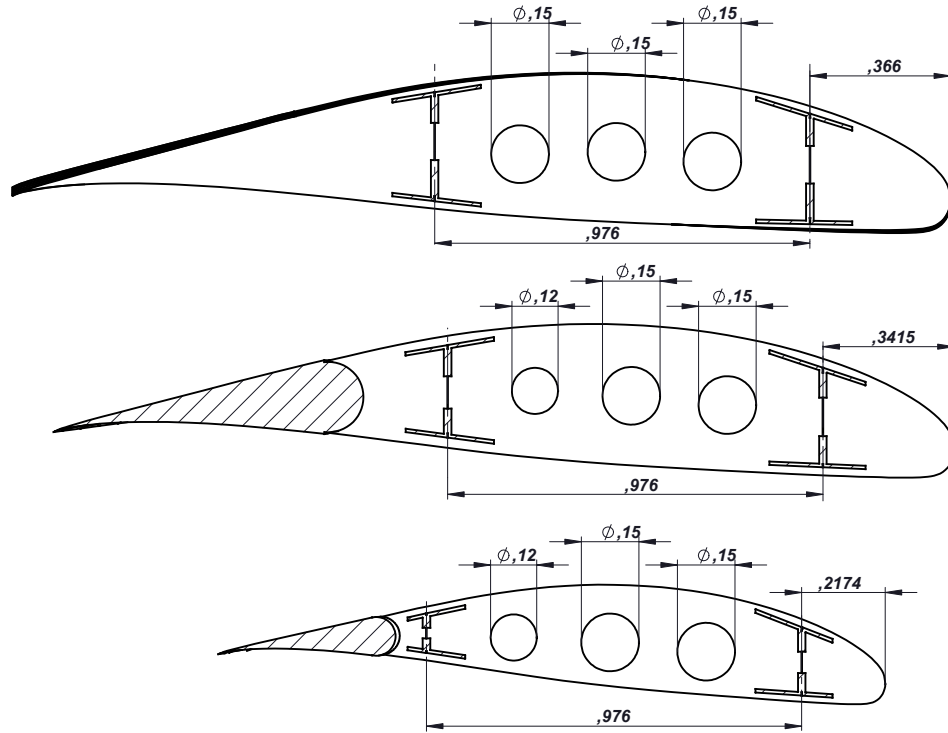


Figure 38: Ribs and spar sections on three different cuts of the wingspan (at 0.90 m, 5.16 m and 10.84 m from the center).

them are parallel to the fuselage as there is no sweepback angle in the wing. The final rib distribution is shown in Figure 39.

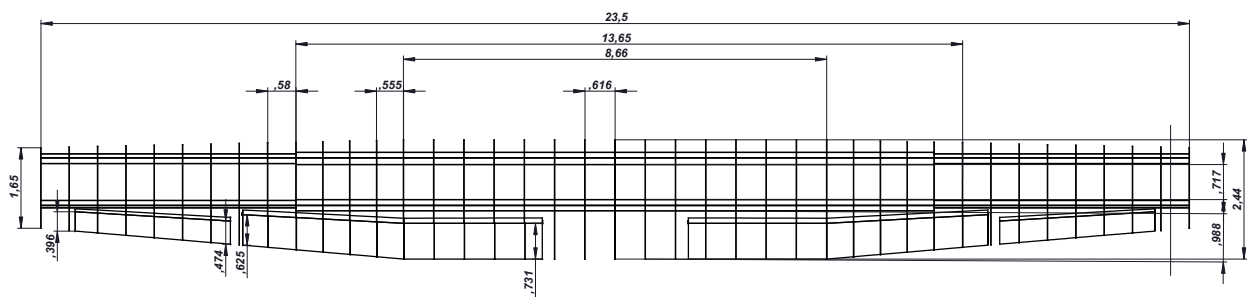


Figure 39: Top view of the internal wing configuration. Note the three different rib spacings.

The final configuration of the wing structure, including ribs, spars, skin, flaps, ailerons is shown in Figure 40.

#### 7.2.1.3 Structural behavior

The resulting wing configuration has been the result of the iterative process developed in the Structures Attach-

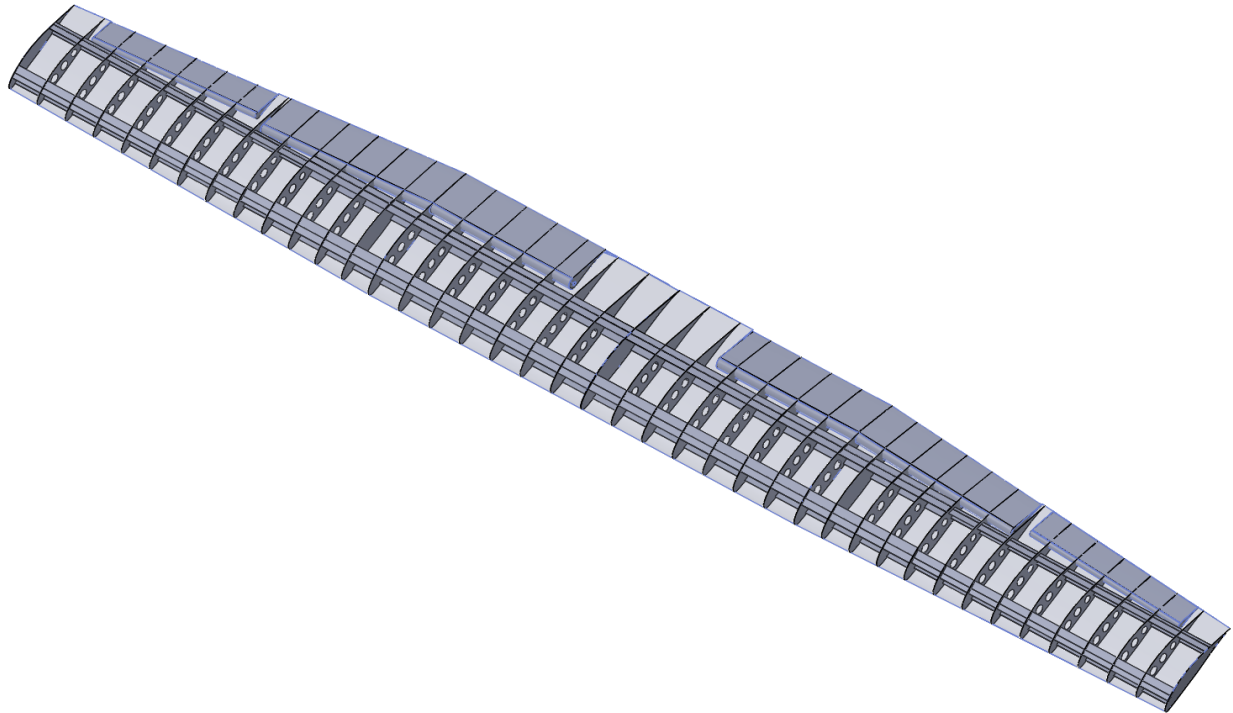


Figure 40: View of the internal wing configuration.

ment, section 2.3.3.1.2. It has consisted of simulating a simplified model of the wing, with the spars as its only elements, with different beam sections until the internal loads result in a factor of safety of 1.5. The simulations have been carried out by a simple one-dimensional finite element code in the first stages of the process and with SolidWorks in the latter.

Figures 41, 42 and 44 show the lift distribution under which the wing is loaded, the predicted deflection and internal loads resulting from the one-dimensional analysis, and the factor of safety plot observed after the accurate simulation, respectively. As it can be seen, some small parts still need to be stiffened, and this will be improved in the joint structure with ribs and skin. The team computers, however, have failed to converge in such complex geometries.

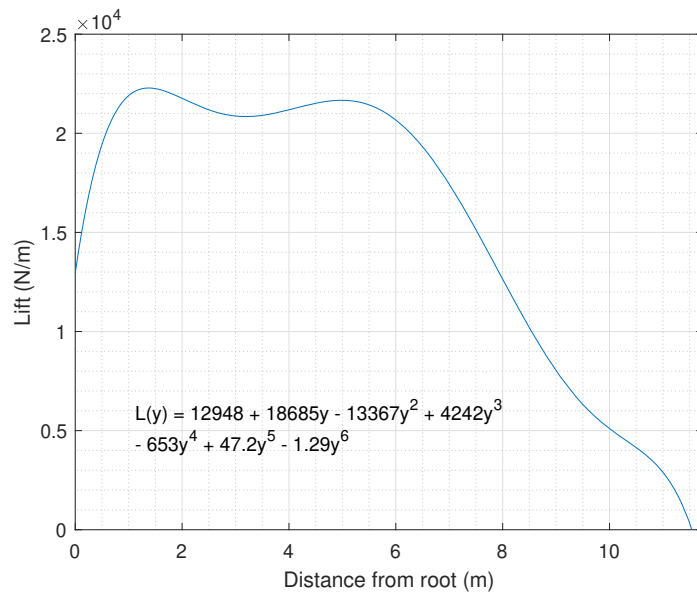


Figure 41: Most demanding lift distribution over the semiwing.

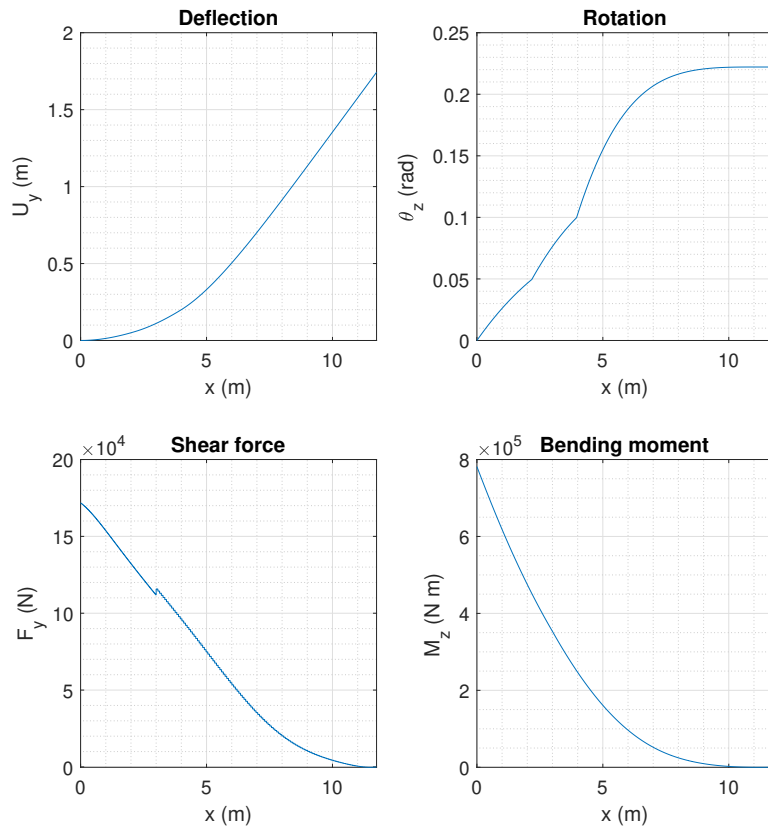


Figure 42: Predicted deflection from one-dimensional analysis.

The displacement obtained by simulating the model is shown in Figure 43. The value obtained in tip deflection is the same as obtained with the one-dimensional analysis.

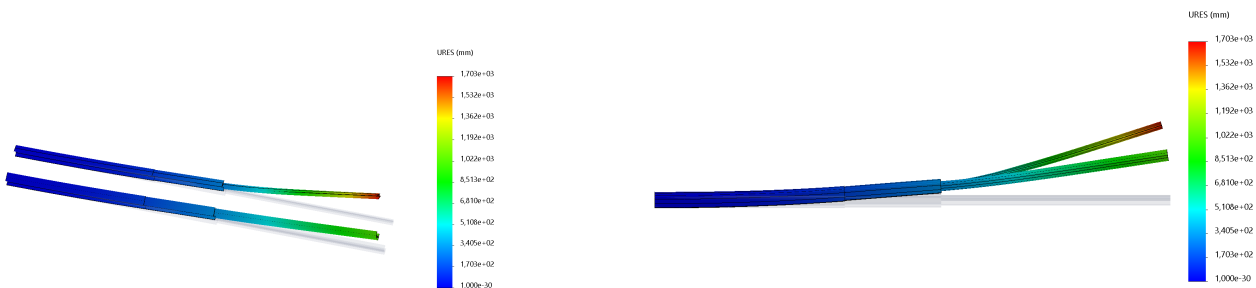


Figure 43: Deflection with combined Titanium-Aluminum configuration.

The factor of safety obtained is observed in Figure 44. Note that there is a small critical area where pink colour indicates a factor of safety smaller than 1.5, yet it is small enough to proceed with the next stage of the design, which consists of checking the performance of the joint structure formed by both the spars and the ribs.

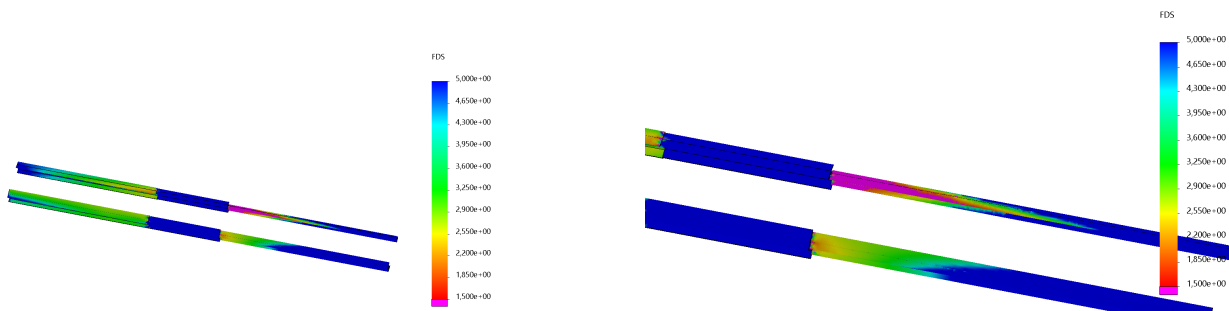


Figure 44: Factor of safety with combined Titanium-Aluminum configuration.

## 7.2.2 Fuselage

### 7.2.2.1 Seating layout

The main interest in terms of the fuselage configuration is to get a low slenderness. Thus, the aim is to design a short and thick fuselage. It is important to consider that passengers do not like three seats in a row, and unless a third aisle is added, the FAR's prohibit more than three seats in a row. Following this reasoning, all seats will be grouped into pairs. By setting this configuration, the fuselage cross section is larger and so, the usable space inside the cabin is more profitable, which is of vital importance in order to develop the operations in the cargo mode of the aircraft.

The seat dimensions chosen will be the ones used in a commuter or commercial aircraft for economy class passenger. Then, the dimensions indicated in the Figure 45 must take the values in Table 15:

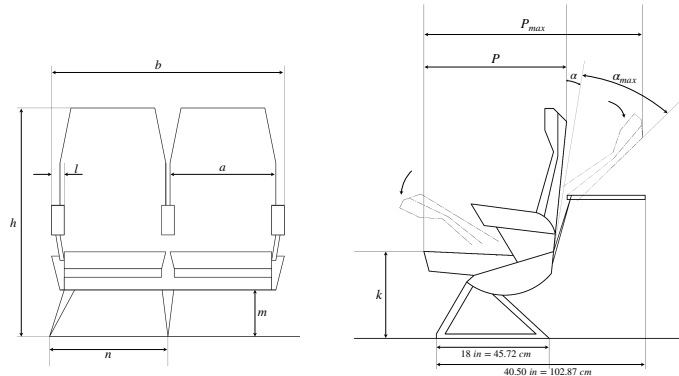


Figure 45: Seat dimensions.

Table 15: Definition of seat dimensions for economy class passengers.

	<i>a</i>	<i>b</i>	<i>l</i>	<i>h</i>	<i>k</i>	<i>m</i>	<i>n</i>	<i>p/p<sub>max</sub></i>	$\alpha/\alpha_{max}$ ( $^{\circ}$ )
(in)	16 - 17	38 - 40	2.0	36 - 41	17.75	8.5	24 - 34	26/35.5	15/38
(cm)	40.64 - 43.18	96.52 - 101.60	5.08	91.44 - 104.14	45.085	21.59	60.96 - 86.36	66.04/90.17	

After some quick calculations following Roskam's book [24], the final chosen dimensions for every row are shown in Figure 46.

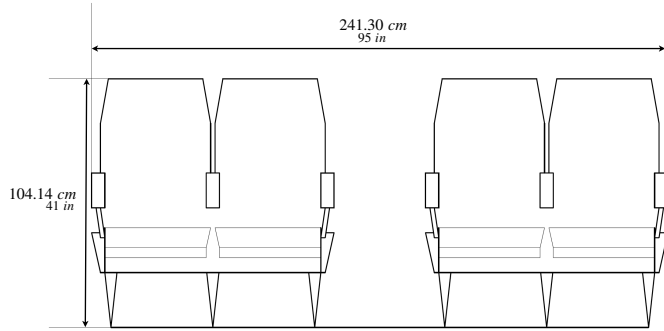


Figure 46: Dimensions for every row.

If the design features an aisle, it should be 76 inches high to allow passengers to move around freely. By taking a value of 41 in (104.14 cm) for the parameter *h* from Table 15 and taking into account the cross section selected above (elliptical) (see Figure 47).

If the desired capacity is 50 passengers, the layout must be of 12-seat-rows versus 4-seats-abreast (2-seats-abreast in each of the both columns) and 1-seat-row versus 2-seats-abreast (in one single column). Moreover, it is important to consider that the crew members must have their assigned seats. Then, the layout would look

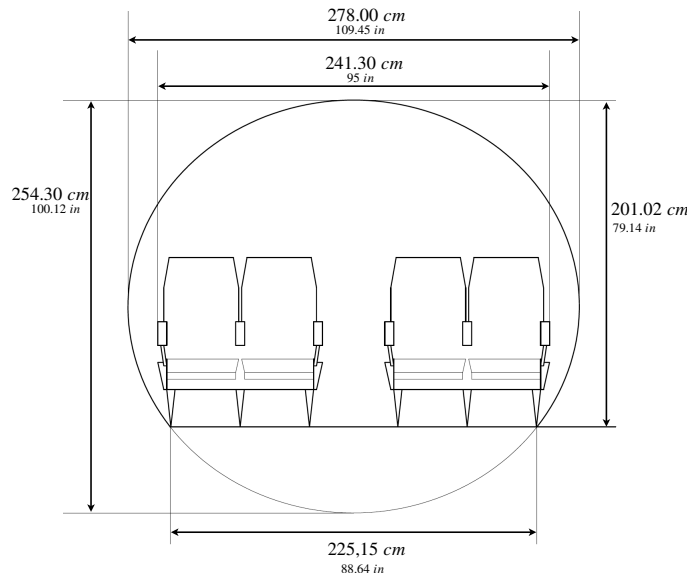


Figure 47: Internal dimensions of the fuselage.

as shown in Figure 48.

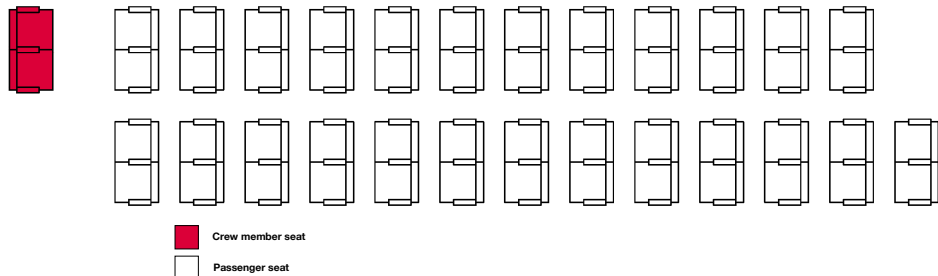


Figure 48: General seating arrangement in passenger operation mode.

Counting the measurements of every seat and adding the measures of the crew members seats, as well as leaving a margin between the passengers and the crew seats, the minimum length increases to 532.5 in (1352.55 cm). The available space that appears as a consequence of the last row of seats, which counts with just two seats-abreast can be used for the implementation of a box office system for the crew.

### 7.2.2.2 Cabin provisions required

As mentioned above, since the aircraft's capacity is equal or higher than 50 passengers, the airplane should have at least one lavatory. It must consist of a sink and a faucet, a counter, mirror, lighting, soap dispensers, amenity racks, and of course the toilet. The lavatory is a module that can be installed anywhere in the aircraft. Figure 49 shows the space claims of a typical aircraft lavatory.

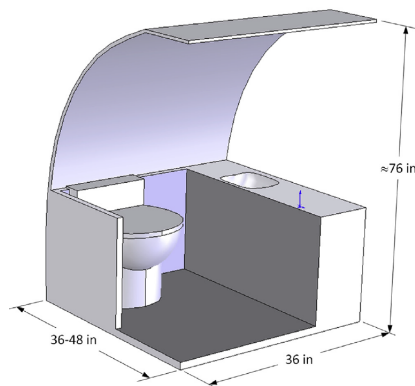


Figure 49: Space claims of a typical aircraft lavatory.

Thus, a module of 36x36 in (91.44x91.44 cm) will be installed next to the crew members sets. By this, the minimum length increases to 568.50 in (14.44 m) (see Figure 50).

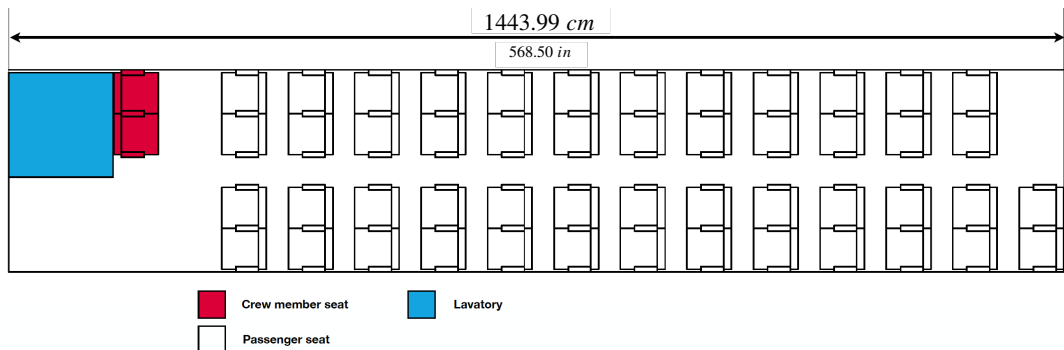


Figure 50: General seating arrangement and lavatory installation.

As the lavatory is a functional module and it is necessary to make some preparations in order to install it, like a centralized waste tank which connects to the toilets using small pipes, it is not a good idea to take it away when changing from the passenger to the cargo configuration.

### 7.2.2.3 Layout of doors

Since the aircraft is carrying less than 80 passengers, one passenger access door is enough, as the installation of any door represents a considerable pressurization leak and, above all, a significant increment in weight. Thus, it is reasonable to have as few doors as possible.

Comfortable sized passenger access doors should be 6x3 ft (182.88x91.44 cm).

The *14 CFR 25.807 - Emergency exits* from FAA states that, for a number of 40 - 50 passengers, the number of required exits on each side of the fuselage is the indicated on the following Table [27]:

Table 16: Number of required exits on each side of the fuselage for 40 - 50 passengers.

Type I	Type II	Type III	Type IV
1	None	None	1

- **Type I:** This type is a floor-level exit with a rectangular opening of not less than 24 inches (60.96 cm) wide by 48 (121.92 cm) inches high, with corner radii not greater than 8 inches (20.32 cm).
- **Type IV:** This type is a rectangular opening of not less than 19 inches (48.26 cm) wide by 26 inches (66.04 cm) high, with corner radii not greater than 6.3 inches (16 cm), located over the wing, with a step-up inside the airplane of not more than 29 inches (73.66 cm) and a step-down outside the airplane of not more than 36 inches (91.44 cm).

Then, the required exit doors on each side of the fuselage for the aircraft we are working in have the following measures (see Figure 51):

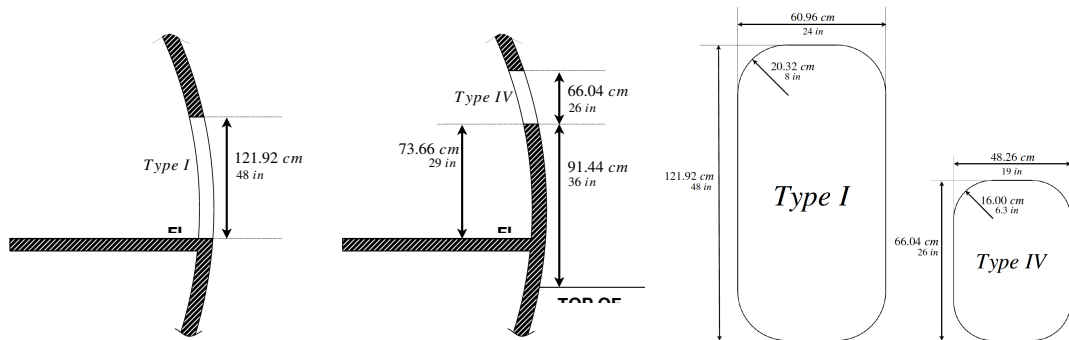


Figure 51: Type I and Type IV doors dimensions.

It is necessary to take into account that all emergency exits must meet the unobstructed access requirement.

- **Type I exits:** 36 in (91.44 cm) of access width
- **Type IV exits:** 18 in (45.72 cm) of access width

Taking into account doors, the minimum length now increases to 611.50 in (15.5321 m). The unobstructed access requirement is reached by taking advantage of the space between the different rows of seats.

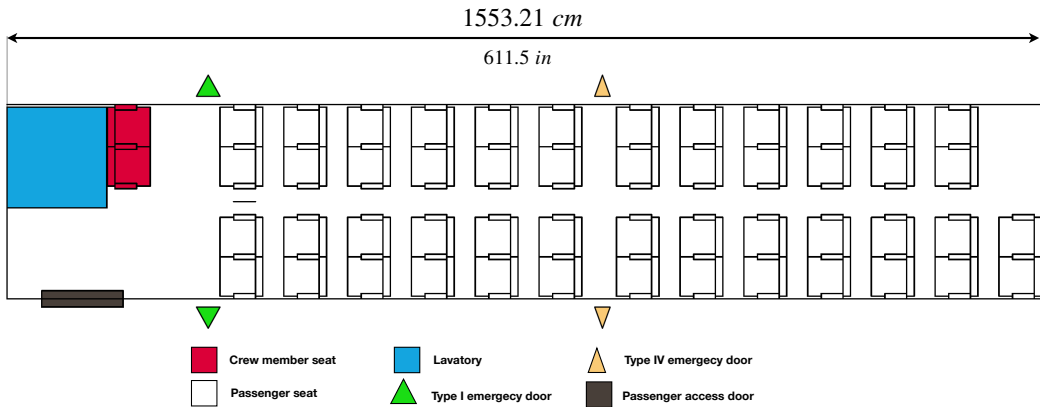


Figure 52: Aircraft's interior layout.

It is necessary to remark that all the Figures representing the aircraft's interior layout (Figures 48, 50 and now 52) are visual schematics used to make the reader understand the distances that are being mentioned. This Figures are not ruled by any scale and they are not a loyal representation of the real design.

#### 7.2.2.4 Design of cockpit layout

Since developing a new cockpit is presented as a particular challenge due to the complexity of the requirements explained above, the best idea for this project is to take an existing cockpit from a similar aircraft. As the objective of this section is to make a first measuring, this method is still valid.

The Fokker F28 Fellowship was a short-haul twin-engine jetliner with a capacity of 65 passengers which presented the cockpit layout shown in Figures 53a and 53b).

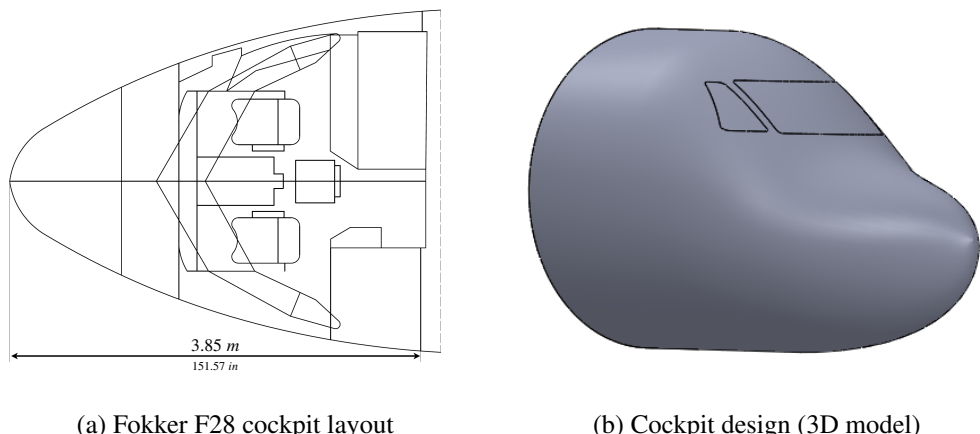


Figure 53: Cockpit design and layout.

In order to simplify the process of measuring, the value of the length of the Quick-Change Regional Aircraft will be the same as the indicated in Figure 53a (3.85 m).

### 7.2.2.5 Structural loads

Once the cabin interior layout is set, it is the moment of adding the appropriate distances to the layout in question to allow for the required structural depth for fuselage frames, bulkheads and skins.

The internal cabin dimensions of the aircraft are the ones in the following Table:

Table 17: Internal cabin dimensions (see Figure 47).

Internal cabin dimensions			
Unit	Length	Max. Width	Max Height
ft	50.96	9.12	6.60
in	611.50	109.35	79.14
m	15.54	2.78	2.01

### 7.2.2.6 Fuselage's frames

Following Roskam's book [24], frame spacings will take a value of 20 in (50.80 cm). As the cross section shape is an elliptical one, the parameter  $d_f$  taken is the major axis of the ellipse ( $d_f = 109.45 \text{ in} = 278.00 \text{ cm}$ ). So, the frame depths take the value of 3.19 in (8.10 cm).

Then, the distribution of the frames for the cabin is the one shown in Figure 54.

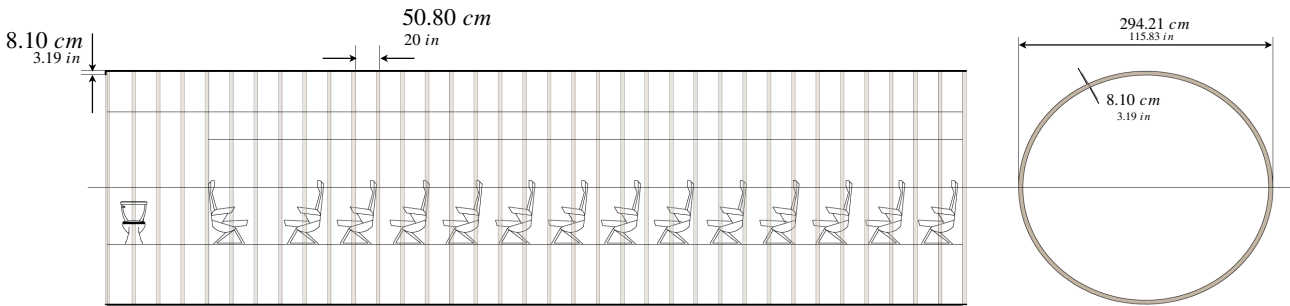


Figure 54: Frame disposition for the cabin.

### 7.2.2.7 Fuselage's longerons

Once again, the distribution of the fuselage's longerons is set according to the data contained in Roskam's book [24]. As the value for the longeron spacings goes from 6 to 12 in, a value of 10 in (25.40 cm) is taken, as shown in Figure 55: So, Figure 56 and Figure 57 show both frames and longerons distribution along the fuselage.

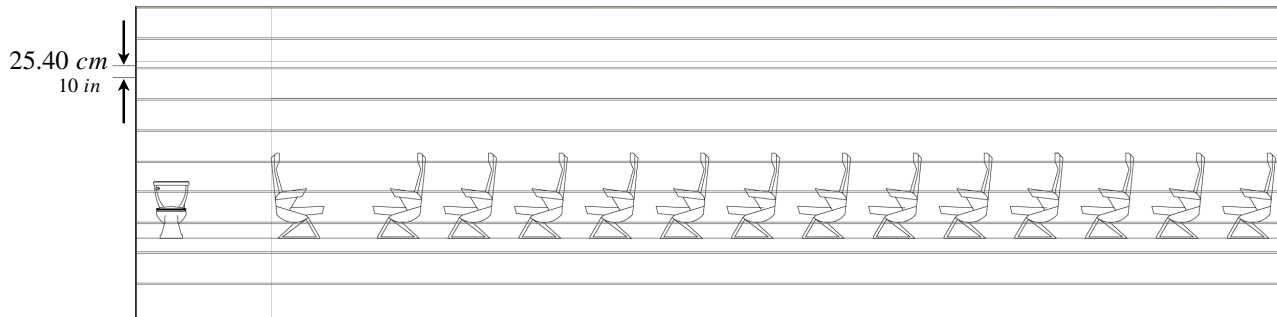


Figure 55: Longeron disposition for the cabin.

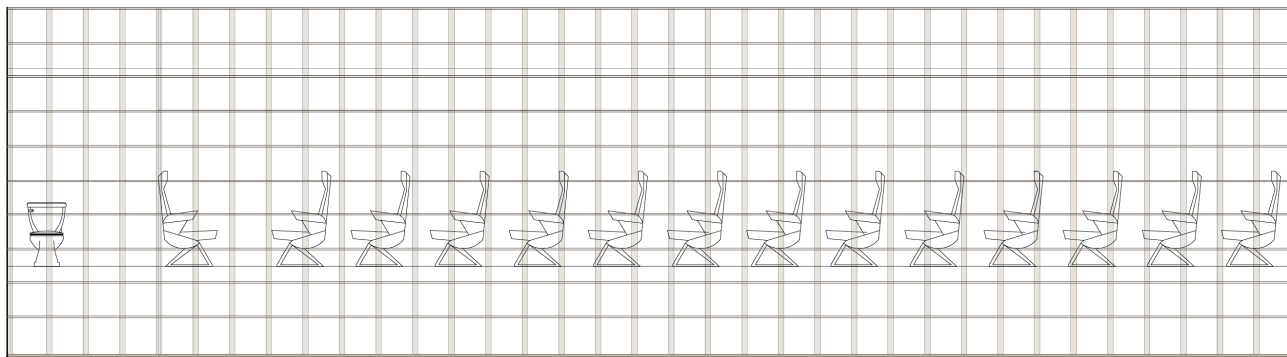


Figure 56: Longeron and frame disposition for the cabin.

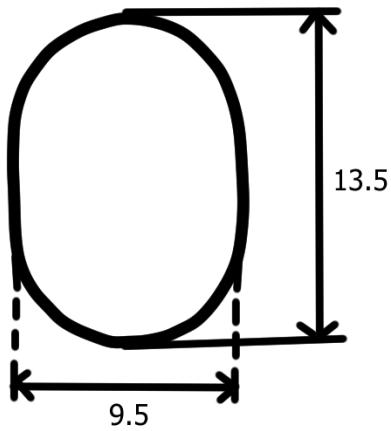


Figure 57: Longeron and frame disposition for the cabin (3D model).

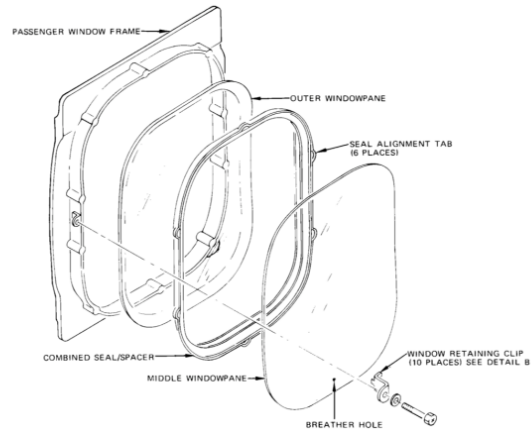
#### 7.2.2.8 Windows layout

After some previous considerations and studying currently existing windows (see Structures Attachment, 2.4.9 section), a 13.5 x 9.5 in (34.29 x 24.13 cm) window like the ones in an Airbus A350 aircraft is chosen. Window measures are represented in Figure 58a. Moreover, a traditional three-pane window structure will be used (see Figure 58b).

Finally, knowing the final size of the windows and taking into account the longeron and frame configuration, it



(a) Final window sizing in inches



(b) Window structure

Figure 58: Window sizing and structure.

is decided that the windows will be placed between frames, at the altitude of passenger's head (see Figure 59).

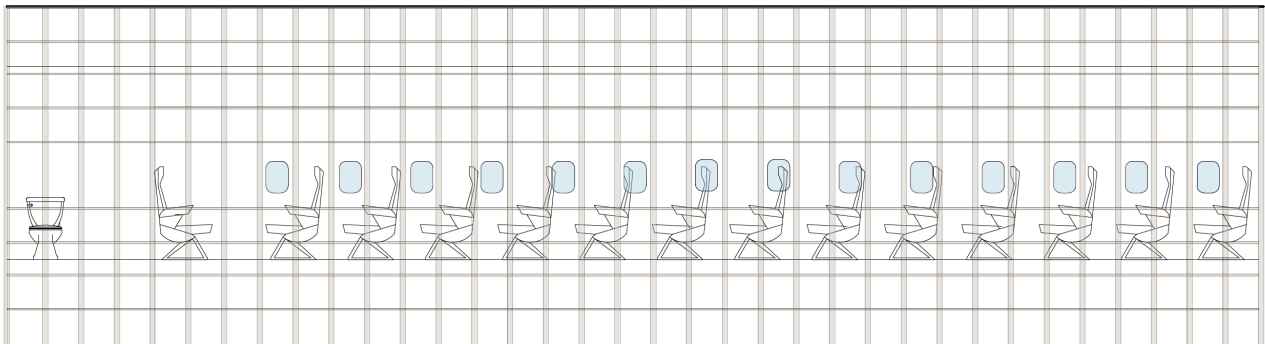


Figure 59: Final window placement.

Notice that one longeron will be removed from the initial configuration. That is not going to cause a problem due to the skin of the plane and the window's frame (specially designed to withstand high tensions) substituting the removed longeron's job.

#### 7.2.2.9 Final design of the entire fuselage

The aim of this section is to get a dimensioned drawing of the entire fuselage, including the cockpit, the cabin and the rear fuselage cone.

The following geometry can be used to estimate the geometric properties of a generic passenger transport aircraft (see Figure 60). Then, the total lenght of the fuselage can be calculated by:

$$L_{fuse} = L_1 + L_2 + L_3, \quad (4)$$

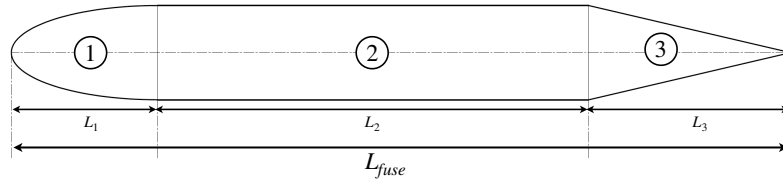


Figure 60: An approximation of a tubular fuselage using elementary solids.

where  $L_1$  is the lenght of the elementary solid which approximates the cockpit (a paraboloid),  $L_2$  is the lenght of the elementary solid which approximates the cabin (an elliptic cylinder) and  $L_3$  is the lenght of the elementary solid which approximates the joint between the fuselage and the tail (a cone) [17].

$$L_1 = 3.85 \text{ m} \quad L_2 = 15.54 \text{ m} \quad L_3 = 6.89 \text{ m}$$

So, by applying the computation of the lenght of each elementary solid, the total lenght of the fuselage results in:

$$L_{fuse} = 26.28 \text{ m}$$

#### 7.2.2.10 Rear cargo door

Once the whole fuselage design is determined, and taking into account tail's design (paying special attention to the Tail-rear fuselage joint subsection), a final design of the cargo door need to be realized.

The most important feature of the door, and the aspect that condition its shape the most as well as the rear fuselage shape is the rail configuration. Since the door must contain a continuation of the inner rail system in order to allow easier pallet loading, the distance between rails along the whole door must be guaranteed.

Secondly, it is necessary to ensure that the door gets in contact with the ground when the landing gear is deployed. Figure 63b shows the accomplishment of this requirement. Figure 61 displays the final cargo door measures.

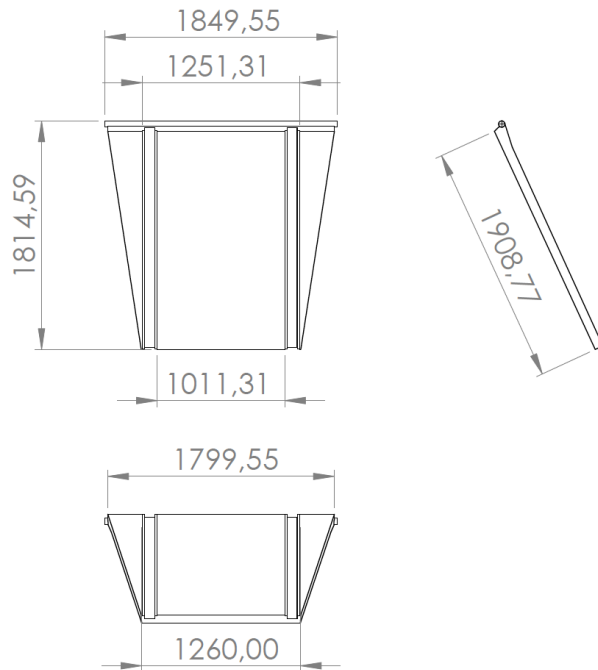
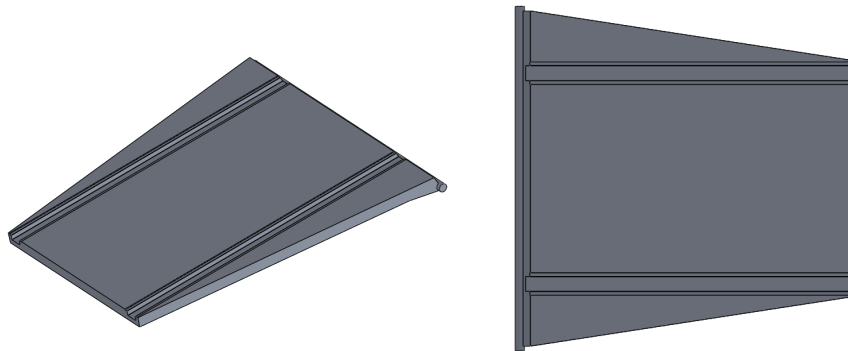


Figure 61: Cargo door dimensions.



(a) Cargo door

(b) Top view of the cargo door

Figure 62: Dismounted cargo door.

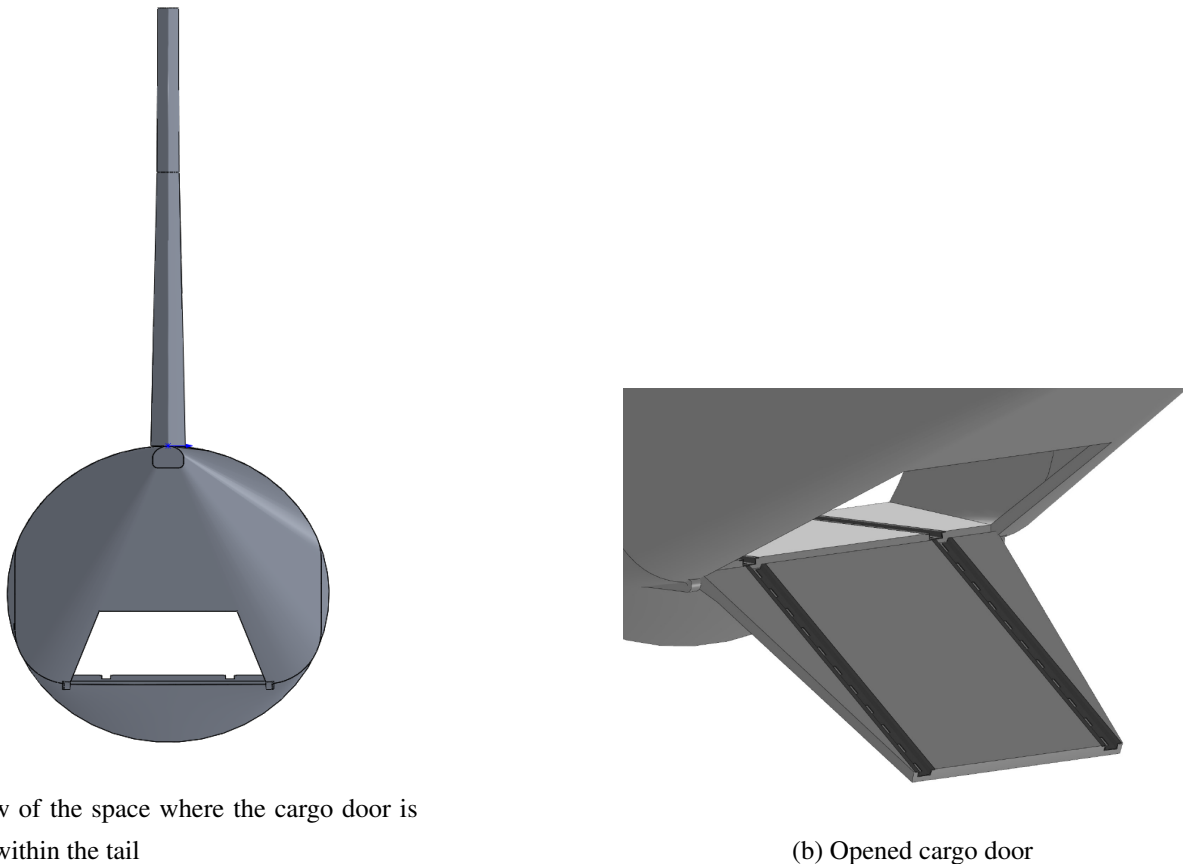


Figure 63: Mounted cargo door.

### 7.2.3 Tail

#### 7.2.3.1 Horizontal Stabilizer (HS) spar distribution

As a general guideline, some typical spar distributions relative to a generic tail chord  $c_t$  are exposed:

Table 18: Typical tail spar positioning in transport aircraft, where  $x_{\text{spar}}$  refers to the chord direction relative to the root's TE. Source: [24]

Spar positioning	$x_{\text{spar}} / c_{t,\text{root}}$
<b>Front spar</b>	0.70-0.75
<b>Rear spar</b>	0.15-0.25

It must be mentioned that the rear spar location is normally subject to the elevator. However, for the sake of simplicity the horizontal tail's airframe will be designed without considering an independent control surface airframe, that is to say, both stabiliser and control surface will be a unique spars, ribs and skin combination.

Bearing in mind the positioning of the elevator provided by Aerodynamics Department, the final spar location is such that:

Table 19: HS spar positioning in QCRA aircraft.

Spar positioning	$x_{spar}/c_{t,root}$
Front spar	0.70
Rear spar	0.45

It is worth noting that the rear spar location is notably different to the guideline provided in Table 18, but needed in order to avoid interfering with the elevator.

#### 7.2.3.2 HS rib distribution

Ribs are required where point loads act, such as control surfaces or intersections between surfaces. Typical rib spacing for “transport” aircraft is around 24inch or 61cm. Since our aircraft is clearly classified in this category, this order of magnitude will be taken into account when deciding the final rib spacing.

In addition, 5 mm thick ribs will be used as a generic size.

#### 7.2.3.3 HS internal airframe final configuration

A partial scheme of the HS airframe drawing can be consulted herebelow, where spars and ribs are indicated (see Figure 68).

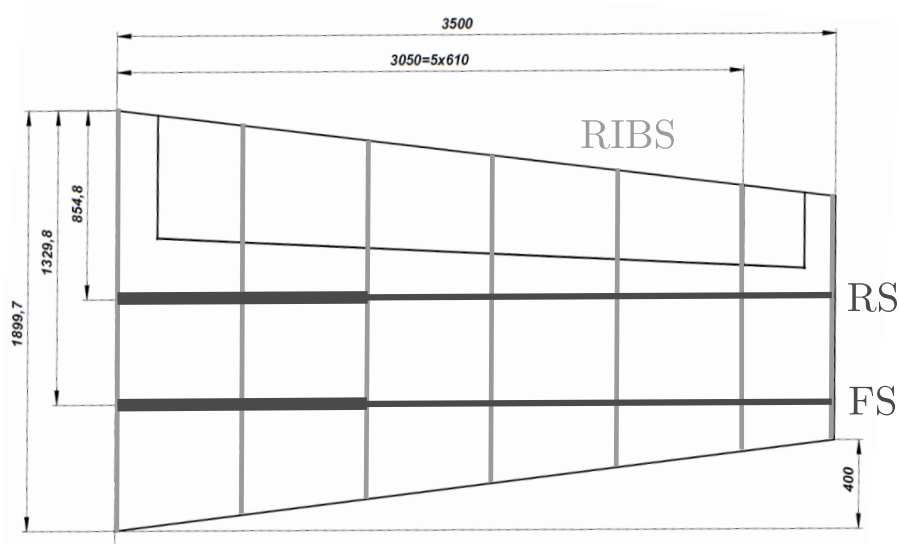


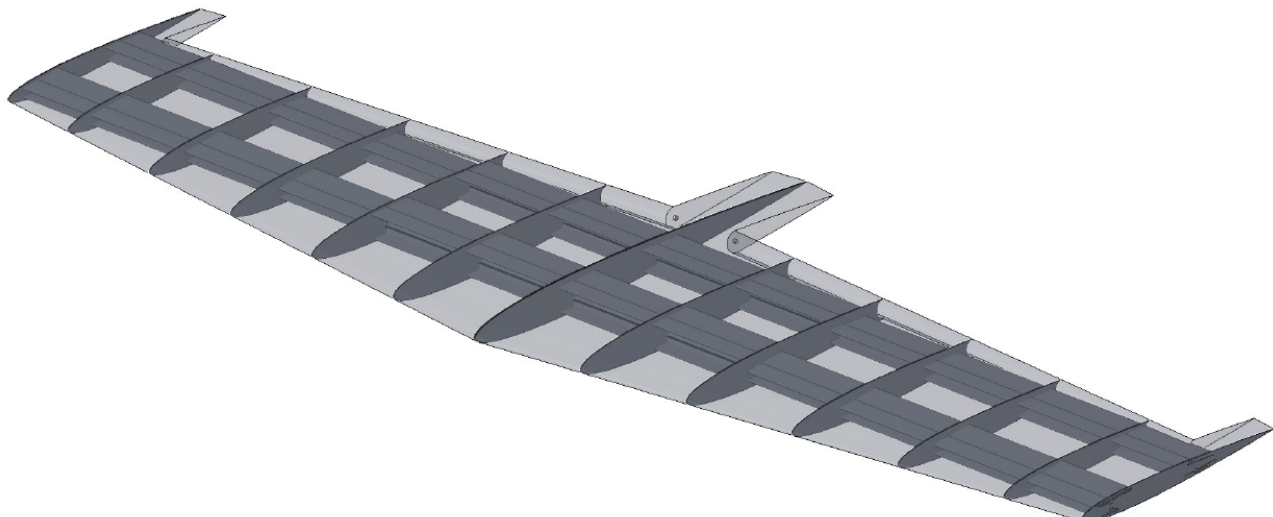
Figure 64: Spars and ribs distribution of the HS.

In fact, the same spar's cross section (Figure 65b) form has been used in comparison with the wing, but only making use of two different sizes along the span, indicated in Table 20:

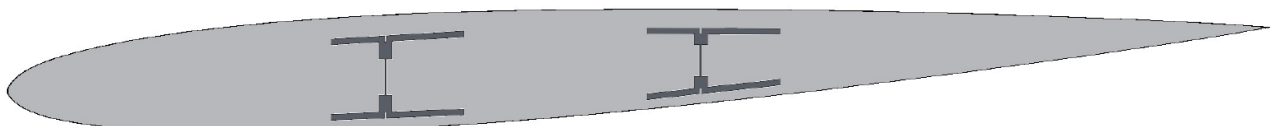
Table 20: HS's spar properties along the span (provided by Solidworks).

Distance from root (m)	Area ( $m^2$ )	Inertia $I_y (m^4)$
<b>0 - 1,22</b>	$9,13484 \cdot 10^{-3}$	$2,102 \cdot 10^{-5}$
<b>1,22 - 3,50</b>	$8,16875 \cdot 10^{-3}$	$4,936 \cdot 10^{-6}$

The resulting spars and ribs model is represented in Figure 65. As it can be seen, the spars are located so that enough space is left for the elevator (Figure 65a).



(a) Horizontal stabiliser's internal airframe



(b) Spars cross section form

Figure 65: Horizontal stabiliser's airframe configuration.

After including the mentioned control surfaces, the entire HS is obtained as shown in Figure 68.

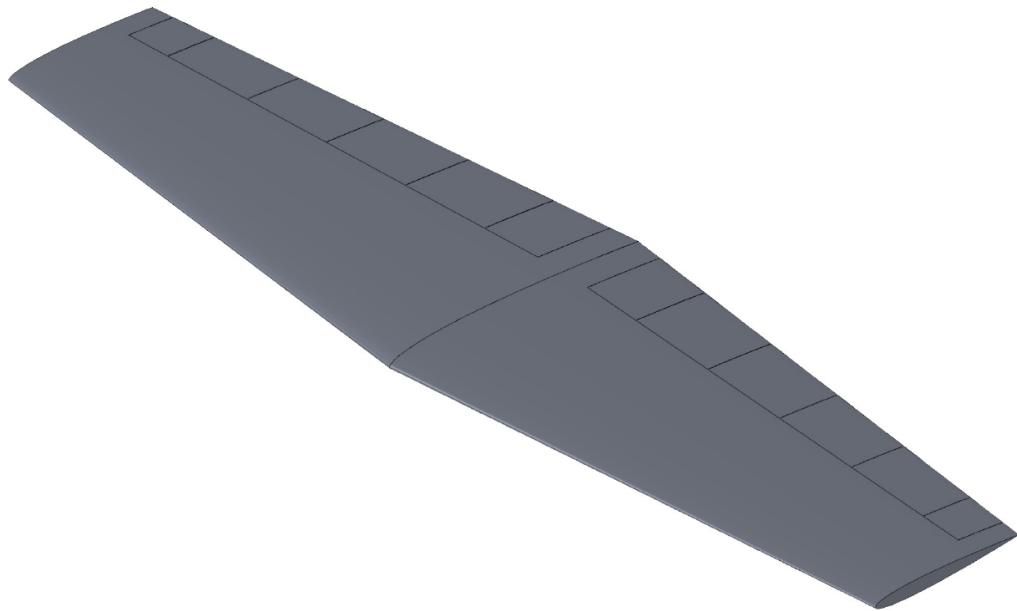


Figure 66: Spars and ribs distribution of the HS.

#### 7.2.3.4 Simulation of the HS's structural behaviour

Analogously to the simulation performed for the wing, the same 1D beam element Matlab script will be used to study the structural behaviour of the HS. Nevertheless, since the horizontal stabiliser analysis is secondary and merely used as ,in this case a structural Solidworks simulation will not be needed.

Taking into account the  $C_L$  distribution along the span provided by Aerodynamics Department, the most structurally demanding situation (cruising speed with maximum elevator deflection up) is analysed. The conditions of the study are:

Table 21: Conditions of the study.

Variable	Value
AoA (°)	-4,4
Elevator deflection (°)	-25
Density (kg/m <sup>3</sup> )	0,5
Cruising speed (m/s)	152,78
Total HS lift in cruise (N)	-31980,0

Hence, the resulting lift distribution for the HS along its span is obtained.

Thereby, considering Aluminium 7075-T651 (see Structures Attachment section 2.2), as the spars' material, the structural behaviour of the HS is described by the graphs in Figure 68.

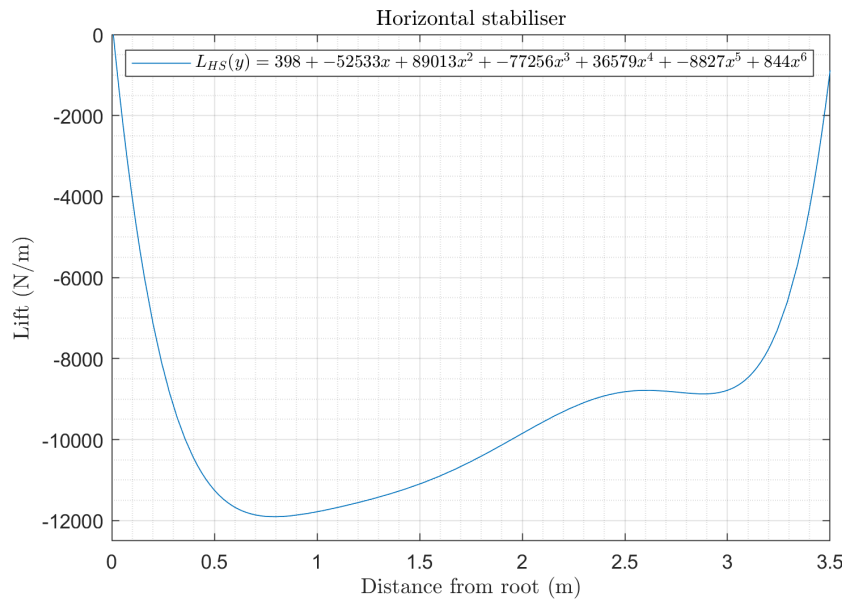


Figure 67: Spars and ribs distribution of the HS.

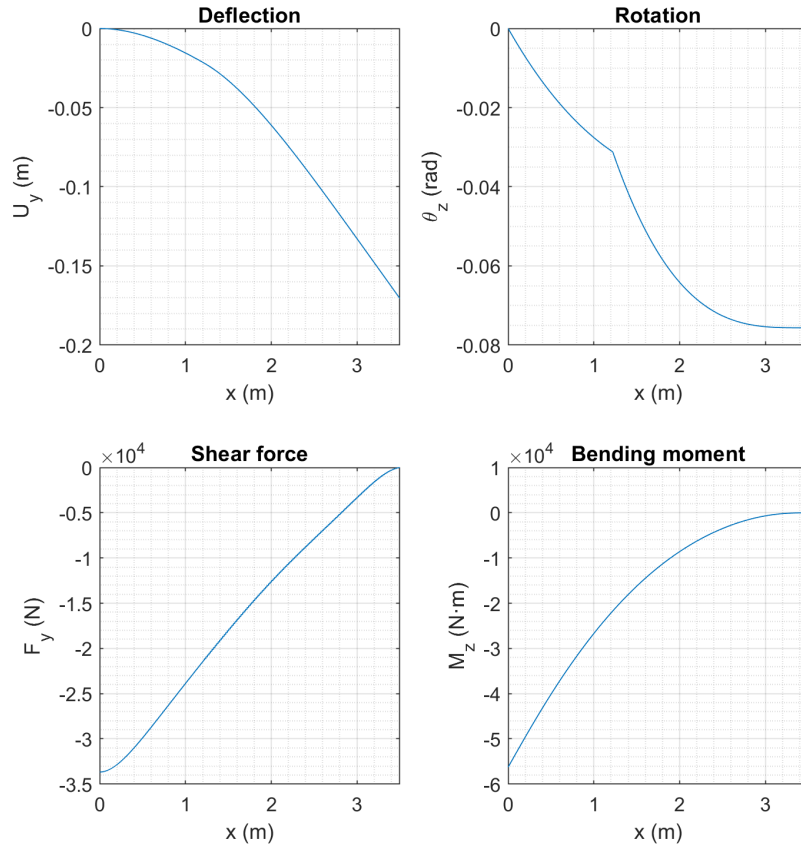


Figure 68: Spars and ribs distribution of the HS.

It is clearly observed that the maximum deflection of  $-0,17\text{ m}$  obtained at the tip is among acceptable values, thereby confirming the structural validity of the spars. Evidently, a change in the section's rotation progression is observed at  $1,22\text{ m}$ , coincident with the spar's section change. In addition, it is obvious that the root is the most structurally demanded part of the HS due to the maximum shear force and bending moment obtained.

### 7.2.3.5 Tail-rear fuselage joint and Vertical Stabilizer (VS)

In order to design the union between the rear fuselage part and the tail, it has been decided to set a tail's ground clearance angle of  $\theta = 20^\circ$ . This can be seen in the partial scheme of the rear fuselage-tail joint design added in Figure 72. The complete drawing is included in the Drawings deliverable.

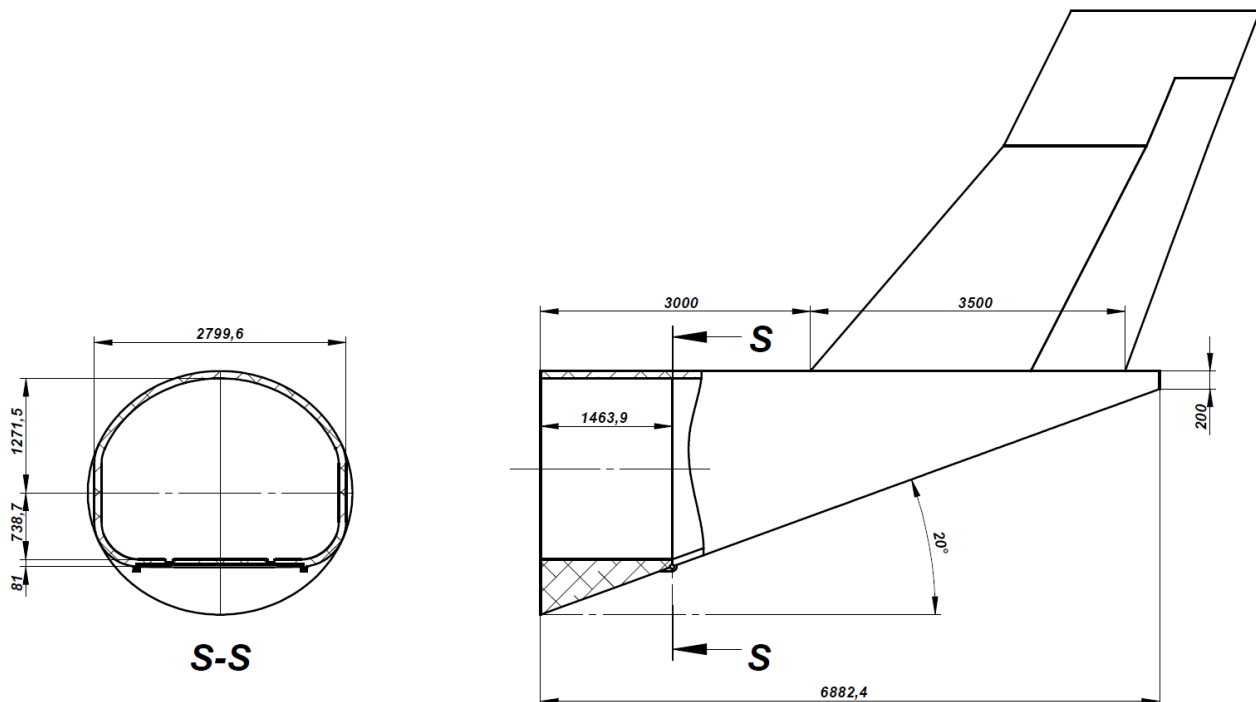


Figure 69: Rear fuselage-tail joint scheme.

In terms of cross section, a transition from the elliptical fuselage section to a special section is needed in order to enable the implementation of a rear cargo door. This is basically due to the fact that if the elliptical section directly converged into the tail, the rear fuselage joint would result in a cone, causing the undesired need of having to fit the flat cargo door in a curved surface. Therefore, such special section with a flat base where the cargo door can be fit is composed by a lower partial rounded rectangle and an upper partial ellipse which matches the original fuselage's cabin cross section. It must be noted that the mentioned special section enables a maximisation of the usable volume, thereby not interfering with the load/unload of the seat pallets of the switch system. Also, it is worth mentioning that the rails are still present in order to enable the switch system correct functioning.

A 3D model representation of the transition from the elliptical section to the special section can be observed in Figure 70:

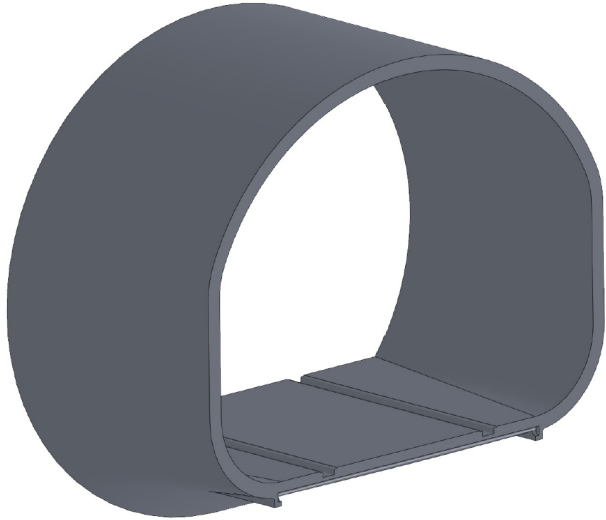


Figure 70: Rear fuselage (elliptical section) to tail (lower rectangular and upper elliptical section) transition.

Such semi elliptical-rectangular section is extruded so that an asymmetric cone is formed. In its flat base, the cargo door will be placed.

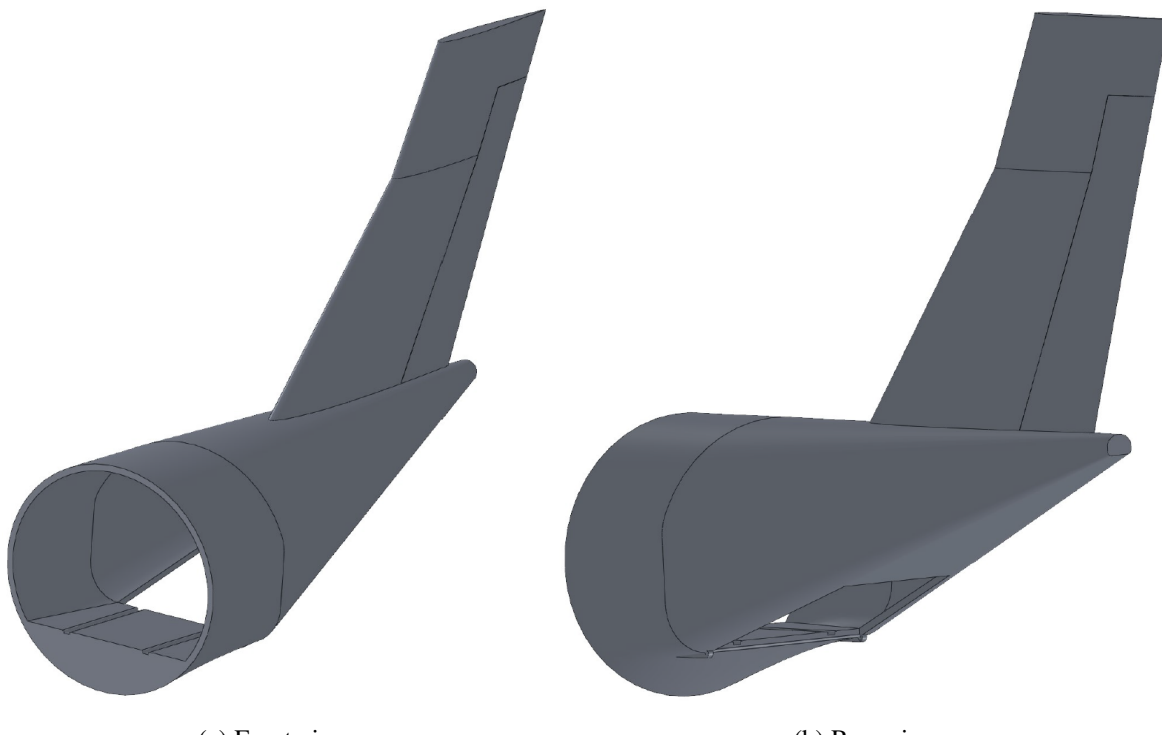


Figure 71: Rear fuselage - tail joint and VS 3D model (cargo door not implemented).

### 7.2.3.6 Final empennage model

The 3D model rendering of the entire empennage is provided for illustrative purposes hereunder.

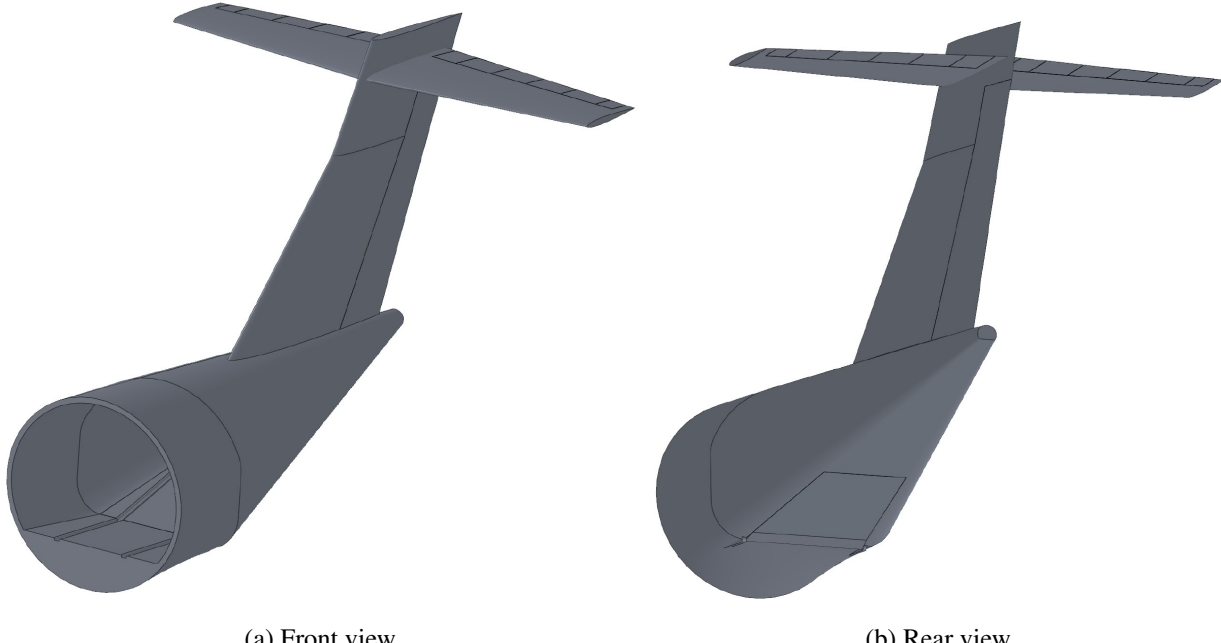


Figure 72: Final empennage 3D model.

## 7.2.4 Landing gear

### 7.2.4.1 Retraction capability

In order to finally define the general layout of the landing gear, the inclusion of a retractable gear must be justified. In this matter, it is commonly known that almost all passenger and cargo aircraft use retractable gear due to the drag penalty that their cruise speed induces. Normally, cruise speeds over 150 kts implies the need of including a retraction feature [28]. Nevertheless, there is a small portion of these airplanes, mainly small-sized aircraft with reduced payload capability, that tend to use a fixed gear configuration.

In the case of QCRA aircraft, since the cruise speed is 300 kts a retractable gear will be needed in order to minimise the drag during flight. It is worth mentioning that the implementation of this gear configuration will imply an increase in weight and structure complexity, however these drawbacks are compensated by the aforementioned drag minimisation.

### 7.2.4.2 Provider

In the matter of the landing gear system provider, Safran Landing Systems [29] is selected. This is not only due to their vast reputation in the sector, but also because some of their main customers are regional aircraft, including the ATR42, the base model in which QCRA aircraft is based on, and also the ATR72, among others.

### 7.2.4.3 Final landing gear positioning and disposition

The landing gear positioning has been performed as an iterative process in conjunction with the CG limits determination. Such iterative methodology is further explained in Structures Attachment, section 2.6.4.

Once the final iteration of weight and balance study has been performed in Section 7.2.5, the final landing gear strut disposition is decided. Specifically, the CG limit positions of the project's aircraft are indicated in Table 22:

Table 22: Estimated most fore-and-aft CG limits for QCRA aircraft, where  $x$  refers to the aircraft's longitudinal axis, being its nose the origin.

Fwd: $\bar{x}_{cg, min}$ (m)	Aft: $\bar{x}_{cg, max}$ (m)
11,21	12,31

Taking into account these data and with the aim of fulfilling both stability and load criteria (further explained in section 2.6.5 of Structures Attachment) the final position of the landing gear and the corresponding stability criteria variables (highlighted in red) are represented in Figure 73.

In fact, such design variables are summed in Table 23:

Table 23: Landing gear's stability design variables.

Criterion	Variable	Value
<b>Tip-over (longitudinal)</b>	-	27,5°
<b>Tip-over (lateral)</b>	$\psi$	55°
<b>Ground clearance (longitudinal)</b>	$\theta$	9,8°
<b>Ground clearance (lateral)</b>	$\phi$	19,8°

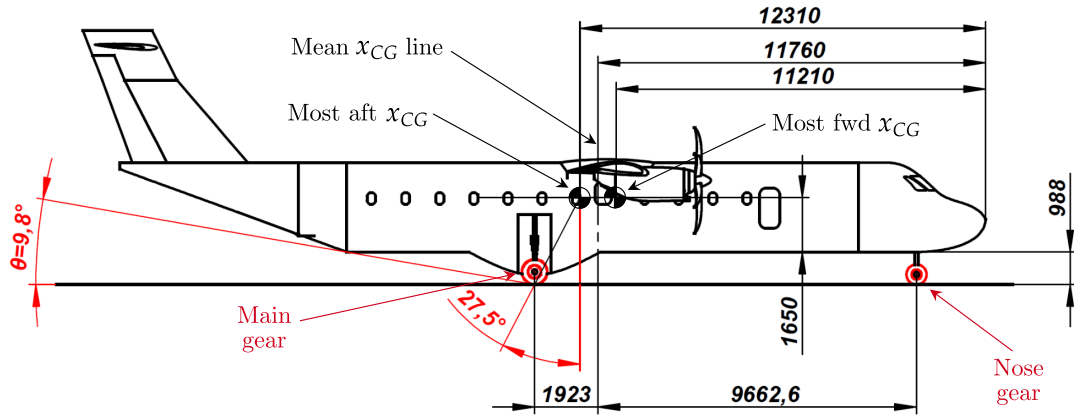
Thereby, the positioning of the landing gear in relation with the x-axis mean CG is specified in Table 24:

Table 24: QCRA's nose and main landing gear distances, being  $l_{nose}$  the distance between the mean CG and the nose, and  $l_{main}$  the one between the main gear and the mean CG. Refer to Figure 73a for a visual representation.

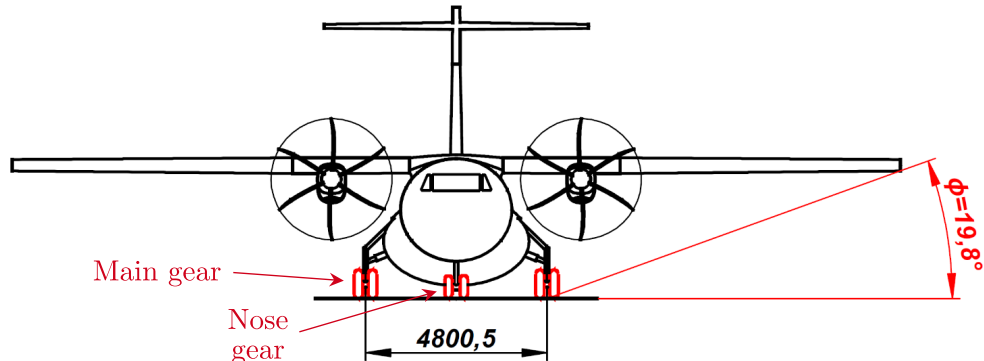
$l_{nose}$ (m)	$l_{main}$ (m)
9,663	1,923

### 7.2.4.4 Landing gear's maximum static load and wheel sizing

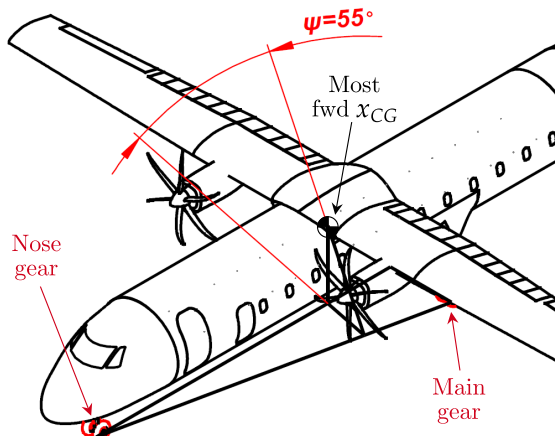
With the goal of determining the static load per strut, both rear and main landing gears have been analysed. The corresponding calculation procedure and further information is added in sections 2.6.6 and 2.6.7 of the



(a) Landing gear disposition scheme (longitudinal)



(b) Landing gear disposition scheme (lateral)



(c) Landing gear disposition scheme (trimetric)

Figure 73: Landing gear disposition scheme according to stability criteria (units in mm).

### Structures Attachment.

In terms of maximum static load, QCRA's main landing gear withstands an 83,4% of the aircraft's weight in

MTOW (18800kg) configuration, whereas the nose gear just 16,6%, being the latter roughly a 10% higher than the commonly found nose loads for Regional Turboprops of 44000lbs category (19958kg) [19].

Due to this fact, the sizing of the nose landing gear wheels has been selected according to heavier transport jets categories (for detailed explanations refer to Structures Attachment, section 2.6.7). Nonetheless, since the main gear load is considered an acceptable value in the Regional Turboprops category, there has not been need of using different categories.

Therefore, wheel sizing properties and the corresponding landing gear loads are included in Table 25.

Table 25: Landing gear loads and wheel sizing.

	<b>Load (kg)</b>	<b>Load ratio</b>	<b>Num. of wheels</b>	<b>Diameter <math>D_t</math> (cm)</b>	<b>Width <math>b_t</math> (cm)</b>	<b>Pressure (psi)</b>
<b>Main gear</b>	7839.4	0.834	2	76.20	22.86	107
<b>Nose gear</b>	3121.1	0.166	2	60.96	19.56	150

It must be mentioned that these sizing values are focused on static structural demandings. In the matter of dynamic analysis, the common type of loads studied and the related regulations are briefly explained in Structures Attachment, sections 2.6.2 and 2.6.3. Obviously, these aspects are not studied in further detail for the QCRA aircraft.

#### 7.2.4.5 Final model

The final landing gear model is represented in Figure 74. For further details of the design and modelling of the landing gear (including retraction features), please see Structures Attachment, section 2.6.8.



Figure 74: 3D model of the landing gear and the corresponding nacelle

Note that this is merely a simplified version. In terms of brakes and hydraulic systems, these are treated by Systems Department in section 7.4.3.3.

### 7.2.5 Stability

Once the aircraft is sized, the range of locations of the center of gravity must be determined in order to set the final dimensions for the landing gear and to guarantee that the aircraft will fly in a stable configuration. Following the guidelines from [19], a weight breakdown has been performed and the center of mass of each part has been located, which allows to calculate the center of mass of the whole aircraft.

The fixed elements weight have been divided into fuselage ( $W_e$ ), wing group ( $W_w$ ), empennage group ( $W_e = W_v + W_h$ ), engine group ( $W_e$ ) and fixed equipment ( $W_{fe}$ ). These elements, along with the fuel weight ( $W_f$ ), trapped fuel and oil weight ( $W_{tfo}$ ) and crew weight ( $W_c$ ) have been considered to have a fix center of mass. The passengers and baggage or cargo weight, however, has been considered to have its center of mass in a variable range (between 40% and 60% of the usable fuselage length). Considering these scenarios for different loading configurations, the excursion diagrams for the center of mass location can be obtained. These are shown in Figures 76 and 77. Note that the resulting most forward and most aft cg positions have been obtained with the passengers/cargo weight  $W_{PL}$  located at 40% and 60% of the usable fuselage length, respectively. From this data, the center of gravity limits from Table 22 are obtained.

The fixed elements weight breakdown and their corresponding centers of mass can be seen in Figure 75. The whole weight breakdown and center of mass computing process is detailed in the Structures Attachment, section 2.7.

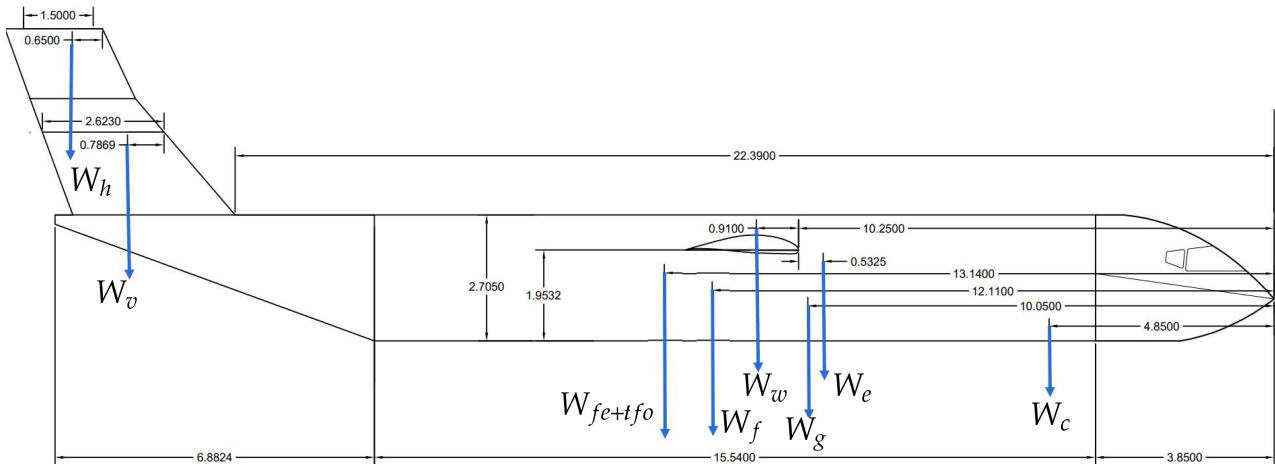


Figure 75: Weight breakdown of the airplane, with the corresponding centers of mass located in the sideview.

According to the aerodynamics data provided by XFLR5, the final wing-body-tail configuration has its neutral point at  $x_{NP} = 12.55\text{m}$ . Bearing in mind that the most aft cg location is  $x_{cg,max} = 12.31\text{m}$ , it is confirmed that the airplane will always be able to fly in a stable configuration, as this gives a minimum static margin of

$$H_{0,min} = x_{NP} - x_{cg,max} = H_{0,min} = 0.24 \text{ m}$$

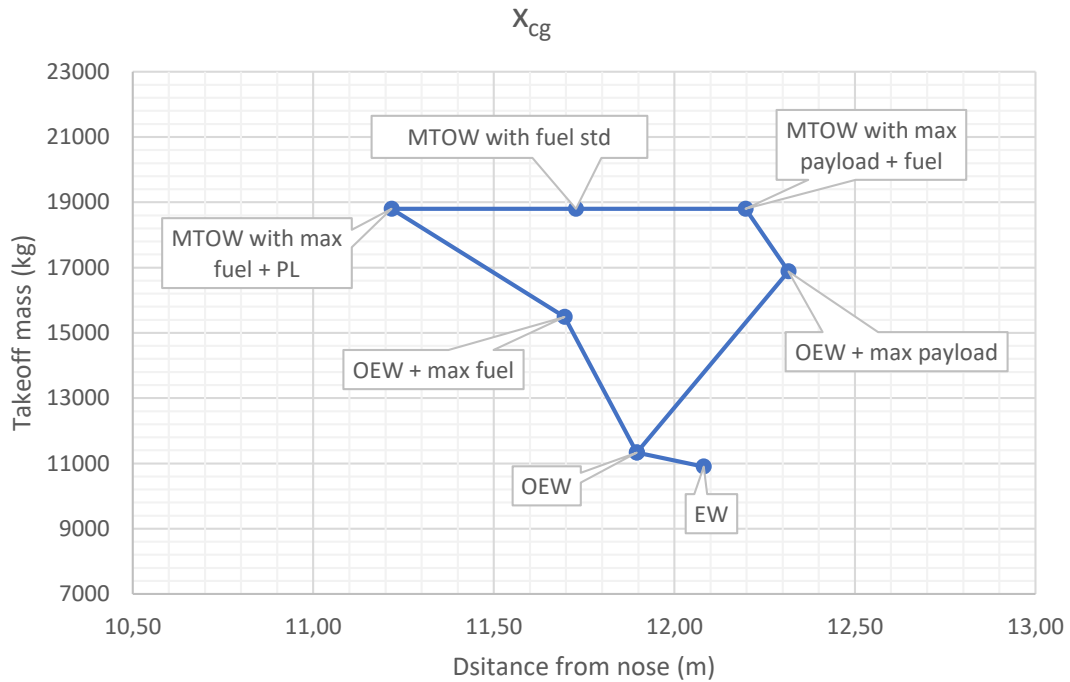


Figure 76: Excursion diagram of the longitudinal position of the estimated center of gravity of the airplane.

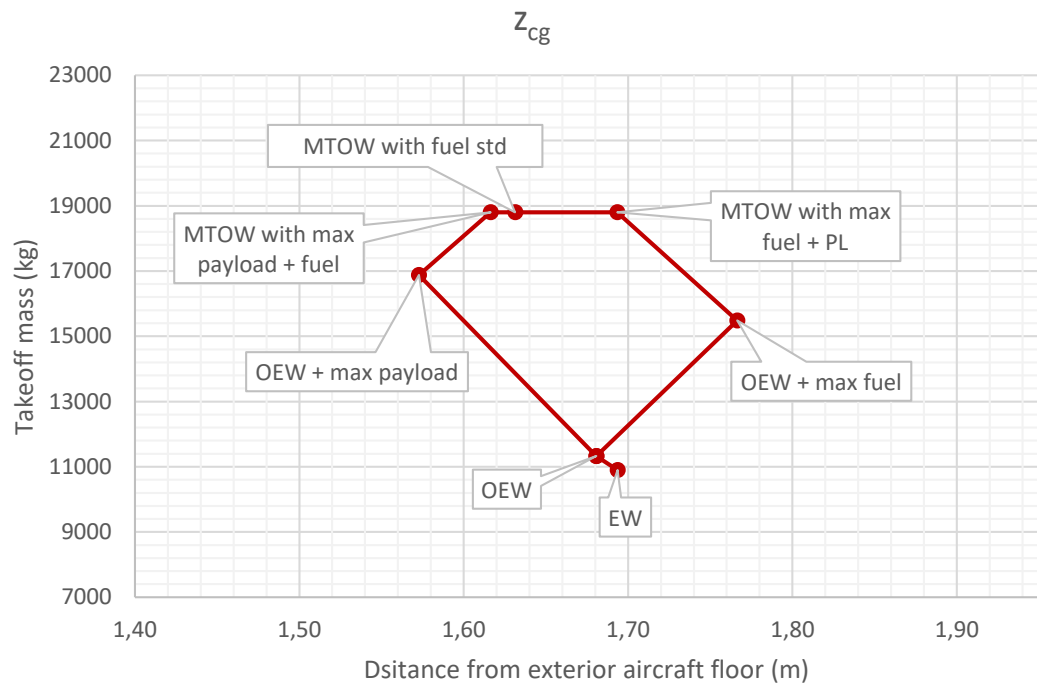


Figure 77: Excursion diagram of the vertical position of the estimated center of gravity of the airplane.

### 7.2.6 Cabin floor rail system

The aim of this section is to determine the rail configuration which will allow to change from one operation mode to the other, taking as inspiration the system exposed in the section 2.8.2.2 of Structures Attachment for the B737-300QC aircraft.

The design features continuous side guide rails to give the seat-pallet floor a continuous finished appearance.

Figures 78a and 78b show a section of the fuselage including the installation of the rail system. This system consists of two different rails located on the fuselage's ground. These two rails take all the cabin length, according to the dimensions stated by Table 17.

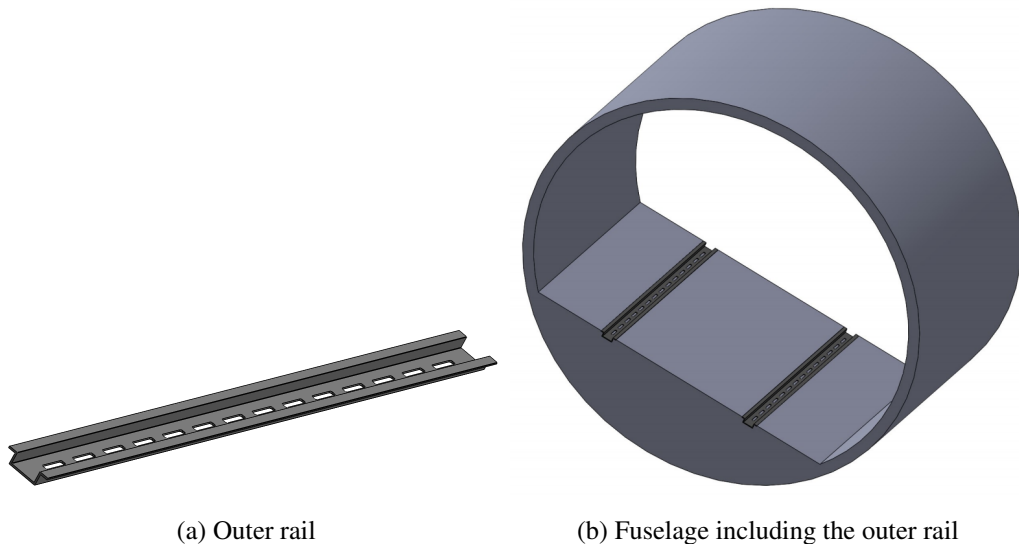


Figure 78: Fuselage rail system.

#### 7.2.6.1 Passenger operation mode

Each pallet is going to include 4-seats-abreast (2-seats-abreast in each side separated by an isle). The dimensions which every row take are the ones indicated in Figure 47.

The length of each pallet would be of 180 cm, as they include two rows of seats. As explained when studying the tail-rear fuselage joint (see subsection 7.2.3.5 *Tail-rear fuselage joint*), a transition from the elliptical fuselage section to a different section is needed to allow the implementation of the cargo door. So, as shown in Figure 72, the pallet must fit in the section S-S. This fact leads to the measuring shown at figure 79a:

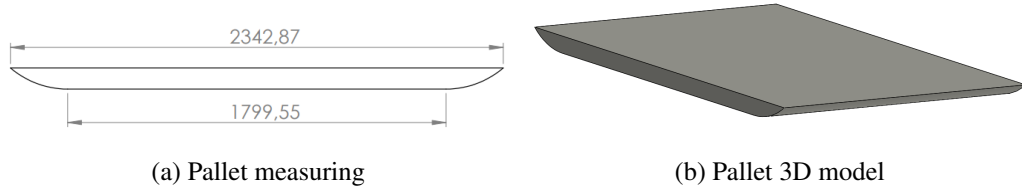


Figure 79: Pallet design.

Moreover, the pallet itself must include the rail system which will allow it to move along the fuselage. So, a piece like the one in Figure 80a must be included in each side of the pallet.

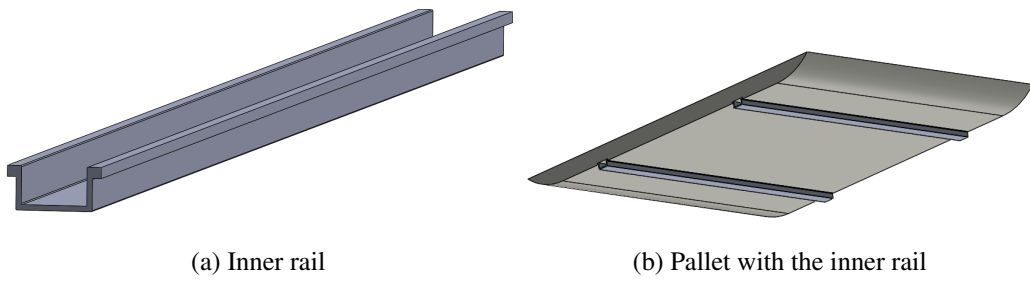


Figure 80: Pallet rail system.

Figures 81a and 81b show the combination of both rails (the inner and the outer one) and the assembly of the pallet and the rail system in the fuselage:

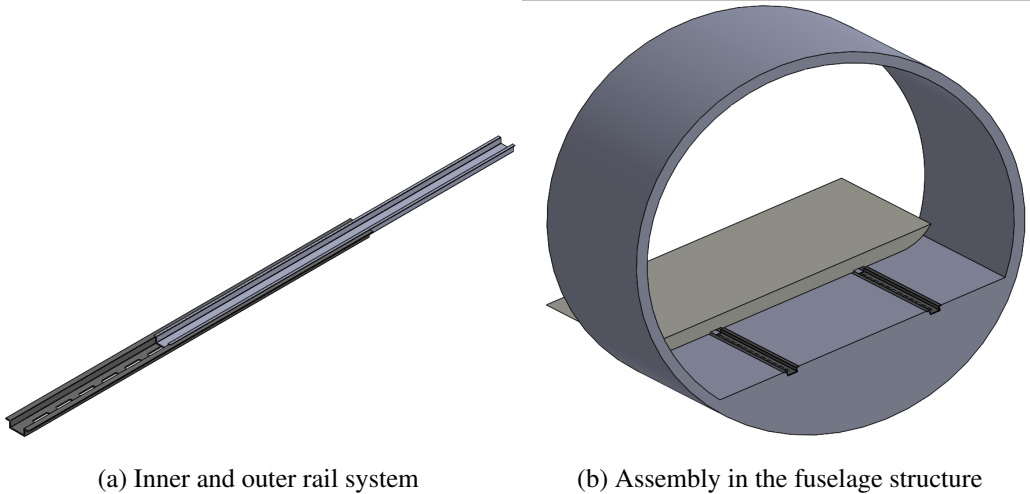


Figure 81: Rail system.

It is worth to remind that the 3D model shown in Figure 81a serves a simplification in order to represent the rail

system in a clear way. So, this system actually shows the following appearance:

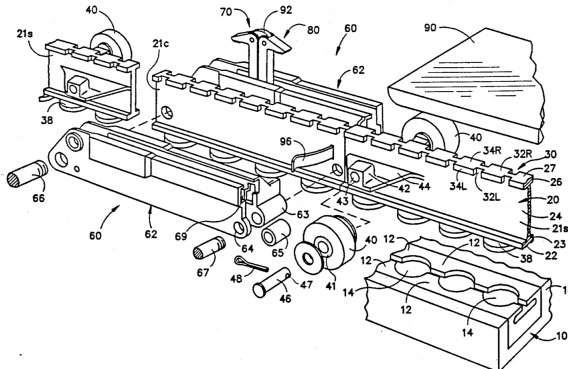


Figure 82: Rail system. Source: [30].

Finally, the pallet must home the seats (see Figure 83). As said, each pallet will include two rows of seats.

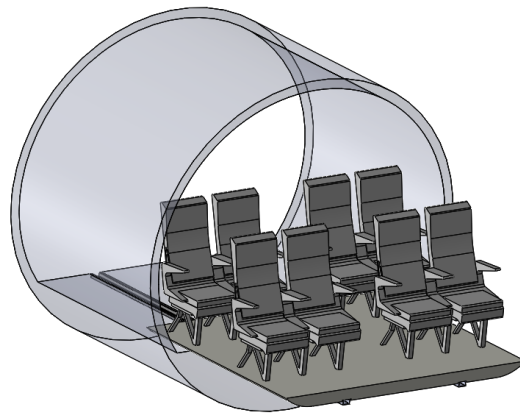


Figure 83: Assembly of the palletized seats in the fuselage structure.

The pallet measures that have been determined are the ones for the standard pallet. However, it is necessary to note that the distance between the rows is not the same one for all the rows along the cabin as a consequence of the presence of the emergency doors, as it can be seen in Figure 52. The QC system was designed to accommodate various passenger interiors that might be engineered to be interchangeable. Therefore, there are going to be four different types of palletized seats, as shown in the following Table, and the disposition of each one of them is specified in Figures 84 and 85:

Table 26: Types of pallets.

Pallet	Standard	Single row	Type I Emergency door	Type IV Emergency door
$d$ (cm)	180	90	241.0	228.3
<b>Number of pallets</b>	4	1	1	1

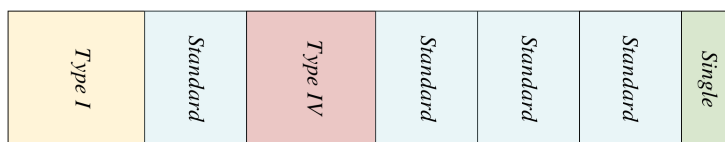


Figure 84: Pallets distribution along the cabin.

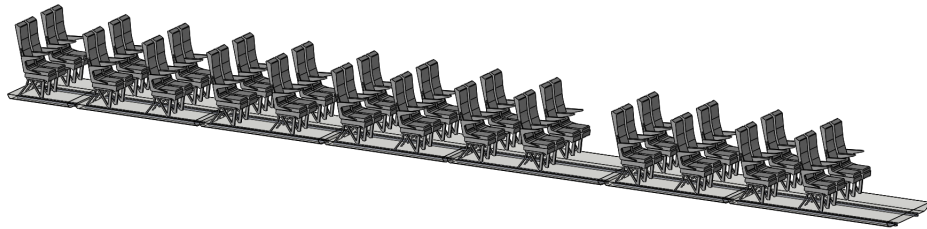


Figure 85: Pallets distribution along the cabin (3D model).

### 7.2.6.2 Cargo operation mode

One of the first things to take into account is that for cargo carrying airplanes, floors need to be equipped with cargo restraint systems.

Also, regarding the different loading systems, modern civil aircraft count with special mechanical loading systems for the agile loading and unloading of containers of standard size. The employed pallets are provided with rollers and have the capability of being adjustable to different values of heights with the aim to fit several aircraft floor levels [31].

Since it is necessary to enable the cargo to be easily moved to its proper position, roller conveyor strips are usually mounted on the fuselage floor, as shown in Figure 86 [24]. The rails used to guide the pallets can be the same ones that are used in the aircraft for the passenger operations.

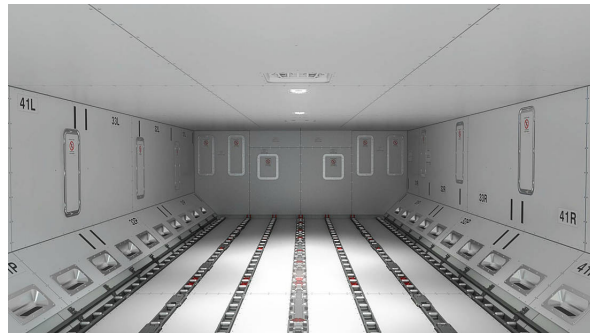


Figure 86: Roller conveyor strips mounted on the fuselage floor. Source: [32].

Finally, it is important to take into account that the containers and pallets must be firmly subjected in order to avoid any kind of movement capable to produce instability or sudden change in weight distribution. So, the floor counts with a track system which includes fixed tabs attached to the rails that prevents any kind of movement. Once the containers and pallets are loaded in the aircraft and, subsequently, located in their corresponding position, the tabs are raised and the freight becomes fixed.

Moreover, it is significant to note that the possibility of liquid spillage exists and so, the floor need to be equipped with a drainage system.

As said, the bathroom and the luggage bins will be fixed elements. Hence, the space they occupy needs to be taken into account when computing the total capacity of the cabin when operating at the freight mode.

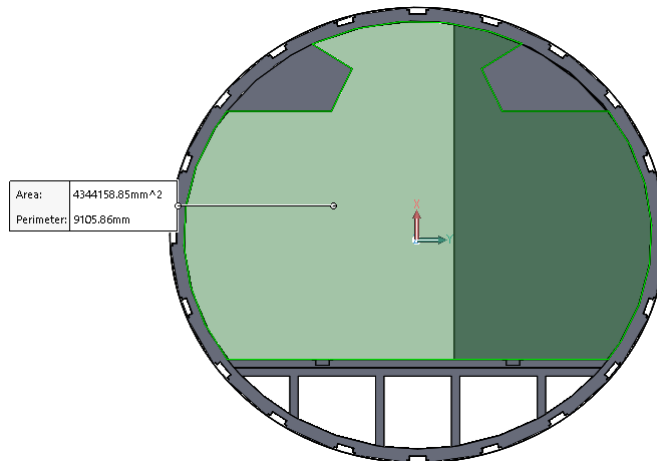


Figure 87: Usable area of the cabin.

$$\text{Hence, } A_{\text{usable}} = 4.34 \text{ m}^2.$$

On the other side, the length of the cabin, excluding the bathroom module, is 14.14 m. So:

$$V_{\text{usable}} = A_{\text{usable}} \cdot L = 61.26 \text{ m}^3$$

### 7.2.6.3 Final quick-change system model

For illustrative purposes, the design of the project's quick-change system is represented in Figure 88, where the previously described pallets, rails and cargo door can be clearly distinguished.

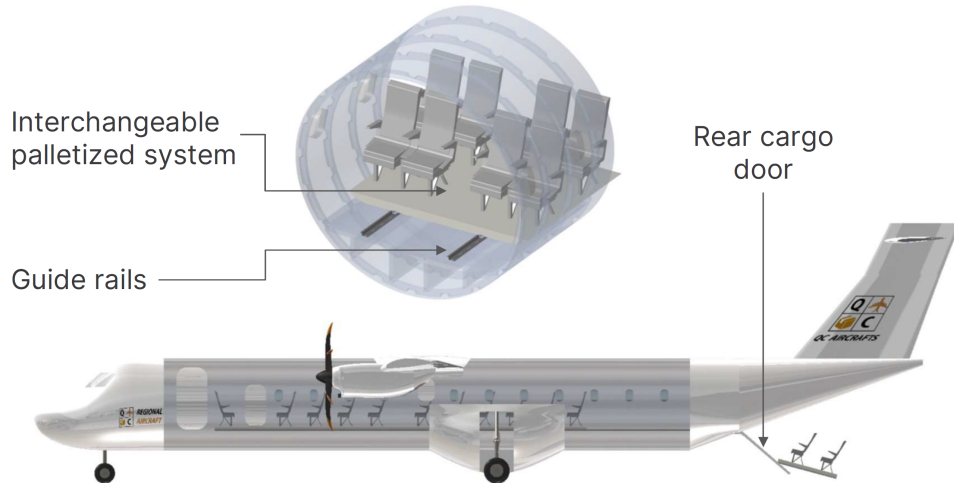


Figure 88: Quick-change system render

Additionally, the cabin configurations for passenger and cargo operation modes are represented in Figure 89.

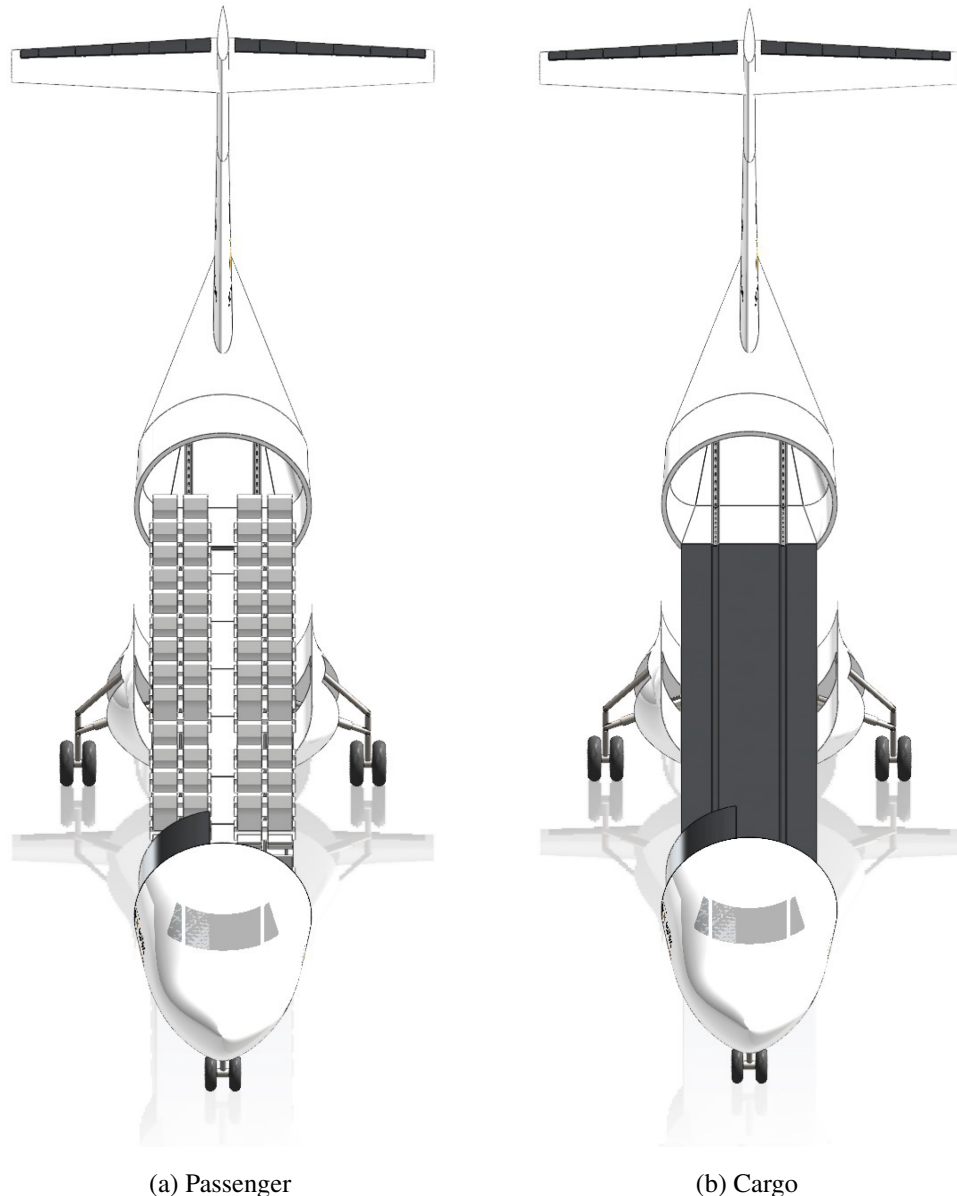


Figure 89: Cabin configuration modes.

### 7.2.7 Final QCRA aircraft CAD model

In order to better appreciate the contribution of the internal structural airframe to the entire aircraft, two comparative CAD renders are added in Figure 90.



(a) Complete aircraft



(b) Internal structural airframe

Figure 90: QCRA aircraft CAD models.

## 7.3 Propulsion

In order to simplify the overall process of design of the plane, the Propulsion Department has decided to acquire an already existing model of turboprop engine. As a consequence, the engine specifications are already determined by the manufacturer, and the role of the Propulsion Department is to determine the power needed for the plane and which is the most suitable engine.

### 7.3.1 Type, positioning and number of engines

The type of engine used will be the **turboprop**, as stated previously in section 6.5.1. The aircraft will be a **twin engine** (see section 6.5.2) and the positioning of the engines will be **under the wings** (see section 6.5.3).

### 7.3.2 Maximum power required

The power required has been calculated in two different ways, explained in more detail in the Propulsion Attachments, section 3.1.2. From a preliminary calculation the value obtained is **1811.8kW** and from empiric calculations **1796.29kW**. From an aerodynamic approach the power required calculated was **1864kW**. The engine selected will have to be able to provide more than the highest of the three powers calculated.

### 7.3.3 Selection of the engine

After a study of the turbopropellers available in the market, the engine selected has been the **PW127N**, which provides a maximum continuous power of 1846kW and maximum take-off power of 2051kW. For more information about the selection see section 6.5.4, and for more information about the engine see the Propulsion Technical Sheets, section 3.5.

### 7.3.4 Propeller

To select the ideal propeller a few calculations have been made. The engine used is only compatible with 6-blade propellers. The next thing that will have to be discussed is the size of the propeller. Its diameter has been calculated with two different approaches: through a preliminary estimation and through empiric calculations. The values obtained were **3.93m** and **3.70m**, respectively (for more information about the calculations see the Propulsion Attachments, section 3.2.1). Finally, the propeller selected is the **Hamilton Standard 568F** propeller, which is used in the ATR-42 aircraft, that runs in a PW127M engine; an older but nearly identical version of our engine selected. Its specifications can be seen in the Propulsion Technical Sheets, section 3.5.

### 7.3.5 Positioning of the engine

In order to determine the engine position within the wingspan it will be used two different criteria: first of all, the placement will allow the aircraft to compensate the yaw moments generated in case of engine failure; and secondly, it will be studied the position of the engines in similar aircraft and determined the average position.

With the first method the longitudinal distance along the wing from the root of the fuselage is **3.16m** and with the second method, **3.41m**. Finally, the distance selected is **3.16m** since the first criteria gave the highest value possible (for more details about the calculations see the Propulsion Attachments section 3.3).

### 7.3.6 Performance

Lastly, the TOFL and the LFL have been calculated for different altitudes. A summary of the results can be seen in Table 27.

Table 27: TOFL and LFL for different altitudes.

Altitude (m)	0	300	600	1200
TOFL (m)	956.1	984.2	1013.2	1074.5
LFL (m)	1527.1	1572.0	1618.3	1716.3

As it can be observed, the take-off landing distance obtained for the different altitudes is **less than 1100m**, one of the requirements of the aircraft. The maximum altitude in which the aircraft still accomplishes this requirement is 1450m of altitude. The landing field lengths are a bit higher as expected. Nevertheless, these values are a first approximation since they will change depending on the runway slope, rolling friction and wind speed. See the Propulsion Attachments, section 3.4, to see more details about the calculations.

To finish the performance study, the fuel consumption of the QCRA aircraft was calculated in the Propulsion Attachments, section 3.4.3, where it was obtained a value of: **2.69 kg/100km/seat**. When comparing this value with similar aircraft, such as the ATR-42, it can be found a substantial reduction of **11.5 %** of the fuel consumption.

## 7.4 Systems

### 7.4.1 Avionics

#### 7.4.1.1 Compulsory instrumentation

In order to determine the compulsory flight instrumentation for our aircraft, the applicable international regulations must be checked. For the type of aircraft considered, the most important ones are the European Union Aviation Safety Agency (EASA) *Certification Specifications (CS)-25* (European) and the Federal Aviation Regulations (FAR) (United States). The requirements extracted from them are presented in the following table:

Table 28: Compulsory instrumentation.

Visible from each pilot station	At each pilot station
<ul style="list-style-type: none"> <li>• Free-air temperature indicator</li> <li>• Clock with hours, minutes and seconds, with second counter</li> <li>• Magnetic direction indicator</li> </ul>	<ul style="list-style-type: none"> <li>• Airspeed indicator</li> <li>• Altimeter</li> <li>• Rate-Of-Climb indicator</li> <li>• Gyroscopic rate of turn indicator combined with an integral slip-skid indicator</li> <li>• Bank and pitch indicator</li> <li>• Direction indicator</li> </ul>

As for the communications instrumentation, the regulations found were more vague. The types of communications that will be included in the QCRA are: human/voice radio communications, transponders, Global Positioning System (GPS), Automatic Dependent Surveillance-Broadcast (ADS-B), Aircraft Communications Addressing and Reporting System (ACARS), SATellite COMmunications (SATCOM) and Fourth Generation Long Term Evolution (4G LTE). More detail in this systems and their corresponding physical equipment is presented in Systems Attachment 4.1.1.

#### 7.4.1.2 Additional instrumentation

In order to provide a better pilot experience and to be more competitive in the regional aircraft market, including just the mandatory instrumentation would not be sufficient. For this reason, additional instrumentation will be equipped: Evolved Horizontal Situation Indicator (EHSI), Source Failure Alert, control panels, weather radar control, Attitude and Heading Reference System Push Button (AHRS PB) and flight data entry panel. A detailed explanation and visual support is offered in section 4.1.2 of the Systems Attachment.

#### 7.4.1.3 Cabin integration

After all the components included in the avionics system the QCRA have been presented, their integration in the cabin must be conducted. Due to the size and complexity of the cabin, it was out of the scope to design it. Figure 91 shows the cockpit design of the ATR42-600, a really similar aircraft, considered to be one of the

most modern turboprop aircraft dashboards according to [33]. The main difference will be the replacement of the yokes by joysticks, as it will be explained shortly in section 7.4.3.



Figure 91: Cockpit of the ATR42-600. Source: [34].

The different sections the cabin has been divided into is: overhead panel, front desk, middle lower controls, lateral site and first's officers rear seat. A detailed list of which components houses each section is presented in Systems Attachment 4.1.3.

#### 7.4.2 Electrical system

The main competent organisms in terms of electrical regulations include both the EASA and Federal Aviation Agency (FAA). The one which has been followed more rigorously is the EASA *CS25.1351*, since they are rather similar.

Apart from the technical limitations of the electrical system, the main requirement established by the different regulations is to ensure alternate electrical power systems with extremely remote probability to fail and also to be totally independent from the main generative systems. The equipment required to do so can be classified in time and non-time limited systems.

To meet all this demands, and to be able offer Direct Current (DC), AC and Alternate Current Wild frequency (ACW), the aircraft will require the following supply systems:

- DC supplying:
  - Batteries: Main and emergency

- DC generators driven by the accessory gearboxes
- DC Ground Power Unit (GPU)
- Transformer-Rectifier Unit (TRU)
- AC supplying:
  - The AC (115/26V 400Hz) is supplied by a Static Inverter (from the DC)
- ACW supplying:
  - ACW generators are driven by the reduction gearboxes
  - AC GPU (Ground Power Unit AC). Since the ACW GPU doesn't exist, the AC GPU supply the ACW busses with 115V/400Hz, which is within the acceptable margins.

#### 7.4.2.1 Power distribution

The power requirements in the aircraft will be similar to the one presented in Figure 92. How these will be met under different circumstances, which include normal working mode (AC powered [94]) and emergency mode (DC powered through generators [93a] and batteries[93b]), are shown below.

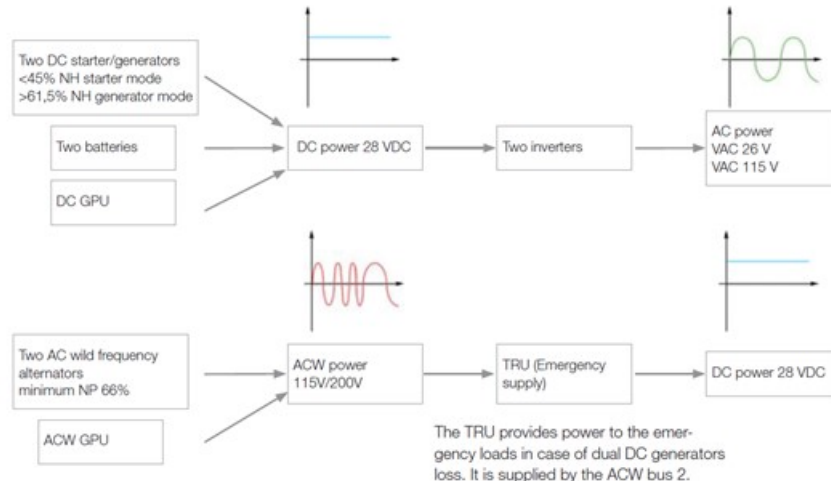
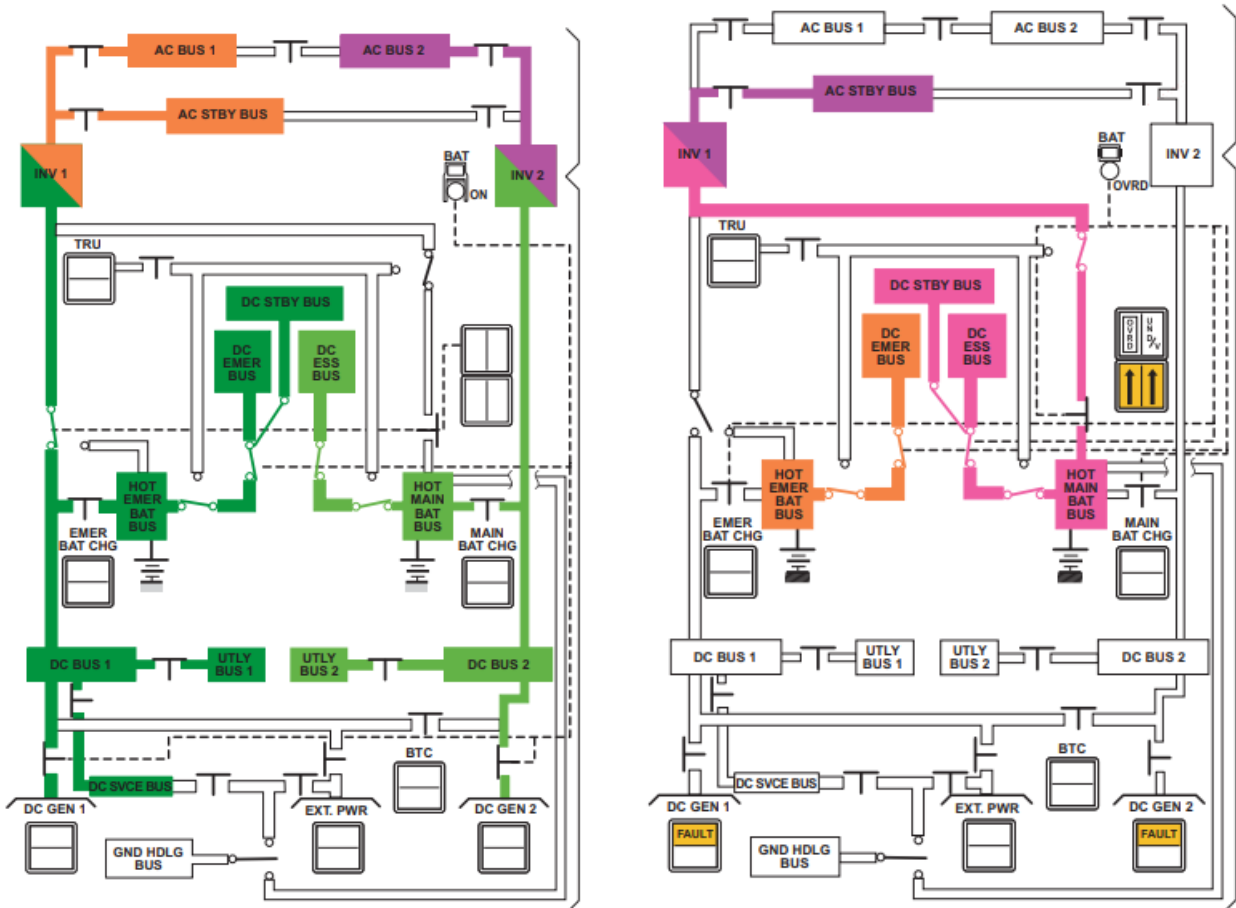


Figure 92: Power Requirements of an ATR 42. Source: [35].

All these power distributions feed: navigation instruments (avionics), communication systems, engine starters, hydraulic pumps, actuators, navigation and interior lightning and refrigeration systems.

#### 7.4.2.2 Illumination



(a) DC circuit scheme with normal supply and both DC generators on line. Source: [35].

(b) DC circuit scheme with emergency supply and failure of both DC generators. Source: [35].

Figure 93: DC powered emergency supplies.

The illumination is crucial for the correct functioning of any aircraft, and regulations are strict to ensure certain standards are met. The different types of illumination the QCRA must include will be studied in this section, with visual help from [36].

- **Exterior lightning**

The exterior lightning of the aircraft provides visibility for the pilots and their crew. They are placed in the exterior part of the fuselage in specified locations (see figure 95), and must meet certain requirements.

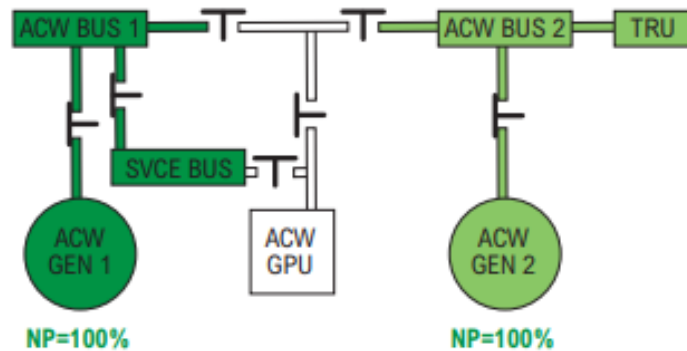


Figure 94: AC circuit scheme with normal supply in flight and both AC generators online. Source: [35].

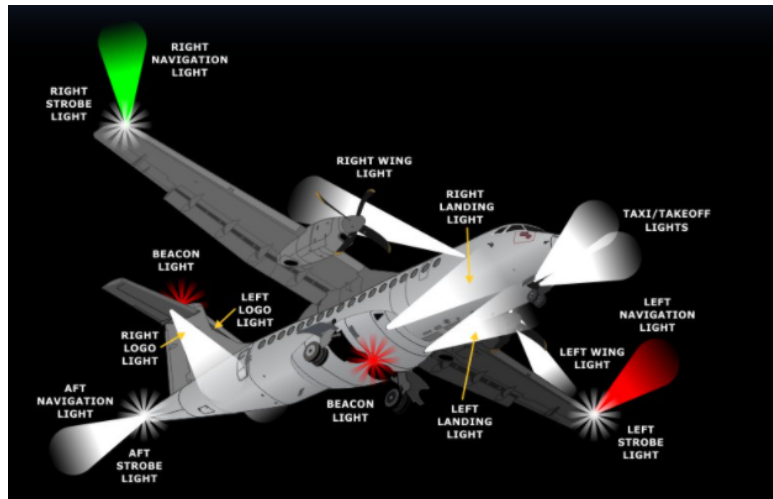


Figure 95: Exterior lightning of the aircraft. Source: [36].

- Navigation lights: Three lights (green, red and white) in the left wing tip, right wing tip and tail cone, respectively.
- Taxi and takeoff lights: Two white lamps on the bottoms side of the fuselage nose. Switched off when the front landing gear retracts.
- Landing lights: Similar to the taxi lights. Placed in front of the main landing gear.
- Wing lights: One light in each side illuminating the leading edge of the wing.
- Beacon lights: Red rotating lights in the top of the tail and in the bottom center of the fuselage.
- Strobe lights: Flashing white lights next to navigation lights.
- Logo lights: Not mandatory. Located in the lower side of the horizontal stabiliser, pointing at the fuse-

lage.

- **Flight compartment lightning**

The flight compartment disposes of several lights which lighten up different areas, so as to make every instrument, indicator or lever clearly visible for the pilots. The most important ones and their names are seen in Figures 96a, 96b and 97.



(a) Dome lights of the ATR flight compartment. Source: [36].



(b) Flood lights of the ATR flight compartment. Source: [36].



Figure 97: Spot lights of the ATR flight compartment. Source: [36].

- **Passenger compartment lightning**

All the lights responsible for illuminating the passenger / cargo zone are presented in Figure 98. Their goal is to offer enough visibility for both configurations and to provide a comfortable atmosphere in the passenger configuration.

Depending if they provide lightning for a single passenger or to the entire cabin, the lights can be further classified into passenger compartment (Figure 99a) and passenger service unit lights (Figure 99b).

- **Service and maintenance lightning**

Provide lightning for the cargo compartment and external cargo loading area. This include all the lights in

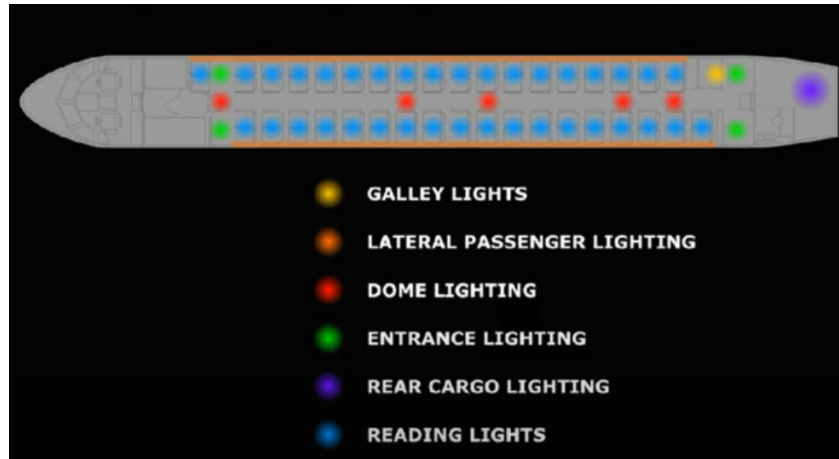


Figure 98: Interior lightning. Source: [36].



(a) Passenger compartment ceiling and lateral lighting.  
Source: [37].



(b) No-smoking, seat-belt lights and reading lights in each Passenger Service Unit (PSU). Source: [38].

7.4.2.2, which will turn off after loading the cargo area, and additional lights located on the floor rails to facilitate the loading process.

- **Emergency lightning**

The emergency lighting is provided for the passengers and crew so as to ease and fasten an evacuation in case of emergency. A similar emergency lighting scheme shown below in Figure 100 will be followed.

#### 7.4.2.3 Electric power generation

All the components that compose the electrical power plant of the aircraft must be acquired from third parties. The Table 29 sums up the choice for some of the most critical components of the electrical system and their sources. An important detail is to verify the compatibility of the elements with the aircraft, specially for the AC generator and Constant Speed Driver (CSD), which have to be installed directly to the engines. Additional details on their specifications and/or functioning can be found in Systems Attachment 4.2.4.

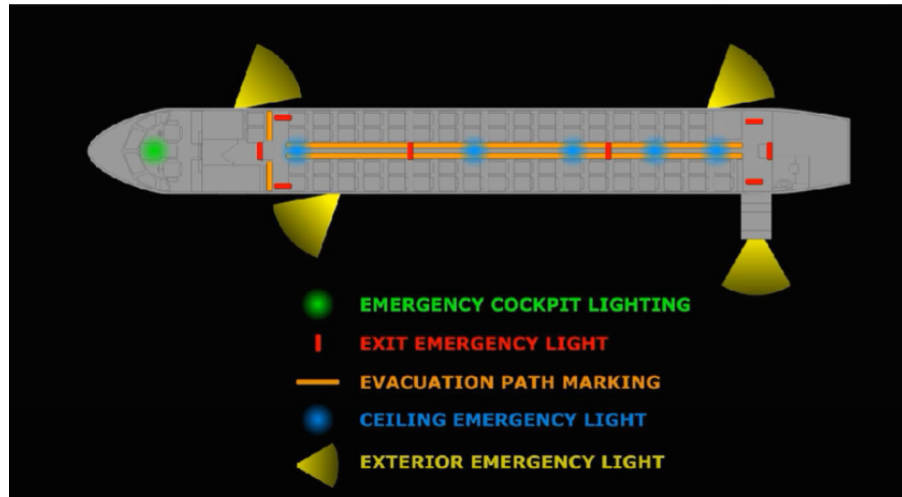


Figure 100: Emergency lighting system of the ATR-42. Source: [36].

Table 29: Commercially available electrical components.

Component	Serial number	Provider
DC battery	RG-380E/44 & RG-42	[39]
DC Generation Control Unit	102-003-11	[40]
Inverter	559-012A	[41]
TRU	28VS50Y-16	[42]
AC Generator + CSD	20032-2	[43]

#### 7.4.3 Control system

The control system consists of all the elements in the cockpit that allow the pilots to operate the mechanisms of the aircraft and the actuators linked to them. One of the more important ones is the pilotage control system.

On such a competitive sector as the aeronautical industry is, the pilotage control system opens a door for innovation. Traditional airplanes of the size of our own QCRA are usually controlled by conventional yokes, but Airbus revolutionized the sector in 1985 by installing joysticks, previously exclusive to fighter jets, in their A320 family [44]. This change also embraced a new control approach, the Fly-By-Wire (FBW), which is now installed in most aircraft regardless of their control system. In order to decide which option will be installed in the QCRA, their advantages and drawbacks were studied.

After taking a look at table *Pilotage control systems comparison* in section 4.3.1 of the Systems Attachment, it can be seen that both options have their strong sides, and it comes down to tradition vs. innovation. Innovation can be used to distinguish the aircraft among the competitors, but tradition will make an easier transition for pilots, hence requiring less training.

By betting that differentiating ourselves from other competitors in the regional aircraft market will make the

QCRA more attractive to airlines, the control system chosen is the joystick. Moreover, it will provide a much clearer view of the dashboard elements and it will take up less space. It will also free one of the pilots' hand to operate other elements.

To eliminate one of the drawbacks this system usually implies, both joysticks will be connected, just like the yoke controls thus preventing any problem resulting from the use of both joysticks at the same time. All in all, this measure will increase the aircraft's safety and make it a competitive option in the market.

Since a FBW approach has been adopted, both the controls located in the cabin and the actuators responsible for providing the movements will have to be selected. The controls included in this section and their classification are presented in Table 30.

Table 30: Control systems.

<b>Primary flight controls</b>	<b>Secondary flight controls</b>	<b>Ground controls</b>
Elevator	Flaps	Landing gear
Ailerons	Spoilers	Wheel brakes
Rudder		

Primary control systems offer the pilot maneuverability capabilities in the three principal axis of the plane: pitch, yaw and roll. The secondary control systems provide the ability to modify the main wing's airfoil, mostly for takeoff and landing operations. Finally, the ground control systems include the landing gear and its wheel brakes. Some key details about them are presented in this report, but a more thorough description is found in Systems Attachment 4.3.

#### 7.4.3.1 Primary control systems

- **Elevator**

The elevator is controlled by the longitudinal movement of the joystick. Moving it forward will cause a positive deflection on the elevator (downwards rotation), taking the nose of the aircraft down, while a backward movement will deflect it negatively (upwards rotation), therefore rising the nose. This deflections will be actuated through an Electro-Mechanical Actuator (EMA) (Figure 102) from the manufacturer *Collins Aerospace* [46], which has been selected as the provider of the actuators required in the aircraft for its reliability, experience and competitive prices. It will be placed in the T junction of the tail, to actuate both sides simultaneously.

- **Ailerons**

The ailerons, whose aerodynamic purpose has been previously explained, are controlled by the lateral movement of the joystick. Moving it to the right will cause a positive deflection on the left aileron and a negative deflection on the right one, inducing a positive rotation along the longitudinal axis of the aircraft (Figure 103).

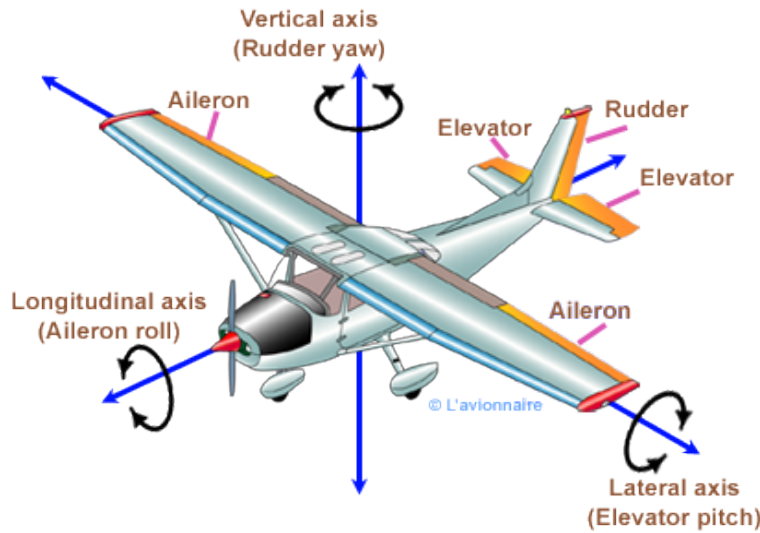


Figure 101: Primary flight controls. Source: [45].



*Electro-Mechanical Actuator (EMA)*

Figure 102: Electro-Mechanical Actuator. Source: [46].

The opposite will happen when moving it to the left. They will be actuated with a smaller version of the system used in the elevator, which will fit in the limited space in the wing at the aileron span position.

- **Rudder**

Unlike the elevator and the ailerons, which are controlled through the joystick, the rudder is controlled by the pedals. Pressing the right pedal will create a side force to the left resulting in the plane turning to the right, and vice versa. Figure 104 shows in detail the system operation in the ATR42-300, which will be similar to our own.



Figure 103: Roll control through the joystick. Source: [47] (modified).

#### 7.4.3.2 Secondary control systems

- **Flaps**

The flaps are controlled in the cabin by the flap lever (Figure 105), situated in the middle lower controls. Its allowable deflections can also be seen in (Figure 105). The actuator used in this case will be the same as for the elevator (Figure 102), through a more complex mechanism. Due to the size of the flaps, two units will be used in each half-wing, and will be powered by a couple of High-Lift Power Drive Unit (HLPDU) from the same manufacturer [46]. For redundancy, an Electric Backup Hydraulic Actuator (EBHA) will be also equipped. The actuators can be placed in the space available inside the wing, but the power units will be installed in the fuselage.

- **Spoilers**

Unlike the other control systems presented so far, the spoilers will not be controlled directly by the pilots. Throughout the history of the spoilers there have been plenty of accidents due to an incorrect usage of the ailerons, so electronic systems will be needed to automatically control their deployment when needed and their retraction. The automatic deployment of spoilers can be seen in Figure 106. Indicators will also be used to show the pilots their state of deployment.

#### 7.4.3.3 Ground control systems

- **Landing gear**

The landing gear has been previously described with high level of detail, with the only thing left being its actuation from the cabin of the aircraft. Since a commercially available unit has been selected, all of its hydraulic

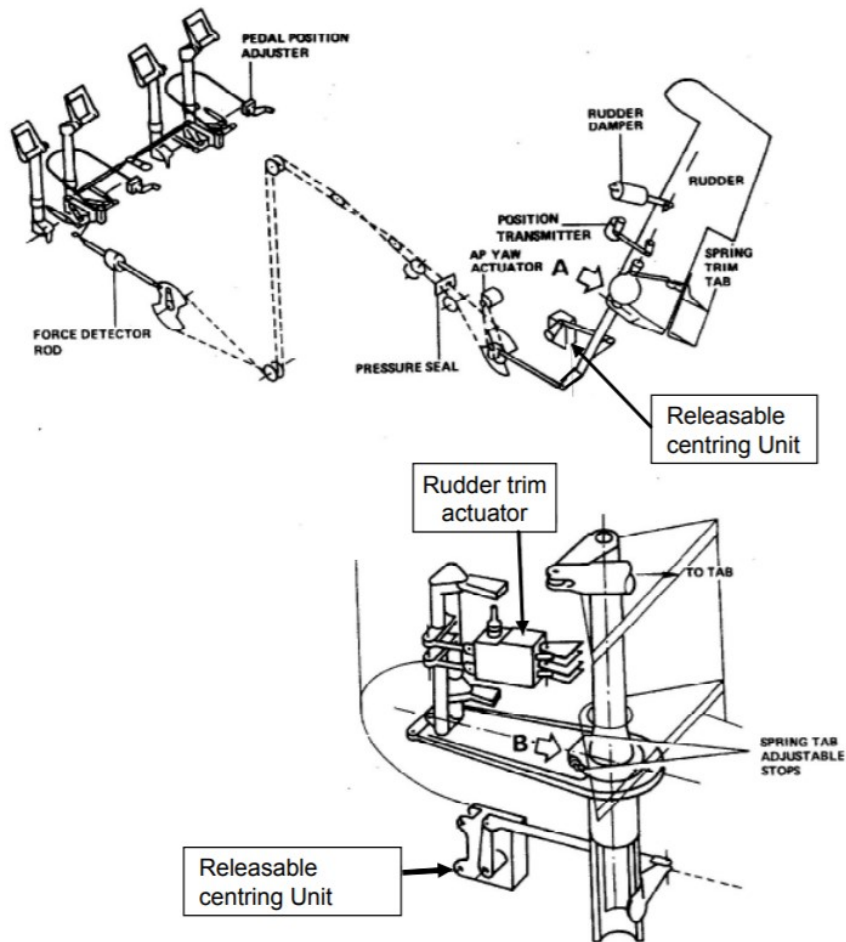


Figure 104: Rudder system layout of the ATR42-300. Source: [48].

actuators are already defined. Its steering control unit will be installed in the front desk in the cabin. A proper connection within components must be ensured to avoid any possible malfunctions, and assistance from the manufacturer will be required. Indicators and alerts will be displayed to ensure its correct deployment during the takeoff and landing.

- **Wheel brakes**

The wheel brakes used in our aircraft are also commercially available from the same manufacturer as the landing gear, to ensure their compatibility. An electric brake, which is the new technology in aircraft brakes, will be used (Figure 107). Its functioning is explained in more detail in Systems Attachments 4.3.3.2.

Some of the most relevant features the braking system includes are:

- **Auto-brake systems:** Designed to be used in case of a failed takeoff attempt. Provides the required brake while minimising brake wear.
- **Brake temperature indicators:** Used for safety reasons, to avoid excessive brake temperature, which



Figure 105: Flap control lever (white) in the ATR42-600s and its allowable deflections. Source: [34].



Figure 106: Boeing 717 approach phase: cruise flight (left), descending flight (center) and landing (right). Source: [49].

may lead to the failure of the system.

- **Parking brake:** Used when the aircraft is stationary on the ground. Activated through an additional lever, which ought to have a different handle color than the main brake one.



Figure 107: Electric brake. Source: [50].

#### 7.4.3.4 Cabin integration

The election of the stick as the main control system of the aircraft, opposed to the conventional yoke, induces some major changes in the cabin distribution. First of all, the stick is installed in the top part of the lateral panel, which will be slightly larger (Figure 108). The instruments previously located in this area have to be moved slightly backwards without being eclipsed by the pilot's arm when controlling the stick. The location of the pedals is not changed. The flap lever location has been already specified (Figure 105). The brake controls will be located in the front desk of the cabin.



Figure 108: Cockpit controls layout in an Airbus A320. Source: [51].

#### 7.4.4 Fuel system

##### 7.4.4.1 Fuel selection

The engines used in the aircraft are the Pratt & Whitney PW127N, which are biofuel compatible. Since one of the main focuses of this project is the reduction of the impact on the environment, the fuel used in this aircraft will be a **50/50 combination in mass of biofuel and Jet A-1 fuel**: the biofuel will be burnt first and then the Jet A-1, so the aircraft will use two different kinds of fuel instead of a blend. The biofuel used will be derived from oilseed crops: 98% of *Camelina sativa* and 2% of *Brassica carinata*. It will be the same fuel used in the Porter Airlines Bombardier Dash Q400 with the turboprop Pratt & Whitney PW150 engines [52]. Both biofuels will meet the requirements stated in the ATM D7566-20b for aviation turbine fuel containing synthesized hydrocarbons [53] (see Systems Attachment section 4.4.1 for more specifications).

##### 7.4.4.2 Fuel required

The different fuel fractions have been calculated, as well as the total amount of fuel required. The results are shown in Table 31:

Table 31: Fuel mass calculations.

Phase	Initial mass (kg)	Weight fraction	Total mass (kg)	Fuel mass (kg)	Real fuel mass (kg) <sup>1</sup>
1	18800.00	0.9900	18612.00	188.00	197.40
2	18612.00	0.9950	18518.94	93.06	97.71
3	18518.94	0.9950	18426.35	92.59	97.22
4	18426.35	0.9890	18223.66	202.69	212.82
5	18223.66	0.8849	16126.11	2097.54	2202.42
6	16126.11	0.9715	15666.52	459.59	482.57
7	15666.52	0.9850	15431.52	235.00	246.75
8	15431.52	0.9646	14885.24	546.28	573.59
9	14885.24	0.9950	14810.82	74.43	78.15
<b>Total</b>	<b>18800.00</b>	<b>0.7878</b>	<b>14810.82</b>	<b>3989.18</b>	<b>4188.64</b>

The total amount of fuel required is 4188.64kg.

##### 7.4.4.3 Fuel tanks

The fuel weight accounts for a notable fraction of the aircraft's weight, and its integration within the structure is of utmost importance. In aircraft of this size, the main tanks are positioned in the wings, for better structural performance, and additional smaller tanks can be distributed in the fuselage or on other aerodynamic surfaces

<sup>1</sup>Adding a 5% contingency factor, as specified by International Civil Aviation Organization (ICAO)'s standards

if more fuel volume is required. Additionally, since the aircraft uses two different kinds of fuel, the tanks will have to be separated in order not to mix them.

The main type of tanks used in similar sized aircraft are the integral fuel tanks (also known as wet wings) and the rigid removable. The advantages and disadvantages of each configuration are presented in the table *Advantages and disadvantages of integral and rigid removable fuel tanks*, in section 4.4.4 of the Systems Attachment.

Although at first sight it may seem that the rigid removable type of fuel tank is a better option, the relevance of each item must be studied.

Reducing the Operational Empty Weight (OEW) of the aircraft improves considerably its performance in terms of range, so lighter fuel tanks are recommended. Also, if all the fuel can be stored in the wings, a less complex pumping system will be required, reducing costs and weights. For this reason, higher volume is sought.

Seeing how fast the materials engineering advances, it is conceivable to assume that improvements in covering materials for the inside of fuel tanks (resins) will be made, then reducing the risk of leakage of integral fuel tanks and their crashworthiness.

For this reasons, integral fuel tanks will be used in the QCRA.

#### 7.4.4.4 Fuel distribution

Knowing that the Maximum Fuel Weight (MFW) is of 4188.64kg, and considering that the aircraft uses a 50/50 mass combination of Jet A1 fuel and biofuel, the volume of fuel required for the most restrictive case (smaller density) would be 2702.35 l and 2755.68 l, respectively, making a total of 5458.03 l.

The fuel tanks will be positioned in the wings and they will be integral fuel tanks, as previously explained. The interior of the wing will have to be sealed with an epoxy resin. The aircraft will have a total of four fuel tanks distributed as shown in Figure 109. Tanks 1 and 4 will store the A1Jet fuel and tanks 2 and 3 the biofuel.

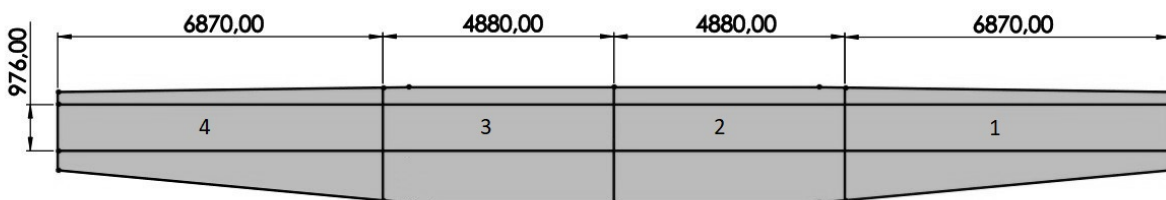


Figure 109: Scheme of the four tanks situated in the wings (the front of the wing corresponds to the top of the image).

Tanks 2 and 3 each have a capacity of around 1400 l (for biofuel) and tanks 1 and 4 of 1460 l (for Jet A1), thus the total fuel tank capacity of the aircraft would be of 5720 l, which is more than the maximum volume of fuel required ( $\approx$  5460 l).

Tanks 1 and 2 will provide fuel to the right engine, and tanks 3 and 4 to the left one. The inner tanks (2 and 3) will feed the engines with biofuel until it runs out, and then the Jet A1 will start to be consumed from the outer tanks (1 and 4). This emptying sequence improves the structural performance of the wing by reducing the bending moment on the root. The tanks with the same fuel type will be connected given that the pilot needs to balance the aircraft or use the fuel for the opposite engine in case of engine failure.

The fueling system will be similar to that in the ATR42. The refueling will be done from the lower part of the wing, and each tank will have to be refuelled separately.

## 8 Economic feasibility analysis

In this section the feasibility of our project is being analysed through the study of several economic indicators such as the Net Present Value, the Payback Time, the Break-Even Point, the Internal Rate of Return and the Return on Investment. These economic parameters are obtained from the Profit & Loss Statement, which refers to the Cash Flow during annual operation. The operational costs, the revenue prediction and the initial investment are explained in depth in the Attachments Economics, section 5.3.

The feasibility study has been developed for the first 15 years. It has been chosen this span by using other aeronautical projects of similar magnitude as a reference. As it is mentioned in the planning and scheduling for the follow up of the project, it has been considered that the revenue starts flowing in during the fourth fiscal year.

As stated in the budget, a QC aircraft will have a materials and manufacturing cost of 13,936,725 € and it will be selling with a gross margin of 40%, at a price of 23.25M €.

Figure 110 is a prediction of the units sold. It must be noted that due to space constraints in our facility, the maximum manufacturing capacity is limited to 10 planes per year.

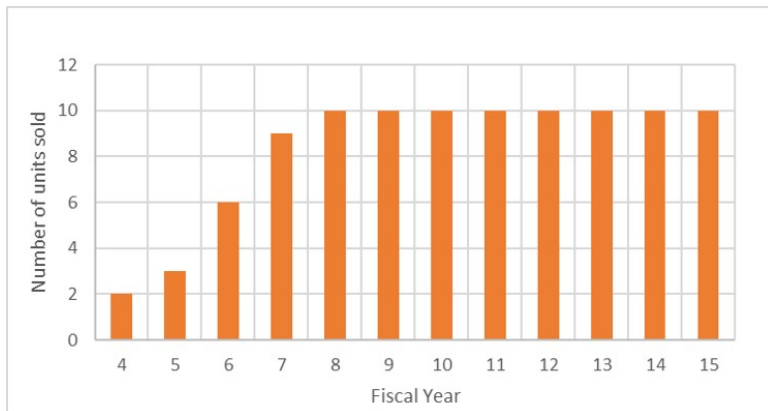


Figure 110: Estimation of the amount of airplanes sold per year.

According to this prediction, the factory will start operating at a full capacity in the eighth fiscal year. The decrease in the cost of mass production has not been taken into account since the aircraft cost has been considered as an average of all the aircraft produced during the project.

### 8.1 Cumulative Cash flow

The feasibility study is analysed through the Profit & Loss statement and it covers three different scenarios.

- **EBITDA:** Before taking into consideration the interests, tax, depreciation and amortisation.
- **EBT:** Taking into consideration the present value of future cash flows, applying a discount rate.

- **EARNINGS:** Taking into consideration the discount rate and the tax deduction. It provides the most valuable information.

As shown in Figure 111, the cumulative net cash flow is the most restrictive (yet realistic) scenario. However, in order to assess the profitability of a project without taking into consideration government policy on taxes, financial performance or depreciation and amortization strategies, evaluating the different parameters using EBITDA can provide us with the capability to extract better conclusions when evaluating businesses.

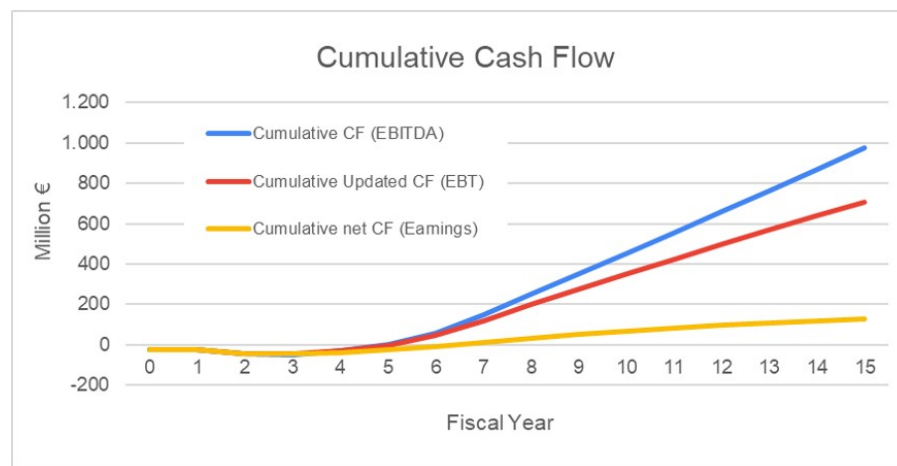


Figure 111: Cumulative cash flow in the three scenarios.

Figure 112 offers a deep view into the net cash flows of our company, deducting tax and accounting for inflation, depreciation and risk factor.

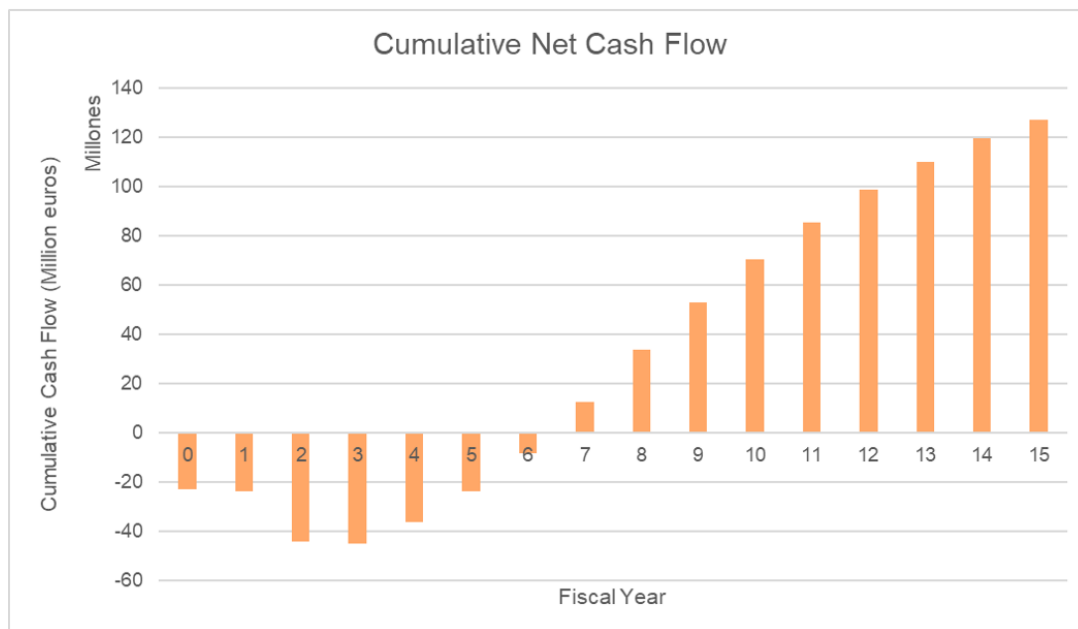


Figure 112: Cumulative Net Cash Flow.

As shown in the figure above, the initial investment will be covered by the revenue in Fiscal Year 7. It seems like seven years is a lot of time to become profitable, but for a company in this niche it is an extraordinary result. When having a look at the cumulative cash flow in the last year (Net Present Value) it becomes obvious that the business is very profitable.

## 8.2 Net present value at the end of the Project

Net present value (NPV) is the difference between the present value of cash inflows and the present value of cash outflows over a period of time, in our case we have considered the full length of the project to asses this parameter.

The NPV obtained is the following:

- NPV (EBITDA): 974,924,552 €
- NPV (EBT): 706,657,057 €
- NPV (NET EARNINGS): 126,927,521 €

As expected, the NPV of our business is smaller in case we account the net earnings after tax deduction, inflation, interest and risk factors. A NPV of 126.9M € is a proof of the profitability our business, as the initial investment was only 23.1M €.

## 8.3 Payback time and Break-even point

The Payback Time is defined as the period of time necessary to recover the initial investment.

The Payback Time has been obtained by a linear interpolation between the year before and the year after the cumulative cash flow becomes positive. Thanks to this method, a very accurate value has been obtained. The results of the PB time in the three different scenarios are the following:

- PBT (EBITDA): 4.98 years
- PBT (EBT): 5.08 years
- PBT (NET EARNINGS): 6.40 years

The payback time sits between five and six and a half years. Having in mind that the mass production doesn't start happening until the fourth fiscal year, it can be said that becoming profitable will not be an issue for the company. The Payback time considering net earnings is the highest as it is taking into consideration the most restrictive case.

The Break Even Point is a parameter based on the net profit which gives us an idea of the number of units that must be sold in order to become profitable. The way in which it has been calculated it is by creating a

polynomial function that represents the total units sold in time. If we substitute the PB time in the equation the BEP is obtained.

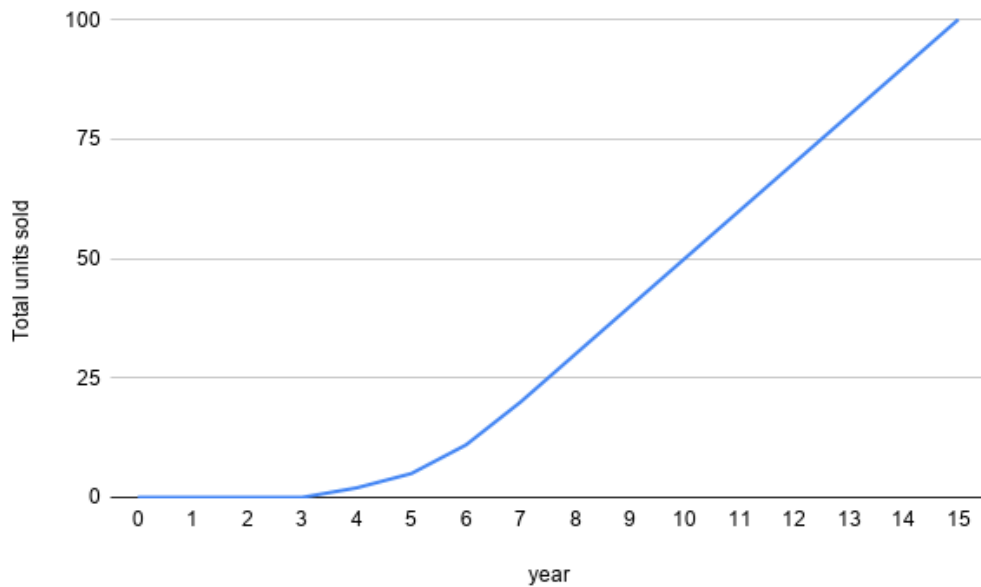


Figure 113: Total units sold per year.

The results obtained have been rounded up, as the Break Even Point can't be represented by decimal numbers. For the break even point, the results obtained are the following:

- BEP (EBITDA): 6 units
- BEP (EBT): 6 units
- BEP (NET EARNINGS): 15 units

When accounting for tax deduction, interests and depreciation the Break Even Point is at 15 airplanes. It seems like this is a very small number but we should take into account that the production in the first years is lower, that is why it has been considered as reasonable.

#### 8.4 Return on Investment

The Return of Investment is defined as an economic indicator which rates the profit of the investment after a defined time. In the case of our project this time is of 15 years and it is computed as follows

$$ROI = \frac{NPV}{Initial\ Investment} \quad (5)$$

Where the initial investment does not only refer to the fiscal year zero, as it has been considered for this

parameter that, on the whole, the initial investment required contemplates those years in which no aircraft are sold. Then, the following results for the different stages are:

- ROI (EBITDA): 21,40
- ROI (EBT): 15,97
- ROI (NET EARNINGS): 3,05

The ROI at the end of the project accounting for tax deduction and inflation is 3.05 or 305%. This means that the capital obtained at the end of the project is 3.05 times the initial investment. The ROI is very dependant on the time frame chosen.

## 8.5 Internal rate of return

The internal rate of return is a metric used in financial analysis to estimate the profitability of potential investments. It is a discount rate that makes the net present value (NPV) of all cash flows equal to zero in a discounted cash flow analysis.

The results obtained are the following:

- IRR (EBITDA): 47,02%
- IRR (EBT): 42,73%
- IRR (NET EARNINGS): 19,59%

The IRR could also be understood as the annualized rate of earnings on an investment. In this case, a 19.59% annual return over-performs the historical average of the stock market, which is around 10%. It can be concluded that although it takes seven years to become profitable, it is a very good investment.

## 8.6 Final conclusions

The results obtained in the feasibility study demonstrate that our company may have great opportunities to succeed. The Net Present Value at the end of the project is 5.5 times greater than the initial investment, which is an extraordinary figure. The fact that we will obtain a profit of more than a 100 M € at the end of project (accounting for inflation, depreciation and tax deduction) demonstrates the great potential of our business.

This huge profitability will give us the chance to reinvest in Research & Development, in new machinery or even in opening other production lines in order to increase the volume of production.

Regarding the risk of the project, it can be argued that it presents a medium to moderate risk since the IRR is quite high at 19.59%, the expected payback time is just 6.40 years (accounting for net profit) and we will recover our investment after only selling 16 units. However, the aerospace industry is a very consolidated industry with very powerful and established companies. Competing against them will not be easy but after

seeing the great results we have obtained in the feasibility study there is no doubt that we may be able to disrupt the sector.

## 9 Environmental impact analysis

### 9.1 General considerations

It is important to make sure that every step of the manufacturing of the aircraft is as environment-friendly as possible. Planes have lots of steps in its fabrication process, so reducing pollution even by a little in each of those steps can end up making a huge difference. That process can be separated between material obtaining process, manufacturing process and product use.

During the material obtaining process, it is important to take into account from who you are buying your materials and how far they are from your manufacturing facilities. The further the material source is from the place planes are being made, the higher the emissions the transport process will cause. Also, if the country can report low environmental impact during material extraction process, the overall impact of the plane will also decrease drastically. Some of this points are further studied in Structures Attachment, Materials subsection.

Another major factor to take into account is the manufacturing process. Even though making a plane requires heavy machinery and installations that tend to cause pollution, it is important to do as much as possible. Replacing fuel-powered machinery with electricity-powered one can be a small step in the right direction, at the same time, the fabric can be equipped with solar panels to provide some of the electricity being used. Also, making sure your electricity supplier obtains a big part of its energy supply from clean sources should not be a problem in a European country (the main installations will be placed in Germany). Some other small initiatives could be placing incentives for the workers to come to work in public transport, bicycle or electric vehicles, like economic rewards, easy access to buses and metro from the factory and the placement of free electric recharge stations for the workers that own an electric vehicle.

Also, when designing the aircraft some aspects like reducing the plane's weight or selecting more modern and environmentally-friendly power plants help reducing aircraft's emissions. On top of that, making the plane compatible with more ecologic fuels (like biofuel) is also a great asset to have. In  $CO_2$  emissions subsection various of this aspects are explained in more detail.

Finally, other factors like recycling materials when the aircraft lifespan is over or reusing some undamaged parts from other planes can help, even by a little bit, to reduce the overall impact on the planet caused by the project.

### 9.2 Structure materials

When designing the aircraft, a lot of factors are taken into account before choosing a material; its properties, the price, the estimated life-span, etc. But other factors need to be taken into account as well, one of them being the environmental impact they have. If the material is widely available in countries near your factory, transport emissions will decrease. Also, if the country from where they proceed have more strict environment protection rules for material-extracting procedures, the impact will be lower. That's why a research about what countries

export aluminium and titanium was conducted.

First of all, a list of the biggest aluminum exporters by country is searched:

1. Canada: US\$5.3 billion (10.1% of total aluminum exports)
2. Netherlands: \$5.12 billion (9.7%)
3. United Arab Emirates: \$5.11 billion (9.7%)
4. Russia: \$4.6 billion (8.8%)
5. India: \$3.8 billion (7.2%)
6. Norway: \$2.8 billion (5.3%)
7. Australia: \$2.78 billion (5.2%)
8. Malaysia: \$2 billion (3.8%)
9. Bahrain: \$1.9 billion (3.6%)
10. Iceland: \$1.4 billion (2.7%)
11. Qatar: \$1.3 billion (2.4%)
12. China: \$1.1 billion (2.1%)
13. United States: \$1.05 billion (2%)
14. South Africa: \$1.01 billion (1.9%)
15. Saudi Arabia: \$967.8 million (1.8%)

Figure 114: Top aluminum exporters in 2019 by dollar value and % share of global sales.

Taking into account that Netherlands shares border with Germany, where the factory is located, and considering it is the world's second biggest aluminum exporter (making them a stable material source), buying it from them would mean a significant reduction on transport emissions (even though they previously import the raw material, once the aluminium is processed it travels a smaller distance compared to buying the final material from a distant country). If not, Russia could be another viable alternative but because of them not being in the European Union, prices would rise and difficulties may appear. Another European source could be Norway, opening both sea routes and land routes through Sweden and Denmark.

After considering everything, Netherlands seems like a great provider both from an environmental point of view (close to Germany and within the European Union, where environmental laws are strict) and a practical point of view (close and stable source of material). Even though it isn't one of the biggest exporters, some aluminium from Germany can also be bought, reducing even further the emissions and inconveniences of exports.

For titanium exporters, data is more faded but world's top exporters include China and Japan as leading exporters and Russia as the third biggest exporter of the world. From these three main countries, for the same reasons previously stated, trading with Russia would be the best option from an environmental point of view. Another good option among titanium exporters is Ukraine, who also export a lot of this material and have close economical relations with the European Union even though it isn't a member of the EU nor the EEA (European Economic Area).

In conclusion, buying from European countries which have common and strict environmental rules and laws and are close to the main factory is always preferable.

### 9.3 $CO_2$ emissions

#### 9.3.1 $CO_2$ emissions in the aviation industry

In many ways, commercial air travel underpins the modern global economy, but this comes with an environmental cost. Jet fuel use is a major contributor to global carbon dioxide ( $CO_2$ ) emissions. In 2019, global commercial aviation emitted around 915 million tonnes of  $CO_2$  [54]. If commercial aviation were counted as a country, it would rank sixth, between Japan (5<sup>th</sup>) and Germany (6<sup>th</sup>), in terms of  $CO_2$  emissions [55]. During recent years, aviation fuel use and  $CO_2$  emissions have significantly grown. As it can be observed in Figure 115, they increased by 44% over the past 10 years.

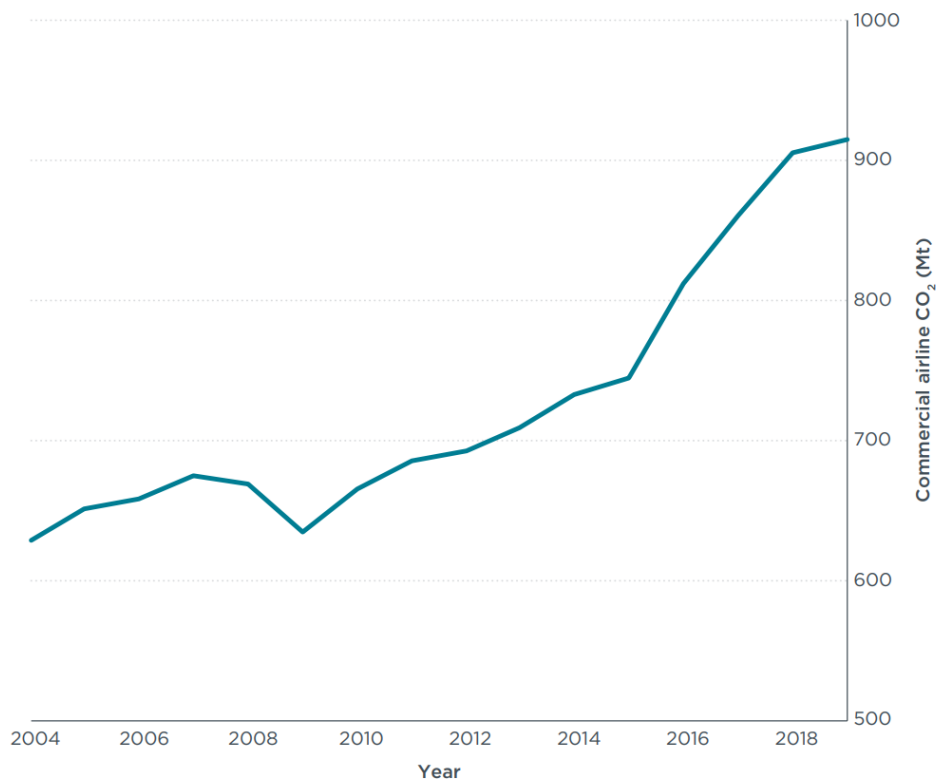


Figure 115:  $CO_2$  emissions from commercial aviation, 2004 to 2019. Source: [56].

Due to this fact, some stakeholders began developing policies to reduce the environmental impact of aviation. In 2012, the European Union began covering  $CO_2$  emissions from domestic and intra-EU flights under its Emissions Trading System [57]. In 2013, the *International Civil Aviation Organization* (ICAO) established a climate goal of carbon neutral growth from 2020 onward [58]. The goal includes an annual 2% fuel efficiency improvement; ICAO has also started analyzing a long-term climate goal for possible adoption in 2022. Addi-

tionally, some airlines and civil society organizations have proposed mid- and long-term  $CO_2$  reduction targets for aviation.

On the other hand, referred to the average fuel burn of new jet aircraft, it fell by about 40% on the block fuel intensity metric from 1970 to 2019, or a compound annual reduction of about 1.0% (Figure 116).

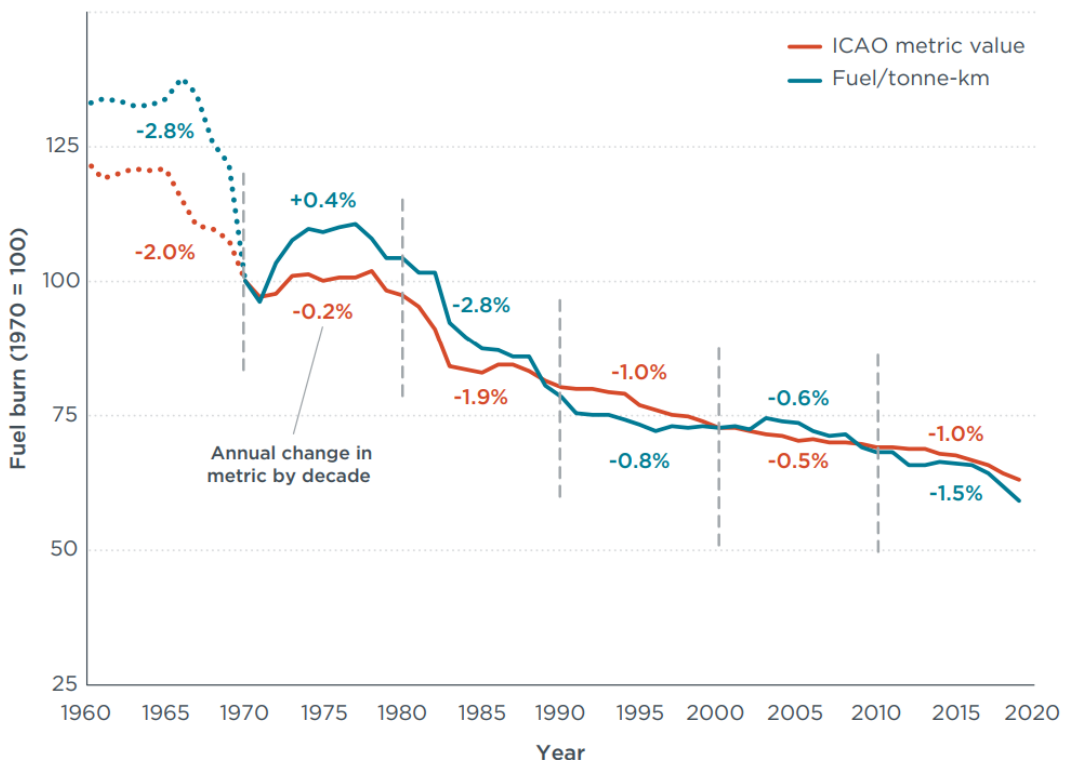


Figure 116: Average fuel burn of new commercial jet aircraft, 1960 to 2019. Source: [56].

In terms of fuel per passenger consumed, the situation is quite different. Nowadays the fuel consumption is usually around 3 to 4 liters per passenger per 100 kilometers. To put into perspective with other means of transport such as cars, according to the United Kingdom Department of Transport, new cars are burning from 8 liters per 100 kilometers (in 2000) to 5.4 liters per 100 kilometers (in 2016), which is higher than most airlines figures per passenger [59].

### 9.3.2 $CO_2$ emissions reduction plan

The engines used in the aircraft are the Pratt & Whitney PW127N. This is one of the latest models of the PW100 series and was designed focusing on reducing fuel consumption and being more environmentally conscious. That is the reason why they are biofuel compatible.

Biofuels are produced from renewable biological resources such as plant material, rather than traditional fossil fuels like coal, oil and natural gas. The biofuels used in aviation are second-generation biofuels which use a

sustainable resource to produce the fuel while not consuming valuable food, land and water resources. These include bio-derived oil, sourced from feedstocks such as jatropha, camelina, algae and halophytes. It can be argued that although the  $CO_2$  emissions are reduced from the use of biofuels, their production (harvesting, processing and distribution) in a large scale still pollutes the environment. Nevertheless, many companies are working towards the reduction of these emissions and there has been a great progress made in the recent years.

Apart from all the environmental benefits biofuels bring, some of the most important properties they offer are lubricity and detergency, which help reduce the formation of deposits in the tanks and also help maintain their cleanliness. They tend to offer a worse performance in high altitudes compared to fossil fuels. In this case this will not be a disadvantage since the aircraft will not fly at such high altitudes, like turbofan powered aircraft, and the fuel used is a 50/50 blend, so the different types of fuel will compensate each others minor deficiencies.

Taking into account the results obtained in section 7.3.6, it is possible to estimate the  $CO_2$  emissions of the QCRA aircraft. The fuel consumption obtained is  $2.69\text{kg}/100\text{km/seat}$ . To convert this fuel consumption to  $CO_2$  emissions it is necessary to use the  $CO_2$  fuel factor, which in this type of aircraft is approximately 3.16 grams of  $CO_2$  per gram of fuel [60]. This equals to an emission of  $8.5\text{kg}/100\text{km/seat}$  of  $CO_2$ .

On average, passenger aviation emitted  $9\text{kg}/100\text{km/seat}$  of  $CO_2$  in 2019 [61]. Comparing both emissions it can be observed that a reduction of 5.5% of the  $CO_2$  emissions has been achieved.

## 10 Safety considerations

The main concern of the aviation field is to guarantee the security of the aircraft and, of course, of its passengers, crew and cargo. In the case of a quick-change airplane, it is necessary to assure its proper functioning when operating with both cargo and passengers configurations. As a consequence, some extra safety measures have to be taken into account.

In order to design the aircraft according to safety standards, it has been performed following the EASA and FAA regulations: CS-25 and FAR 25 respectively. Moreover, all equipment installed is approved by the authorities that ensure their correct operation. This reduces the risk of an accident provoked by component failure, controlling air traffic problems or severe weather conditions, such as lightning or icing. Including fire extinguishers and life jackets, also approved, may reduce the damage resulting from an accident.

Emergency doors are also included. Following the aforementioned regulations, four of them are needed. Two emergency exits are located in front of the first row of seats and other two are located in the middle part of the seats zone. This arrangement would allow a correct evacuation if needed. (see Structures Attachment, section 4.6.3).

However, there are some aspects that determine the safety of each singular flight and must be controlled before and during each operation. Thus, it is essential to take into account the following safety considerations.

First of all, the pilot and copilot must have the corresponding flying license and specific training, as the aircraft has been designed considering that the crew has the basic knowledge necessary to pilot it without extra assistance.

Regarding the aerodynamics and structure of the aircraft, the TOW must not surpass the established value of 18800 kg. The pilot and copilot have to ensure that the flying angle of attack is between -10° and 20° and the maximum load factor of 2g is never exceeded. As a consequence, the aircraft can not perform any aerobatic manoeuvres.

Concerning the fuel, it must be compatible with the engine PW127N, for instance, the 50/50 blend of biofuel and Jet A-1. The fuel quantity must be enough to complete the flight path and must also take into account the taxi stage and the reserve fuel.

When flying with both configurations, but especially in cargo configuration, the ground staff has to properly secure the cargo pallets, so they don't move during the flight, even in the worst flying conditions. Its distribution is also important, as it may provoke a variation of the center of gravity of the aircraft, principally in case of a flight where the cargo compartment has empty spaces. When flying in passenger configuration, in order to ensure their own safety, the passengers must fasten their seat belt and remain seated following the corresponding sign located over the seat, according to general flight regulations.

Finally, the proper maintenance of the aircraft is essential to ensure the correct operation during its lifespan.

## 11 Planning and scheduling for the follow-up of the project

The preliminary design and study of a quick change regional aircraft has proven to be feasible both economically and technically. This leads us to defining the future steps that we would need to take in order to make our project reality.

Once the preliminary design phase has been finished, the following steps would be a more exhaustive and precise: design phase, a construction of the first prototype, the certification and testing of the aircraft and finally, a manufacturing phase. The project will last 15 years and the time frame of the first four years is illustrated in Figure 117.

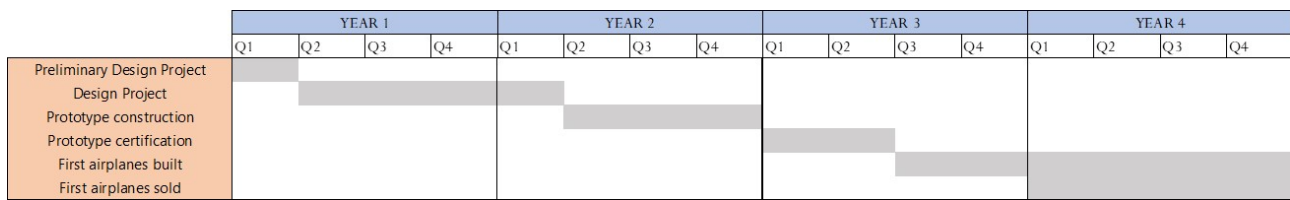


Figure 117: Planning and scheduling for the follow up of the project.

### 11.1 Preliminary Design

The Preliminary design has been developed by a team of 15 engineers who are spread across five main departments; aerodynamics, propulsion, structures, systems and economics. Each department has a coordinator whose job is to communicate with the project manager and with the other departments.

The organization chart of the team is shown in Figure 118.

The duration of this phase is three months and the goal is to have a first iteration of the project. The relative error that we can accept in this initial stage must be below 30%. To jump to the next phase, the aircraft should meet all of the initial requirements and the economic feasibility of the project must be proven.

The most important objective to accomplish during this part of the project is to make sure that there is a good communication between departments in order to avoid making mistakes that can affect the integrity of the aircraft.

The process that has been followed for the planning of the different tasks of the preliminary design has enabled the team to organise and work efficiently. The first step was to develop the Work Breakdown Structure (WBS) that contained the activities that had to be developed by every department. Once the tasks were defined, some tables were created where a brief explanation was added, as well as its preceding tasks and the resources (in units of time) required. Please refer to the Organization, Planning and Scheduling Attachment for the corresponding WBS, task identification and resources distribution and other important aspects.

Additionally, the Gantt diagram with all of the tasks is included in the Organization, Planning and Scheduling

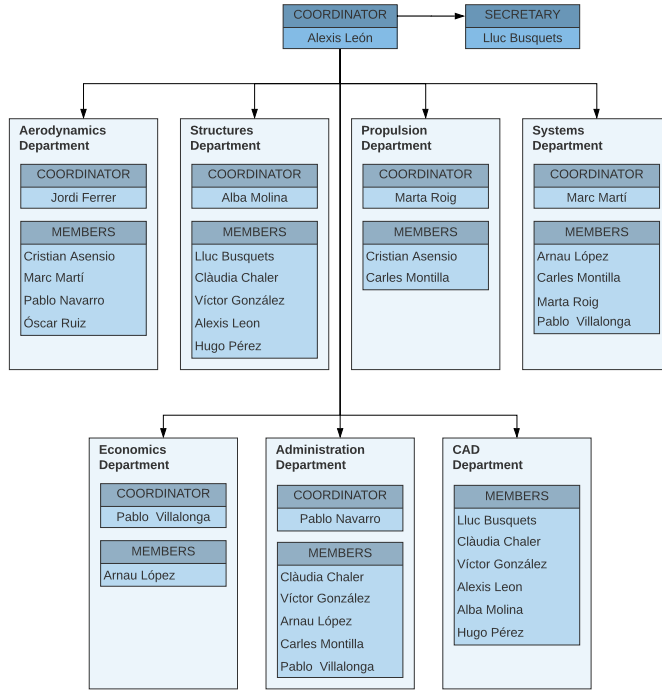


Figure 118: Internal organization structure.

Attachment, section 6.3.

## 11.2 Design Phase

The design phase will start once the preliminary design is successfully completed and it will have a duration of one year. There will be no major changes in the structure of the team, as we will have a workforce of 15 employees distributed across 5 different departments.

The main idea is to carry out several iterations of the preliminary study in order to obtain a more accurate design and to minimize errors. We will also focus on improving the weak points of our design.

## 11.3 Prototyping Phase

The aim of this stage is to build the first aircraft of its kind. In order to develop this phase, we will need to have our factory and equipment ready. The duration is set to nine months due to the complexity of the operation. In terms of the manpower required, the coordinator, the secretary and the team coordinators will stay in their respective roles and the other engineers will be relocated in a new project. We will also need to hire the first factory technicians and mechanics.

## 11.4 Certification Phase

Once the prototype is successfully built the certification period will begin. It will start with several weeks of ground testing and system certification until the first test flights are conducted. We will need to hire an expert in certification and several testing and validation engineers to accelerate the process and two test pilots. We estimate a duration of around six months until it is approved and we can start building it in mass.

## 11.5 Manufacturing Phase

A smooth manufacturing stage will be one of the main pillars to become cash flow positive. It is estimated we will begin manufacturing at the beginning of the fourth fiscal year. Our facility can build up to 10 planes per year, but it will not be until the eighth fiscal year that we will be operating at maximum capacity.

According to our estimations, the factory team will be formed by 20 members that include factory technicians, process engineers and controllers in order to deliver the volume of aircraft that has been predicted.

## 12 Conclusions and recommendations

To sum up, we are proud to say that the initial goal of designing the best quick change regional aircraft in the market has been accomplished.

However, it hasn't been a bed of roses, as we have faced many obstacles along the way. It has been a tough battle to design an aircraft that met our customer's constraints and requirements, and a great internal communication between departments has been crucial to coordinate a project of this magnitude. Regular team meetings have been the main channel used in order to update and debate with the other departments, and the coordinator has played a key role in detecting the weak points that needed more attention.

From the **structural** point of view, our main difficulty has been to draw the line between the tasks that were essential to the preliminary study and those who weren't. We have also had some issues correcting calculus errors, this is because taking a step back and recalculating the whole structure has been very time consuming. However, we have managed to develop a very accurate structural calculation of the wing using the finite element theory, we have defined the main structural parameters required in a preliminary design and we have also designed a cad version of the aircraft. We have also put a lot of focus on synchronizing and catching up with the aerodynamics department, as many points were dependant on their decisions.

When it comes to the **aerodynamics** of our aircraft, the biggest challenge has been the analysis of the aerodynamic surfaces and of the fuselage-wing assembly using XFLR5. While the results from simple analysis converged and were accurate enough compared to reference aircrafts, they were not converging if we added additional elements such as control surfaces or flaps. The biggest accomplishment from the aerodynamic point of view has been the segregated study of integration of different parameters and elements (such as winglets, high-lift devices, twist and torsion). Having done a deep analysis in all of this parameters has allowed us to better integrate our design with the other key departments. It is also important to mention that the requirement of reducing the fuel consumption a 10% has been the key motivator to focus on maximizing the aerodynamic efficiency.

In relationship to the **propulsion** system, we have chosen a turboprop engine due to its high efficiency in the range of velocities in which our aircraft operates. It has also been a perfect match because of its performance in short take off and landings, which was one of the requirements from our customer. The fuel selected is a mixture between bio-fuel and kerosene so as to offer a more ecofriendly alternative to air travel. The main drawback has been the limitations and lack of innovation when choosing an already existing model of engine.

As far as the **systems** of our aircraft goes, we have been able to research and define the main circuits, instruments and elements that are present in an aircraft of this characteristics. The main limitation has been the lack of information about their assembly and configuration.

Aiming to accomplish the initial requirements presented by our customer, both technical and soft skills have been developed in order to achieve our goals and delivering on time. We have pushed the boundaries of

engineering and we have created a great working environment where respect, empathy and hard work have been the core to our success.

The learning process has been exponential, as all of the members have had the chance to choose the department they were willing to contribute with. This has motivated us to work hard and become very efficient.

## 13 Bibliography and regulations

- [1] M. Heinemann, M. A. H. (1967). Quick-change (qc) airplane system: A prospective [DOI: 10.2514/3.43792]. *Journal of Aircraft*, 4(1).
- [2] Lucy Budd, S. I. (2016). The role of dedicated freighter aircraft in the provision of global airfreight services [<https://doi.org/10.1016/j.jairtraman.2016.06.003>]. *Journal of Air Transport Management*.
- [3] Netz, J. (2003). Concept and future of quick change operations between freight and passenger configurations [DOI: 10.2514/6.2003-2501]. *AIAA International Air and Space Symposium and Exposition: The Next 100 Years*.
- [4] J. M. Nelson, R. T. K., & Gregg, R. D. (2001). *A study of the economic benefit potential of inter-modal transports* (tech. rep.). NASA. <https://ntrs.nasa.gov/api/citations/20010039146/downloads/20010039146.pdf>
- [5] Murdo Morrison. (2020). *How coronavirus has turned the airfreight market on its head*. <https://www.aircargonews.net/freighters-world/how-coronavirus-has-turned-the-airfreight-market-on-its-head> (accessed: 9-12-2020)
- [6] Boeing. (n.d.[a]). 737 classic passenger. [https://www.boeing.com/resources/boeingdotcom/company/about\\_bca/startup/pdf/historical/737-classic-passenger.pdf](https://www.boeing.com/resources/boeingdotcom/company/about_bca/startup/pdf/historical/737-classic-passenger.pdf)
- [7] ATR. (n.d.[a]). Atr 42-500. <http://1tr779ud5r1jjgc938wedppw-wpengine.netdna-ssl.com/wp-content/uploads/2020/07/42-500.pdf>
- [8] ATR. (n.d.[b]). Atr 72-500. <http://1tr779ud5r1jjgc938wedppw-wpengine.netdna-ssl.com/wp-content/uploads/2020/07/72-500.pdf>
- [9] AircraftCompare. (n.d.). British aerospace atp. <https://www.aircraftcompare.com/aircraft/british-aerospace-atp/>
- [10] Flugzeug. (n.d.). Regional airliner fokker 50. [http://www.flugzeuginfo.net/acdata\\_php/acdata\\_fokker50\\_en.php](http://www.flugzeuginfo.net/acdata_php/acdata_fokker50_en.php)
- [11] SAAB. (n.d.). Saab 340. <https://www.saab.com/products/saab-340>
- [12] of Canada Limited, D. H. A. (n.d.). Dash 8-400 —the world's most advanced turboprop. <https://dehavilland.com/en>
- [13] EFW. (n.d.[a]). The market for a320 and a321 freighters. [http://www.team.aero/images/aviation\\_data\\_insert/109\\_FRT.pdf](http://www.team.aero/images/aviation_data_insert/109_FRT.pdf)
- [14] COMPANY, A. (n.d.[a]). An-140 regional airplane. <https://antonov.com/en/history/an-140>
- [15] COMPANY, A. (n.d.[b]). An-140 regional airplane. <https://antonov.com/en/history/an-140>

- [16] Torenbeek, E. (1982a). *Synthesis of subsonic airplane design : an introduction to the preliminary design, of subsonic general aviation and transport aircraft, with emphasis on layout, aerodynamic design, propulsion, and performance*. SPRINGER-SCIENCE+BUSINESS MEDIA, B.V. <https://doi.org/10.1007/978-94-017-3202-4>
- [17] Gudmundsson, S. (2014). *General aviation aircraft design: Applied methods and procedures*. Elsevier.
- [18] Coma Company, M. *Arquitectura de aviones*. Escola Superior d'Enginyeries Industrial, Aeroespacial i Audiovisual de Terrassa. Grau en Enginyeria en Tecnologies Aeroespacials (Pla 2010). *Disseny d'Aeronaus*. 2017.
- [19] Roskam, D. J. (1986a). Airplane design. DARcorporation.
- [20] Meier, N. (2005). Civil turboshaft/turboprop specifications. <http://www.jet-engine.net/civtsspec.html>
- [21] *Type-certificate data sheet for engine pw100 series engines* (tech. rep.). (2018). EASA. <https://www.easa.europa.eu/sites/default/files/dfu/EASA%5C%20IM.E.041%5C%20TCDS%5C%20Issue%5C%204.pdf>
- [22] Sadraey, M. H. (2012). *Aircraft design: A systems engineering approach*. John Wiley & Sons.
- [23] *Survey on standard weights of passengers and baggage* (tech. rep.). (2009). EASA. <https://www.easa.europa.eu/sites/default/files/dfu/Weight%5C%20Survey%5C%20R20090095%5C%20Final.pdf>
- [24] Roskam, D. J. (1986b). Airplane design. DARcorporation.
- [25] Tools, A. (n.d.). Douglas la203a. <http://airfoiltools.com/airfoil/details?airfoil=la203a-il>
- [26] Vergün, T. and Tola, C. (2019). Rib Spacing Optimization of a Generic UAV Wing to Increase the Aeroelastic Endurance [DOI: 10.36287/setsci.4.6.032].
- [27] *14 cfr 25.807 - emergency exits*. (1965). Federal Aviation Administration. <https://www.law.cornell.edu/cfr/text/14/25.807>
- [28] Roskam, D. J. (1986c). Airplane design. DARcorporation.
- [29] Safran Landing Systems. (2020a). *Atr 42/72 landing gear*. <https://www.safran-landing-systems.com/landing-gears/regional-aircraft/atr-42/72> (accessed: 25-10-2020)
- [30] Nordstrom, A. (1992). Seat pallet and cargo pallet restraining system [United States Patent 5131606]. <https://www.freepatentonline.com/5131606.pdf>
- [31] Torenbeek, E. (1982b). *Synthesis of subsonic airplane design : an introduction to the preliminary design, of subsonic general aviation and transport aircraft, with emphasis on layout, aerodynamic design, propulsion, and performance*. SPRINGER-SCIENCE+BUSINESS MEDIA, B.V. <https://doi.org/10.1007/978-94-017-3202-4>

- [32] EFW. (n.d.[b]). *Cabin interiors & aircraft monuments*. <https://www.elbeflugzeugwerke.com/en/engineering/cabin-interior-aircraft-monuments/> (accessed: 20-11-2020)
- [33] Blog, P. (n.d.). Atr72 600 cockpit review. [https://www.youtube.com/watch?v=zJSpkXX3tso&ab\\_channel=PilotBlog](https://www.youtube.com/watch?v=zJSpkXX3tso&ab_channel=PilotBlog)
- [34] ATR. (n.d.[c]). Explore the cockpit. <https://www.atr-aircraft.com/our-aircraft/atr-42-600/>
- [35] ATR. (n.d.[d]). Systems atr 42-72. <https://www.theairlinepilots.com/forumarchive/atr/atr-systems.pdf>
- [36] Atr lighting system. (n.d.). <https://www.youtube.com/watch?v=w-k0V1Z6FaU>
- [37] Caswell, M. (n.d.). Lufthansa to offer 24 “lighting scenarios” on a350. <https://www.businesstraveller.com/business-travel/2017/02/06/lufthansa-offer-24-lighting-scenarios-a350/>
- [38] Boeing. (n.d.[b]). Qtr411. [https://www.boeing.com/commercial/aeromagazine/articles/2011\\_q4/pdfs/AERO\\_2011q4.pdf](https://www.boeing.com/commercial/aeromagazine/articles/2011_q4/pdfs/AERO_2011q4.pdf)
- [39] Concorde batteries. (n.d.). <http://concordebattery.com>
- [40] Batteries, C. (n.d.). Rg-380e/44 battery. <https://www.145.aero/Concorde-RG-380E-44-24-Volt-Aircraft-Battery-p/rg-380e-44.htm%20308E>
- [41] MidContinent. (2020a). *Inverter 6431200-6*. <https://www.mcico.com/inverters-3/6431200-6-1> (accessed: 2-11-2020)
- [42] Aeroval. (2020). *28vs50y-16 - transformer, rectifier, unit*. <https://aeroval.com/ref/235999/28VS50Y-16/> (accessed: 2-11-2020)
- [43] MidContinent. (2020b). *Ac generator 20032-2*. <https://myduncan.aero/online/parts/detail/20032-2>
- [44] Pranjal Pande, S. F. (2020). Why airbus aircraft have side sticks while boeings have yokes. <https://simpleflying.com/airbus-sidestick-boeing-yoke/>
- [45] L'avionnaire. (n.d.). Flight controls. <https://www.lavionnaire.fr/VocabFlightControl.php>
- [46] Collins Aerospace. (2020). *Power, controls & actuation*. <https://www.collinsaerospace.com/what-we-do/Commercial-Aviation/Power-Controls-Actuation/Actuation> (accessed: 11-11-2020)
- [47] Thrustmaster. (n.d.). Tca sidestick airbus edition. [http://www.thrustmaster.com/es\\_ES/productos/tca-sidestick-airbus-edition](http://www.thrustmaster.com/es_ES/productos/tca-sidestick-airbus-edition)
- [48] Atr42-300. (n.d.). [https://assets.publishing.service.gov.uk/media/5423016940f0b61346000b8b/ATR42-300\\_\\_EI-SLD\\_08-08.pdf](https://assets.publishing.service.gov.uk/media/5423016940f0b61346000b8b/ATR42-300__EI-SLD_08-08.pdf)
- [49] Harley, C. D. (n.d.). Aerodynamic performance of low form factor spoilers. <https://core.ac.uk/download/pdf/40024336.pdf>

- [50] Safran Landing Systems. (2020b). *Electric brake*. <https://www.safran-landing-systems.com/wheels-and-brakes/technologies/electric-brake> (accessed: 21-11-2020)
- [51] Airbus. (2020). *Cockpits*. <https://www.airbus.com/aircraft/passenger-aircraft/cockpits.html> (accessed: 19-11-2020)
- [52] Cicero, B., & Duchesne, M. (2012). Porter airlines operates bombardier q400 aircraft in canada's first biofuel-powered revenue flight. [https://skynrg.com/wp-content/uploads/2019/03/20120417\\_Press\\_Release\\_Porter-Biofuel-Powered-Flight\\_EN.pdf](https://skynrg.com/wp-content/uploads/2019/03/20120417_Press_Release_Porter-Biofuel-Powered-Flight_EN.pdf)
- [53] International, A. (2011). Astm aviation fuel standard now specifies bioderived components. <https://www.astm.org/cms/drupal-7.51/newsroom/astm-aviation-fuel-standard-now-specifies-bioderived-components>
- [54] International Air Transport Association. (2019). Industry statistics: Fact sheet. <https://www.iata.org/en/iata-repository/publications/economic-reports/airline-industry-economic-performance---december-2019---data-tables/>
- [55] Global Carbon Atlas. (n.d.). CO2 emissions. <http://www.globalcarbonatlas.org/en/CO2-emissions>
- [56] Zheng, X. S. (2020). Fuel burn of new commercial jet aircraft: 1960 to 2019. <https://theicct.org/sites/default/files/publications/Aircraft-fuel-burn-trends-sept2020.pdf>
- [57] European Comission. (2020). Reducing emissions from aviation. [https://ec.europa.eu/clima/policies/transport/aviation\\_en](https://ec.europa.eu/clima/policies/transport/aviation_en)
- [58] International Civil Aviation Organization. (2019). Climate change. <https://www.icao.int/environmental-protection/pages/climate-change.aspx>
- [59] OpenAirlines. (2018). How much fuel per passenger an aircraft is consuming? <https://blog.openairlines.com/how-much-fuel-per-passenger-an-aircraft-is-consuming>
- [60] Carbon Independent. (2020). Aviation. <https://www.carbonindependent.org/files/B851vs2.4.pdf>
- [61] ICCT. (2020). Co2 emissions from commercial aviation: 2013, 2018, and 2019. <https://theicct.org/publications/co2-emissions-commercial-aviation-2020>